Doctoral Dissertation

博士論文

Evolutionary biological studies on transition from heterothallism to homothallism based on the comparative analyses of sex-determining regions in the green algal genus *Volvox*

(緑藻ボルボックス属の性染色体領域比較解析による

ホモタリック種出現の進化生物学的研究)

A Dissertation Submitted for the Degree of Doctor of Science

December 2020

令和 2 年 12 月博士（理学）申請

Department of Biological Sciences, Graduate School of Science, The University of Tokyo

東京大学大学院理学系研究科生物科学専攻

Kayoko Yamamoto

山本　荷葉子

Table of contents

Abstract

Transitions between self-incompatible (dioecy, heterothallism) and self-compatible (monoecy, homothallism) mating systems are common across eukaryotes, but have not been extensively studied in the context of haploid (UV) sex chromosomes which are found in many algae and early diverging land plants. *Volvox* is a very interesting oogamous organism that exhibits various types of sexuality and/or sexual spheroids depending upon species or strains. However, molecular bases of such sexual reproduction characteristics have not been studied in this genus.

In the model species *V. carteri,* an ortholog of the *minus* mating type-determining or *minus* dominance gene (*MID*) of isogamous *Chlamydomonas reinhardtii* is male-specific and determines the sperm formation. Male and female genders are genetically determined (heterothallism) in *V. carteri*, whereas in several other species of *Volvox* both male and female gametes (sperm and eggs) are formed within the same clonal culture (homothallism). In this thesis, I investigated the transition from heterothallism to homothallism in *Volvox* and the fates of the haploid sex chromosomes after this transition, based on comparison of two closely related heterothallic *V. reticuliferus* and homothallic *V. africanus*.

In Chapter 2, I identified *MID* orthologs in two homothallic species *V. africanus* and *V. ferrisii.* Comparison of synonymous and nonsynonymous nucleotide substitutions in *MID* genes between homothallic and heterothallic volvocacean species suggests that the *MID* gene of *V. africanus* and *V. ferrisii* evolved under the same degree of functional constraint as those of the heterothallic species. Based on RT-PCR [semi quantitative reverse transcription polymerase chain reaction analyses] using the asexual, male and monoecious spheroids isolated from a sexually induced homothallic *V. africanus* culture, the *MID* mRNA level was significantly upregulated in the male spheroids but suppressed in the monoecious spheroids. These results suggest that the monoecious spheroid-specific down regulation of gene expression of the *MID* homolog correlates with the formation of both eggs and sperm in the same spheroid in *V. africanus*.

In Chapter 3, I analyzed three *de novo* whole genome sequences of heterothallic *V.*

reticuliferus (male and female strains) and homothallic *V. africanus* to identify a heteromorphic sex-determining region (SDR) of ca. 1 Mbp in *V. reticuliferus* and a homologous sex-determining-like region (SDLR) in *V. africanus* that retained distinct hallmark features of a SDR. Phylogenetic analyses indicated that in *V. africanus* most of the ancestral male gametologs (orthologs present in the SDR of both sexes) from the presumed heterothallic ancestor were lost during the transition to homothallism while a large region of the ancestral female SDR and its gametologs was retained. Interestingly, the predicted male-determining gene, *MID*, formed an unlinked multicopy array in *V. africanus* while a second conserved male gene, *MTD1* moved to a different genomic location from the SDLR. Those data help date the origins of the *Volvox* expanded SDR within this genus at least 75 MYA and establish a framework for understanding how a homothallic mating system arose from ancestral haploid sex chromosomes.

This study can suggest that UV sex chromosome system in an ancestral heterothallic volvocine algae was modified to produce a homothallic mating system in *V. africanus*. Even the ancestral male SDR degenerated to SDLR in *V. africanus*, the *MID* gene has been maintained and still has a role for male gametogenesis. The *V. africanus* female-like SDLR genes may also play a role in governing developmental patterning that gives rise to monoecious versus male sexual forms in this species. Further studies in gametologs in common with other *Volvox* and genomic analyses of different *V. africanus* linages will elucidate the molecular genetic basis of the evolution of *Volvox* from heterothallism to homothallism.

Chapter 1.

General introduction

A principal advantage of sexual reproduction is the resultant mixing of genomes through meiotic recombination that can maintain or improve fitness of a population. As first noted by Darwin when studying plant sexuality, self-fertilization can lead to inbreeding depression, though this potential disadvantage may be offset by higher probability of fertilization success (Darwin and Burkhardt, 1861; Charlesworth et al., 1990). Transitions between self-incompatible (dioecy, heterothallism) and self-compatible (monoecy, homothallism) mating systems have been documented in sexual systems across a broad range of taxa including animals, land plants, algae, protists and fungi (Jarne and Auld, 2006; Wong and Wolfner, 2017; Coelho et al., 2018; Hanschen et al., 2018). Hermaphroditic sexual systems in diploid animals and plants are fairly common, and the molecular genetic bases of monoecism and dioecism were recently studied in the land plant spinach (Yamamoto et al., 2014). However, transitions between heterothallism and homothallism have not been well-studied in systems with haploid (UV) sex chromosomes (Coelho et al., 2018) (Fig. 1.1). The fates of sex-determining and sex-related genes present on ancestral sex chromosomes, as well as the resolution of differentiated gametologs [genes with orthologs in both the male and female sex-determining regions (SDRs)], some of which may have undergone antagonistic selection, are unknown.

The volvocine green lineage is a unique model encompassing a progression of complexity and sexual dimorphism, from unicellular isogamous *Chlamydomonas* to multicellular oogamous *Volvox* (Kirk, 2005; Nozaki et al., 2006; Ferris et al., 2010; Hanschen et al., 2016; Hamaji et al., 2018; Umen and Coelho, 2019). Ferris and Goodenough (1994) identified the first mating-type locus (*MT*) in *Chlamydomonas reinhardtii* that was discovered to have some features of a typical sex chromosome including large size and suppressed recombination. Subsequent studies revealed conservation of the mating-type determining gene *MID* in *MT* of *minus* or male strains in heterothallic species of isogamous *Gonium* and *Yamagishiella*, anisogamous *Eudorina*, and oogamous *Volvox* (Ferris et al., 2010; Hamaji et al., 2016, 2018). The mating type *MT* haplotypes

or SDRs in heterothallic volvocine algae range from 7 kbp to 1 Mbp and are structurally heteromorphic with rearrangements between haplotypes which exhibit differing degrees of differentiation (Hamaji et al., 2018). The ca.1 Mbp, highly-differentiated *Volvox carteri* SDR was expanded about five-fold relative to that in *Chlamydomonas* (Ferris et al., 2010), and this was likely to have occurred after the transition from isogamy to anisogamy/oogamy (Hamaji et al., 2018). The timing of the SDR expansion in the genus *Volvox* and its significance with respect to the evolution of sexual dimorphism remains unresolved.

During the evolution of the volvocine lineage, transitions from heterothallism to homothallism might have occurred in many times (Hanschen et al., 2018). However, it remains unknown how sex-specific genes and SDR of ancestral heterothallic species evolved during the transition except for a previous study that reported the presence of an ortholog of minus dominance gene (*MID*) in the homothallic, isogamous volvocine species *Gonium multicoccum* (Hamaji et al., 2008).

In volvocine linage, oogamous *Volvox* is a genus of spheroidal, multicellular green algae with a surface layer of thousands of biflagellated somatic cells, and a much smaller number of non-flagellated germ cells that develop into asexual progeny. During sexual reproduction, heterothallic, dioecious species produce male spheroids (containing sperm packets) or female spheroids (containing eggs) are formed in the male or female strain, respectively, some homothallic species formed monoecious spheroids, containing sperm and egg from the same strain (Figs. 1.2, 1.3). This genus exhibits various types of sexuality and/or sexual spheroids that have been used to define separate taxa within *Volvox* (Smith, 1944; Isaka et al., 2012; Nozaki et al., 2015).

In many species of genus *Volvox,* heterothallic *Volvox carteri* is mainly studied. *V. carteri* has long (ca.1 Mbp), highly-differentiated SDR, which expanded about five-fold relative to that in *Chlamydomonas* (Ferris et al., 2010). Artificial knock-down of *VcMID* in *Volvox carteri* male strain resulted in “pseudo monoecious spheroid”, with many eggs and several sperm packets in

same sexual spheroid (Geng et al., 2014). These experiments suggested that sex determination in *Volvox* gametogenesis needed only *MID* gene, and also MID expression regulated in monoecious spheroids. However, in wild strain of homothallic *Volvox*, existence of *MID* is still unknown, and there is no data for seeking ancestral SDR's trace. In this thesis, I performed comparative molecular analyses and genomics of two related *Volvox* species, heterothallic *V. reticuliferus* and homothallic *V. africanus*, in order to resolve molecular genetic bases for evolution of homothallism.

FIGURES

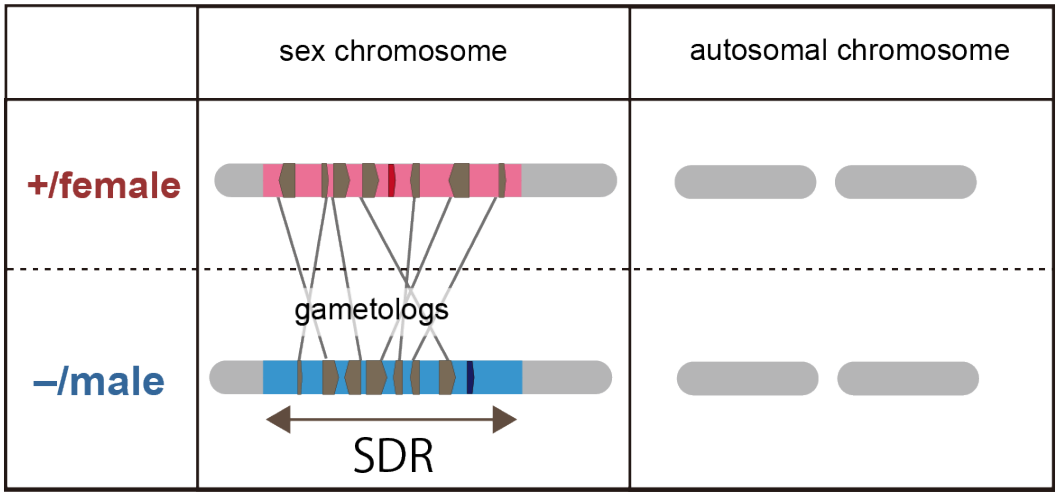

Figure 1.1. Sex-determining region (SDR) in haploid heterothallic species. Haploid individuals have single chromosome set, a sex chromosome (U or V) and autosomal chromosomes. SDR (sex determining region) is highly rearranged, non-recombining sequence in a sex chromosome. SDR contains two types of genes; “gametologs (gray markers)” exist as pairs of ortholog that are derived from a single ancestral gene; “sex specific genes (red or blue markers)” exist only on one side of sex.

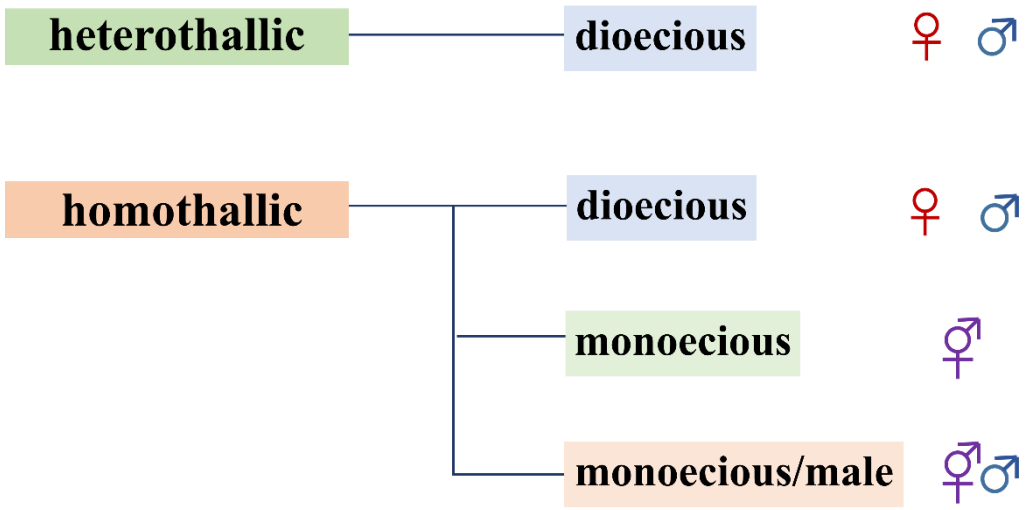

Figure 1.2. Four sexual types *Volvox africanus*-like algae recognized by Starr (1971).

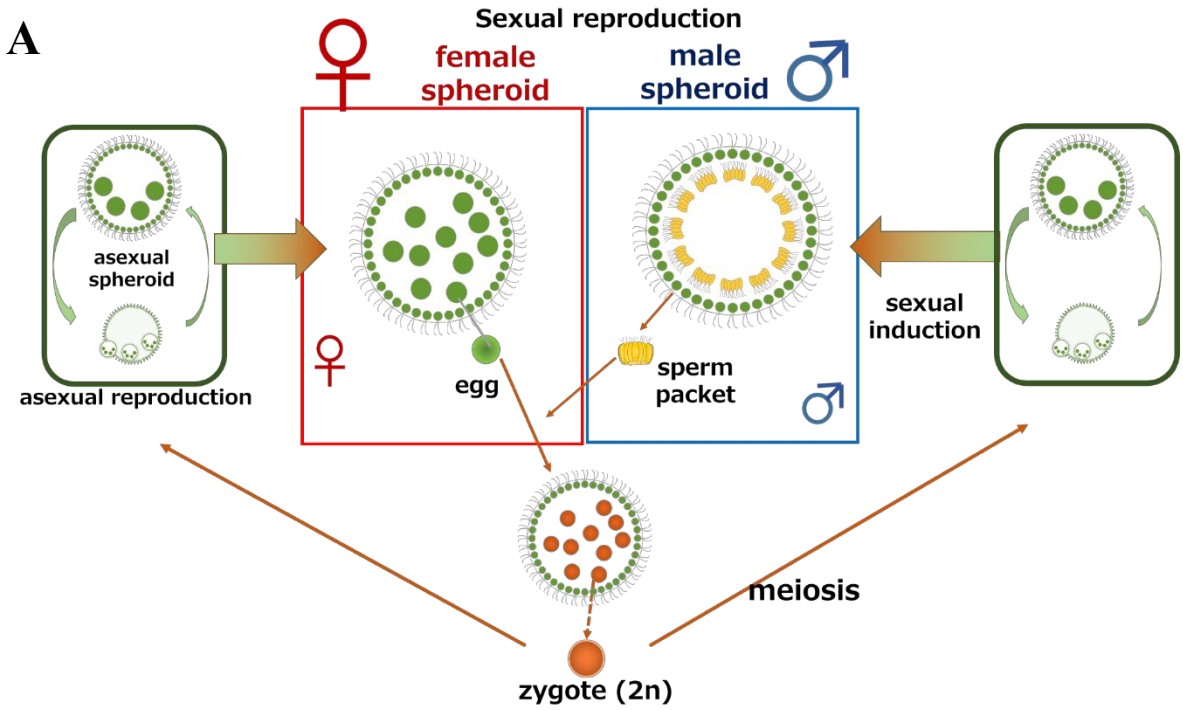

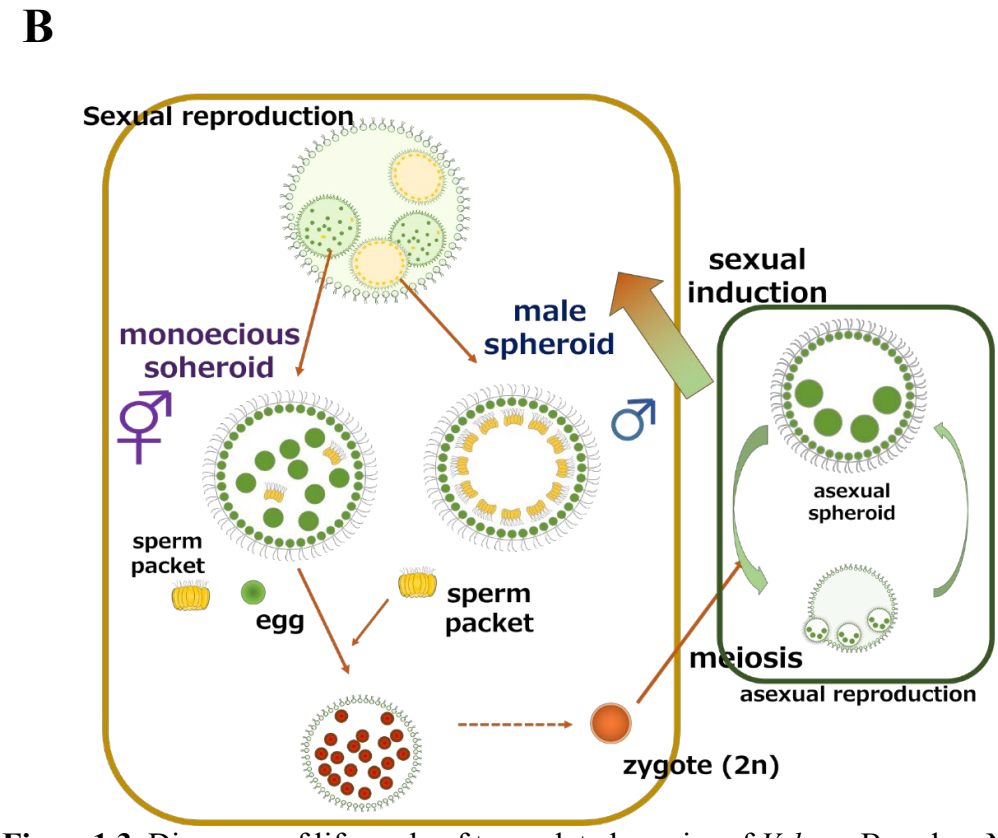

Figure1.3. Diagrams of life cycle of two related species of *Volvox*. Based on Nozaki et al. (2015). A. *V. reticuliferus* (heterothallic, dioecious type), B. *V. africanus* (homothallic, monoecious with male type)

Chapter 2.

Identification and expression analyses of minus-dominance orthologs in three *Volvox* species

INTRODUCTION

Starr (1971) recognized four types of sexuality in several strains identified as *Volvox africanus* originating from locations around the world (Fig. 1.2) heterothallic, dioecious type: male spheroids (containing sperm packets) or female spheroids (containing eggs) are formed in the male or female strain, respectively; 2) homothallic, dioecious type: separate male and female spheroids are formed in the same strain; 3) homothallic, monoecious type: monoecious spheroids (containing both eggs and sperm packets) are formed; and 4) homothallic, monoecious with males type: monoecious spheroids and male spheroids are both formed in the same strain. Coleman (1999) resolved a small clade composed of these four sexual types of *V. africanus* based on the internal transcribed spacer-2 (ITS-2) of nuclear ribosomal DNA (rDNA) sequences. Thus, these related strains may be very useful for studying the diversity and evolution of monoecy and/or homothallism in *Volvox*. However, further studies of sexuality in these strains have been lacking except for the heterothallic, dioecious type (Hiraide et al., 2013), since strains exhibiting the three types of homothallic sexuality are not available (Nozaki et al., 2015). Recently, new Japanese strains of two *V. africanus*-like species were isolated from water samples collected in Lake Biwa, Japan (Isaka et al., 2012). One that corresponds to sexual type 1 (heterothallic, dioecious type) by Starr 1971 was renamed as a new species, *V. reticuliferus* (Fig. 1.3A, 2.1D and 2.1E). The other was re-identified as *V. africanus and* produces both monoecious and male spheroids in a single strain [sexual type 4 of Starr (1971); Figs. 1.3B and 2.1D, E, F].

In the heterothallic isogamous species *Chlamydomonas reinhardtii*, two sexes or mating types are determined by the presence or absence of the mating type-specific minus dominance gene (*MID*) (Ferris and Goodenough, 1997). In anisogamous volvocine *Pleodorina starrii* and oogamous *Volvox carteri*, a *MID* ortholog is present only in male strains (Nozaki et al., 2006; Ferris et al., 2010). Although *MID* is the master gene determining mating type minus of *C. reinhardtii* (Ferris and Goodenough, 1997), the *MID* ortholog in *V. carteri* (*VcMID*) was recently

reported to act as regulating formation of sperm packets, but not formation of male-specific sexual spheroids (Nozaki et al., 2006; Ferris et al., 2010; Geng et al., 2014). The *MID* ortholog is present in only one of the two heterothallic mating types in the isogamous volvocine *Gonium*, but it is present in a homothallic strain of *Gonium multicoccum* (Hamaji et al., 2008).

In the male strain of heterothallic *V. carteri*, experimental knock-down of *VcMID* results in sexual spheroids with eggs and sperm packets (similar to monoecious spheroids in wild monoecious species) or female-like sexual spheroids (with eggs and no sperm packets), depending upon the degree of suppression of *VcMID* expression (Geng et al., 2014). This implies *MID* gene expression may be important for formation of monoecious spheroids in homothallic wild species of *Volvox*. However, *MID* orthologs in wild homothallic *Volvox* species with monoecious spheroids, like sexual type 3 or 4 of Starr 1971, have not been previously reported.

To understand the evolution and development of monoecious spheroids in wild *Volvox* species, comparative analysis of their *MID* genes with those of closely related heterothallic dioecious species should be fruitful. In this chapter, I examined *MID* homologs from two closely related species of *Volvox* sect. *Merrillosphaera*: *V. africanus* and *V. reticuliferus*, identified by Nozaki et al., 2015. Since these two species are heterothallic, dioecious type and homothallic, monoecious with males type (sexual types 1 and 4 by Starr1971, respectively), comparative analyses of *MID* orthologs from these two species will lead to a greater understanding of the evolution of monoecy or homothallism in *Volvox*. In addition, in order to elucidate general *MID* characteristics of monoecious spheroids, the *MID* homolog from *V. ferrisii* which produces only monoecious sexual spheroids (Isaka et al., 2012) was also studied. *V. ferrisii* is belongs to *Volvox* sect. *Volvox* that is phylogenetically separated from *Volvox* sect. *Merrillosphaera* (Nozaki et al., 2015).

MATERIALS AND METHODS

Strains and culture conditions

Volvox africanus and *V. reticuliferus*

Volvox africanus strain NIES-3780 (Table2.1) and six strains of *V. reticuliferus* (Table 2.4) were obtained from previous study (Nozaki et al., 2015; unpublished data). The cultures were maintained in screw-cap tubes (18 × 150 mm) containing 10 ml AF-6/3 medium (Nozaki et al., 2015) at 20°C on a 14-h light: 10-h dark schedule or at 25°C on a 12-h light:12-h dark schedule under cool-white fluorescent lamps at an intensity of 55–80 μmol·m^{-2}·s^{-1}.

To induce sexual reproduction, about 0.5 ml of growing cultures were transferred into 10 ml of USVT medium (Nozaki et al., 2015) diluted one to two with distilled water and grown at 25°C on a 12-h light:12-h dark schedule under cool-white fluorescent lamps at an intensity of 160–180 μmol·m^{-2}·s^{-1}. Sexual spheroids developed after 4~5 days (*V. africanus*) or 7~10 days (*V. reticuliferus*).

Volvox ferrisii

Volvox ferrisii strain NIES-3986 (Table2.1) was cultured in screw-cap tubes containing 10 ml AF-6 medium (KATO, 1982; Kasai et al., 2009) at 20°C on a 14-h light: 10-h dark schedule under cool-white fluorescent lamps at an intensity of 55–80 μmol·m^{-2}·s^{-1}.

To induce sexual reproduction, about 0.5 ml of growing cultures were transferred into 10 ml of VTAC medium(Nozaki, 1983; Kasai et al., 2009) and grown at 25°C on a 12-h light:12-h dark schedule under cool-white fluorescent lamps at an intensity of 160–180 μmol·m^{-2}·s^{-1} . After 7~10 days sexual spheroids developed abundantly.

Identification of *MID* orthologs

V. africanus

Total RNA was isolated from cultures in which sexual reproduction was induced as described

above, using RNeasy Mini kit (Qiagen, Hilden, Germany) after the cells had been homogenized with ceramic beads and a wash brush (Nozaki et al., 1997, 2006). Amplification of cDNA was carried out by Superscript 3 reverse transcriptase (Thermo Fisher Scientific, MA, USA) and 3'-RACE CDS Primer A in SMARTer™ RACE cDNA Amplification Kit (Clontech Laboratories, Inc., CA, USA). Nested PCR using this cDNA as templates with the degenerate primers with *MID*-gene (Table 2.2) yielded the partial fragment of *VaMID*. The primers used in in the first PCR were dMT-dF3 (Hamaji et al., 2008) (Table 2.2) and Nested Universal Primer A (Clontech Laboratories); the primers used in the second PCR were dMT-dF3 and SMID-R6. The PCR reactions were carried out using rTaq polymerase (TAKARA, Shiga, Japan) using the cycling conditions described previously (Nozaki et al., 1995). The resulting fragments were TA subcloned using TOPO TA Cloning kit (Thermo Fisher Scientific) and sequenced using an ABI PRISM 3100 Genetic Analyzer (Thermo Fisher Scientific) with a BigDye Terminator Cycle Sequencing Ready Reaction Kit v. 3.1 (Thermo Fisher Scientific), as described previously (Nozaki et al., 2006).

To determine the 3' terminus sequence of *VaMID*, 3'RACE was performed with Nested Universal Primer A and gene specific primers, VaMID_F1, VaMID_F2 and VaMID_F3 (Table 2.3). The resulting fragments were TA subcloned using TOPO TA Cloning kit and sequenced as described above.

The 5' terminus sequence was determined using the GeneRacer kit (Thermo Fisher Scientific) according to the manufacturer's protocol; the antisense gene specific primer was VaMID_5'R1 (Table 2.3). Nested PCR were performed with GeneRacer5' Primer and gene specific primers, VaMID5'R1, VaMID5'R2 and VaMID5'R3 (Table 2.3). The resulting fragments were TA subcloned and sequenced as described above.

To determine the intron-exon structure of *VaMID,* genomic PCR using total DNA extracted as described previously [18] was performed, followed by DNA sequencing of the product. The PCR reaction used KOD FX Neo DNA polymerase (TOYOBO, Osaka, Japan) and *VaMID*-

specific primers (VaMID_AR and VaMID_ValR2; Table 2.3) with cycling conditions 2 min at 94℃, followed by 35 cycles of 10 sec at 98℃ and 30 sec at 68℃.

V. reticuliferus

Polyadenylated mRNAs were isolated from cultures that were sexually induced, using dynabeads oligo $(dT)_{25}$ (Thermo Fisher Scientific), and reverse transcribed with Superscript 3 reverse transcriptase (Invitrogen).

5' and 3'RACE were performed with GeneRacer kit and *V. reticuliferus MID* (*VrMID*) specific primers based on the partial *MID* sequences of "*V. africanus* UTEX 1890" (Hiraide et al., 2013). 5' nested PCR was performed with Gene Racer 5' Primer and gene specific primers, F1-7MID_R1 and F1-7MIDR2 (Table 2.3). 3' PCR were performed with Gene Racer 3' Primer and a gene specific primer, F1-7MID_3'F1 (Table 2.3).

The intron-exon structure of *VrMID* was determined using genomic PCR as described above for *VaMID* but using *VrMID*-specific primers (F1-7MID_AF and F1-7MID_AR; Table 2.3).

V. ferrisii

A partial sequence of *V. ferrisii MID* (*VfMID*) mRNA was obtained by PCR amplification and sequencing as described for *VaMID* except for the primers used for the nested PCR and determination of 3' and 5' termini (Table 2.2). Degenerate primers SMID-F1 and SMID-R5 were used for the first PCR, and SMID-F1 and SMID-R4 for the second PCR (Table 2.3). To determine the 3'-terminus sequence of *VfMID*, 3'-RACE was performed with Nested Universal Primer A and *VfMID*-specific primers VfMID_F1, VfMID_F2, VfMID_F3, VfMID_F4, VfMID_F5 and VfMID_F6 (Table 2.3). Specific primers VfMID_R1 and VfMID5'R (Table 2.3) were used for amplifying the 5'-terminus sequence.

The intron-exon structure of *VfMID* was determined using genomic PCR as described above

for *VaMID* but using *VfMID*-specific primers (VfMID_Af and VfMID_AR; Table 2.3).

Phylogenetic analysis of *MID* orthologs

Phylogenetic analyses were performed using MUSCLE (Edgar, 2004) -aligned entire protein sequences of sixteen MID homologs of the Volvocales (Table 2.1). Maximum likelihood (ML) method, based on LG model (Le and Gascuel, 2008) and neighbor joining method, using JTT model (Jones et al., 1992) by MEGA 6.0 (Tamura et al., 2013) were carried out with bootstrap values from 1000 replications.

A molecular evolutionary analysis of non-synonymous and synonymous substitutions was performed between *MID* homologs of *G. pectorale* and those of other six Volvocales by MEGA 6.0, using modified Nei-Gojobori model (Nei and Gojobori, 1986; Nei and Kumar, 2000) (assumed transition/transversion bias = 1.55).

Detection of *VrMID* based on genomic PCR of *V. reticuliferus*

Genomic PCR was performed in six strains of *V. reticuliferus* (Table 2.4) using total DNA extracted as described previously (Miller et al., 1993), KOD FX Neo DNA polymerase and a pair of *VrMID* specific primers (F1-7MID_AF and F1-7MID_AR; Table2.2). The ITS2 sequence was amplified as a control, using an ITS2-specific primer pair designed based on the ITS2 sequence of NIES-3782 (Table 2.4). PCR cycles were 2 min at 94℃, followed by 30 (ITS2) and 35 (*VrMID*) cycles of 10 sec at 98℃ and 30 sec at 68℃.

Southern blot analysis

Genomic DNA of *V. africanu*s (NIES-3780)*, V. reticuliferus* (male strain: NIES-3786, female strain: NIES-3785) (Table 2.1) was prepared as described previously (Miller et al., 1993). Restriction enzyme digests of genomic DNA (2 μg) were separated by 1.0% agarose gel

electrophoresis and transferred onto a Hybond-N+ nylon membrane (GE Healthcare, UK). A hybridization probe containing part of the *VrMID* gene (Fig. 2.2) labeled with digoxigenin-11-dUTP was prepared by PCR using a plasmid clone of the *VrMID* gene as template and the primer pair F1-7_southMID_F and F1-7_MID_R1 (Table2.3) using PCR DIG Probe Synthesis Kit (Roche Diagnostics, Germany), and hybridized at 42°C. A hybridization probe containing part of the *V. reticuliferus* elongation factor 1-like gene (*EF1-like*) labeled with digoxigenin-11-dUTP was prepared by PCR using a plasmid clone of the *EF1-like* gene as template and the primer pair (CV_EF1A1-R2 and GpEF1A-INT3-R(Hamaji et al., 2008); Table2.3) using KOD FX Neo DNA Polymerase, and hybridized at 42°C. The signals were detected using DIG-High Prime DNA Labeling and Detection Starter Kit II (Roche Diagnostics) and ChemiDoc XRS (Bio-Rad, Hercules, CA, USA). The resulting image was processed with a median filter (diameter: 1 pixel) in ImageJ (National Institutes of Health, Bethesda, MD, USA) to remove random noise produced by long exposure (2 hr.).

Estimation of genome sizes of *Volvox africanus* and *V. reticuliferus*

To estimate relative genome size of *V. africanus* and *V. reticuliferus*, 4',6-diamidine-2-phenylindole (DAPI)-staining was performed using somatic cells of *V. africanus*, male and female strains of *V. reticuliferus* (NIES-3782 and NIES-3783, respectively), and *V. carteri* strain EVE (control). One ml of each vegetative sample was fixed with 0.25% glutaraldehyde, followed by postfixation in 100% methanol for reducing autofluorescence, and washed with phosphate-buffered saline. Fixed samples were stained with 0.1 μg/μl DAPI overnight. DAPI-stained somatic cells of *V. africanus* and *V. reticuliferus* male and female were mixed separately with DAPI-stained *V. carteri* strain EVE and mounted in the same slide. The images were obtained using a BX-60 Microscope and DP Controller 1. 2. 1108 (Olympus, Tokyo, Japan). The image analyses were performed using ImageJ, measuring the mean gray value of 10 nuclei for each exposure time (0.50,

0.67, 1.0, 1.5, 2.0 and 2.5 s).

Semi-quantitative RT-PCR analyses

To use elongation factor-1 like (*EF-1 like*) genes as an internal control, PCR amplifications were performed using full-length cDNA, with primer sets, CV_EF1A1-R2 and GpEF1A-INT3-R (Hamaji et al., 2008). From direct sequence of PCR-products, gene specific primer pairs (Table 2.3) for semi-quantitative RT-PCR analyses were designed.

Thirty asexual, male or monoecious spheroids were collected by a micropipette from cultures that were sexually induced or not. Polyadenylated mRNAs were isolated from these 30 spheroids of identical type and reverse transcribed as described in *V. reticuliferus MID* determination.

PCR analyses were performed using KOD FX Neo DNA polymerase. PCR cycles and primer pairs are described in Table 2.3. The amplified products were electrophoresed on 2% (wt/vol) agarose gels and stained with ethidium bromide. The gel images were captured using a ChemiDoc XRS system with Quantity One software (Bio-Rad), level adjusted and gradation inverted with Adobe Photoshop CS6 (Adobe Systems Inc., San Jose, CA).

RESULTS

Identification and characterization of *MID* orthologs

I identified full-length cDNA sequences and exon-intron structures of *VaMID, VrMID* and *VfMID* (Figs. 2.2, 2.3). The genomic sequences of the three genes determined in this study covered the entire DNA sequences and demonstrated that all of the three genes contained four introns. Deduced protein sequences of the three genes were composed of 163-167 amino acids that contained DNA binding RWP-RK domain in C-terminus. RWP-RK domains of seven volvocine MID proteins

were highly conserved even among homothallic and heterothallic volvocine species (Fig. 2.4).

Three alternative splicing variants of *VaMID* were also identified. All these variants were identified as the intron retention (Kianianmomeni et al., 2014) (Fig. 2.5). No alternative splicing variants were identified in *VrMID* and *VfMID*.

Based on the phylogenetic analysis of 14 colonial volvocine MID proteins, a large clade composed of seven genes of the Volvocaceae was resolved with 83-85 % bootstrap values in ML and NJ methods (Fig. 2.6). However, phylogenetic relationships of *Gonium* MID proteins were not well resolved. Within the volvocacean clade, MID proteins from *V. carteri*, *V. reticuliferus*, *V. africanus, Pleodorina starrii* and *Eudorina* sp. formed a robust monophyletic group (with 98-99 % bootstrap values in both analyses) from which *Yamagishiella unicocca* and *V. ferrisii* MID proteins were separated. These results were consistent with the phylogenetic relationships of the colonial volvocine algae based on chloroplast genes (e. g. Nozaki et al., 2014).

A molecular evolutionary analysis of the volvocacean *MID* genes demonstrated that non-synonymous and synonymous substitutions of the genes from two homothallic species of *Volvox* (*V. africanus* and *V. ferrisii*) fell within the range of those of heterothallic species (Fig. 2.6).

Genomic PCR and Southern blot analysis of *MID* genes of *Volvox africanus* and *V. reticuliferus*

Results of genomic PCR using *VrMID*-specific primers (Table 2.3) for strains of *V. reticuliferus* (Table 2.4) are shown in Fig. 2.7. All three male strains of *V. reticuliferus* demonstrated the presence of *VrMID* based on a single band whereas all three female *V. reticuliferus* strains lacked the gene. Four of the *V. reticuliferus* strains are F1 progeny in which the *MID* gene band is found only in phenotypically male strains. This is consistent with the expectation that a *MID* gene containing MT locus is the genetic determiner of sex, although more progenies are needed to be definitive. In the homothallic species *V. africanus*, a single band of *VaMID* was detected (not

shown).

Southern blot analysis of *V. reticuliferus* demonstrated the presence of a single copy of the *VrMID* gene in the male genome and the complete absence of the gene in the female (Fig 2.8A). The genome of the homothallic species *V. africanus* was shown to encode two possible copies of *VaMID* based on the blot analysis (Fig. 2.8A). However, only a single copy of *EF-1 like* gene was detected in each strain of *V. africanus* and *V. reticuliferus* (Fig. 2.8B).

Estimation of genome sizes of *Volvox africanus* and *V. reticuliferus* based on epifluorescence microscopy of DAPI-stained somatic cells

Since *V. africanus* or *V. reticuliferus* might have originated from their common ancestor by duplication of the whole genome, relative genome sizes of these two species were measured based on the degree of fluorescence of DAPI-stained nuclei in somatic cells using epifluorescence microscopy. By using the fluorescence value of nuclei of *V. carteri* EVE somatic cells as a control, both *V. africanus* and *V. reticuliferus* genome sizes could be 0.9-1.1 times the genome size of *V. carteri* EVE (Fig. 2.9).

Semi-quantitative RT-PCR analyses of expression of *MID* genes

Results of semi-quantitative RT-PCR analyses of expression of *MID* genes in *V. africanus* homothallic strain, *V. reticuliferus* male strain and *V. ferrisii* homothallic strain are shown in Figure 2.10. In sexually induced *V. africanus* culture, *VaMID* expression was extremely high whereas the expression was low in monoecious and asexual spheroids (Fig. 2.10A, D). The *VaMID* expression of asexual spheroids in sexually uninduced culture was slightly higher than that of sexually induced culture (Fig. 2.10A). In heterothallic *V. reticuliferus*, *VrMID* level was highly upregulated in male spheroids when compared that of asexual spheroids in the same culture (Fig. 2.10B, E). In contrast to *V. africanus*, *VrMID* expression of asexual spheroids in sexually induced culture was

slightly higher than that in sexually uninduced culture (Fig. 2.10E).

In contrast to *V. africanus*, *VfMID* level in monoecious spheroids of *V. ferrisii* was higher than that of asexual spheroids in sexually induced and sexually uninduced cultures. *VfMID* transcription level in monoecious spheroids was more than 2.5 times higher than that of asexual spheroids in both cultures.

DISCUSSION

MID orthologs in homothallic species of *Volvox* with monoecious spheroids

The present study demonstrated that two homothallic species of *Volvox* with monoecious spheroids, *V. africanus* and *V. ferrisii*, have *MID* orthologs (Figs. 2.5, 2.6). *MID* orthologs (*VaMID* and *VfMID*) of these two homothallic species are essentially consistent with those of other heterothallic colonial volvocacean species (Nozaki et al. 2006; Ferris et al., 2010) in containing 5 exons, 4 introns, and DNA binding RWP-RK domain in C-terminus. Phylogenetic relationships of *MID* orthologs within the Volvocaceae (Fig. 2.5) were consistent with those of the species phylogeny based on chloroplast genes (Isaka et al., 2012; Nozaki et al., 2015). Moreover, comparison of synonymous and nonsynonymous substitutions of *MID* genes between homothallic and heterothallic volvocacean species suggested that the *MID* gene of the two homothallic species have evolved under the same degree of functional constraint as those of the heterothallic species. Nozaki et al. (2006) reported that MID protein expression is strong in nuclei of the male gametes of male strain of *Pleodorina starrii*. Geng et al. (2014) demonstrated that the *MID* ortholog (*VcMID*) of the heterothallic species *Volvox carteri* controls the sperm packet formation of sexual reproductive cells (androgonidia). The present study showed that expression of *VaMID* in homothallic *V. africanus* is very high in male spheroids (Fig. 2.10). Therefore, the *MID* orthologs of the two homothallic species of *Volvox* may control sperm packet formation as in the heterothallic species. Thus, the evolution of *Volvox* species with monoecious spheroids cannot be explained by evolution

of *MID* sequences.

VaMID **transcription in monoecious and male spheroids**

The number of sperm packets in monoecious spheroid is very small, 1–4 in *V. africanus* (Nozaki et al., 2015) or 3–5 in *V. ferrisii* (Isaka et al., 2012). In contrast, the male spheroid of *V. africanus* contains 100-260 androgonidia that divide to form sperm packets. The present semi-quantitative RT-PCR showed *MID* suppression in monoecious spheroid of *V. africanus* and high upregulation in male spheroid of *V. africanus*, suggesting that *VaMID* transcriptional level is correlated with the quantity of sperm packets in monoecious or male spheroids. It indicates that *V. africanus* has the spheroid-specific regulation of *VaMID*. In heterothallic *V. carteri*, VcMID protein is localized in the sperm nucleus and controls formation of sperm packets (Geng et al. 2014). As discussed above, *VaMID* may also control formation of sperm packets. Thus, *V. africanus* determines the fate of reproductive cells in monoecious spheroid by differently controlling *VaMID* expression between eggs and androgonidia. Further analyses of the localization of VaMID in the monoecious spheroid at cellular level is required to confirm this hypothesis.

FIGURES

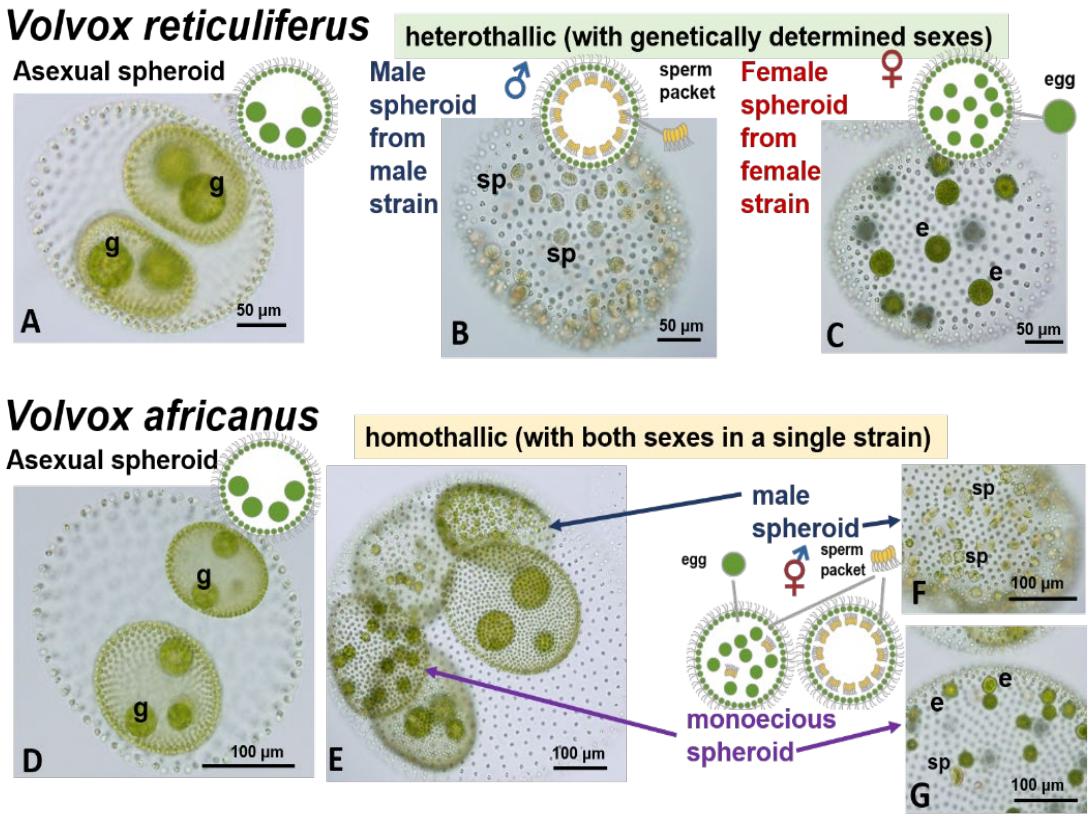

Figure 2.1. Light microscopic images of *Volvox reticuliferus* (heterothallic dioecious type) and *V. africanus* (homothallic, monoecious with male type).

V. reticuliferus (male strain: NIES-3786, female strain: NIES-3785): A. Asexual spheroid. B. Male spheroid. C. Female spheroid.

V. africanus (NIES-3780): D. Asexual spheroid. E. Parental spheroids containing one monoecious spheroid and two male spheroids. F. Male spheroid. G. Monoecious spheroid.

sp: sperm packet, e: egg, g: gonidium [an asexual reproductive cell].

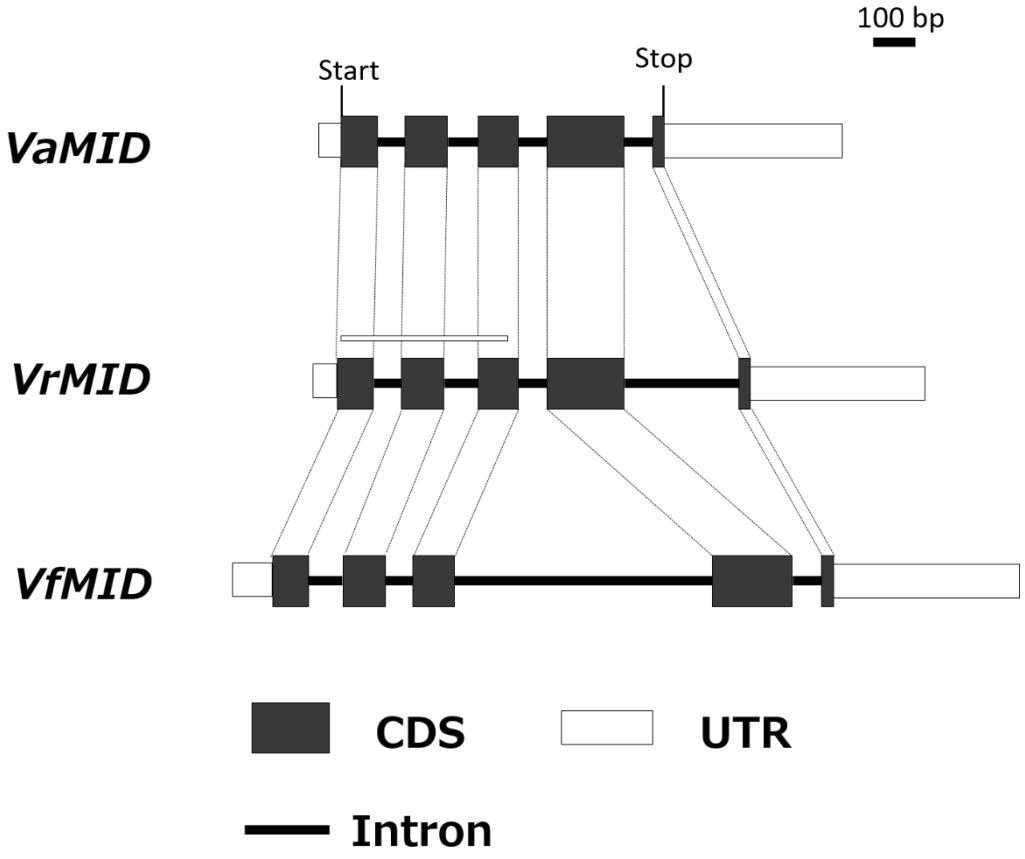

Figure 2.2. Exon-intron structures of *MID* orthologs, *VaMID* (*V. africanus*), *VrMID* (*V. reticuliferus*), and *VfMID* (*V. ferrisii*). White bar represents *VrMID* probe for Southern blotting (Fig. 10).

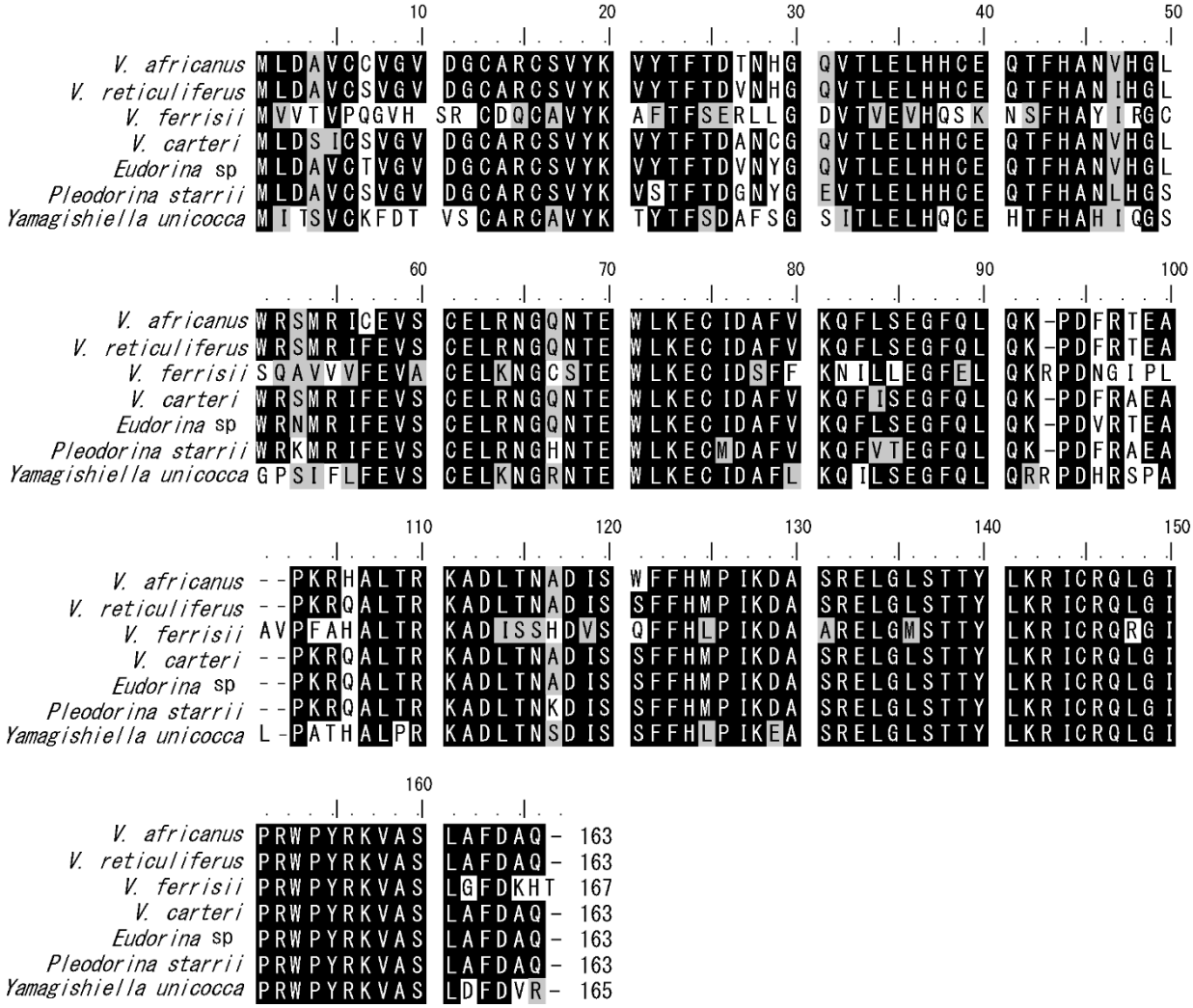

Figure 2.3. Alignment of seven MID homologs from *Volvox africanus, V, reticuliferus, V. carteri, V. ferrisii, Eudorina* sp.*, Pleodorina starrii,* and *Yamagishiella unicocca.*

Black back color indicates 100%, gray back color indicates over 70% of identity or similarity, respectively.

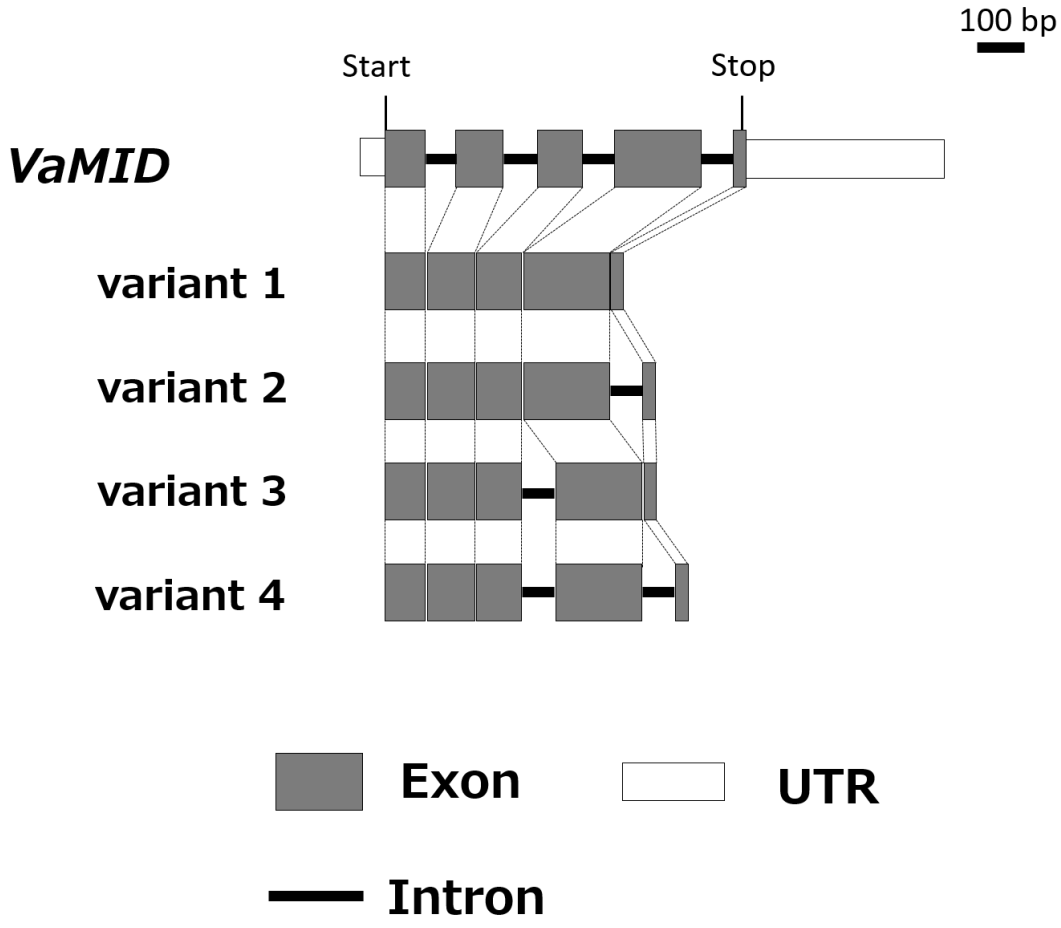

Figure 2.4. Alternative splicing variants of *Volvox africanus MID* orthologs (*VaMID*).

Variant 2-4 are intron retention.

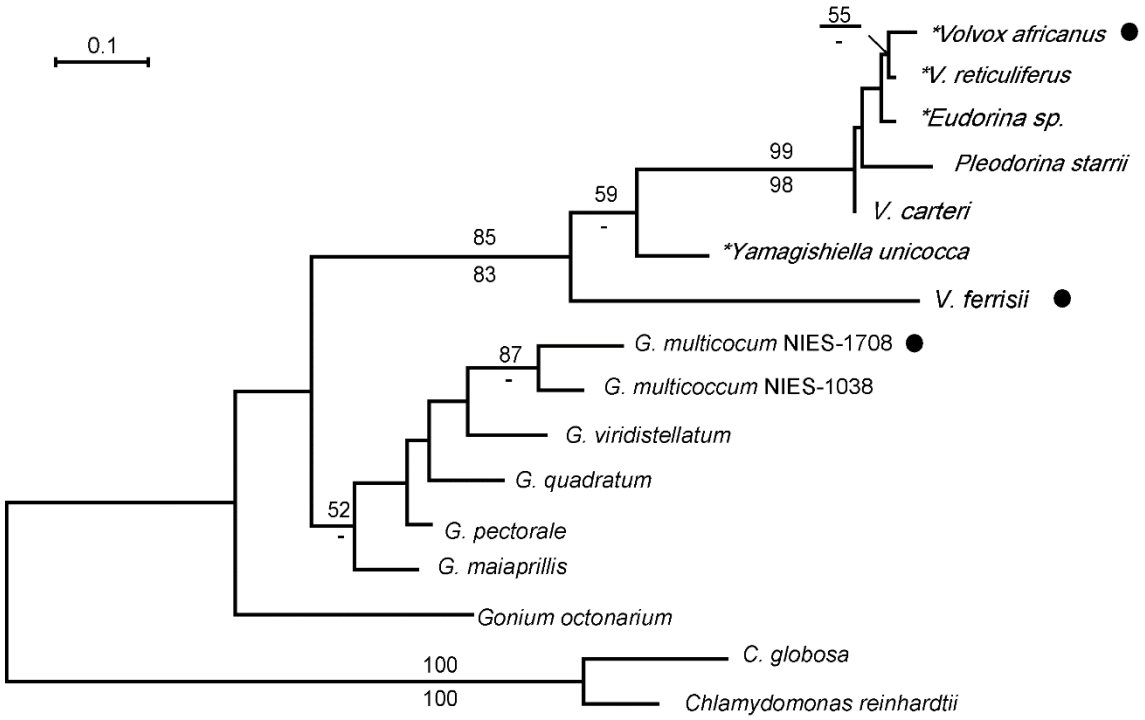

Figure 2.5. Maximum-likelihood (ML) tree (based on LG model) of the full-length sequence of 16 MID proteins from colonial volvocine species and two species of *Chlamydomonas*. Branch lengths are proportional to the estimated amino acid substitutions, which are indicated by the scale bar below the tree. Numbers above and below branch points indicate bootstrap values of the ML and neighbor-joining (based on the JTT model), analyses, respectively. MID homologs with asterisks (*) are determined in this study; a filled circle (●) indicates the homothallic strain.

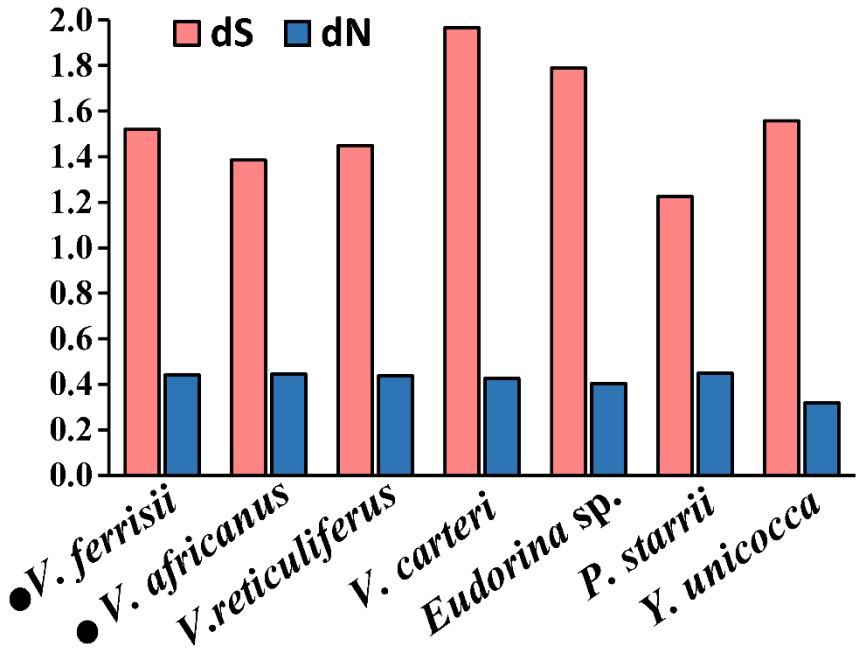

Figure 2.6. Non-synonymous/synonymous substitutions of *MID* genes in volvocine algae. Analyses were conducted with the outgroup *Gonium pectorale MID* gene (AB353340) using the modified Nei-Gojobori (assumed transition/transversion bias = 1.55) model (Nei and Gojobori, 1986; Nei and Kumar, 2000) by MEGA6 (Tamura et al., 2013). All positions containing gaps and missing data were eliminated. There was a total of 162 positions in the final dataset. Filled circles (●) indicate the homothallic strain.

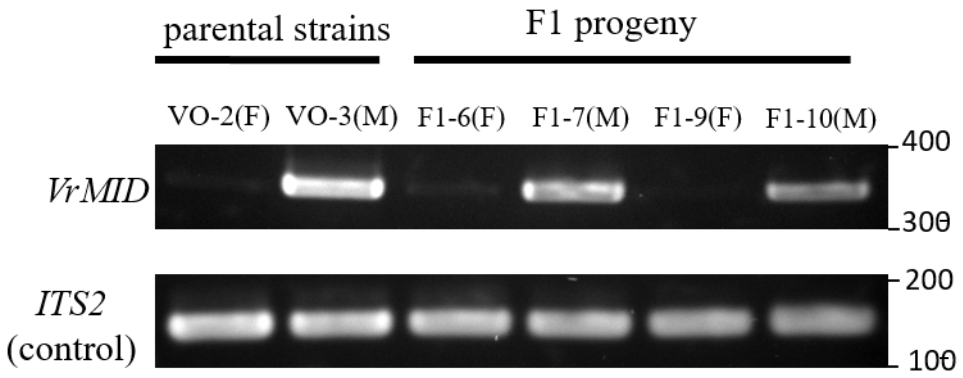

Figure 2.7. Results of genomic PCR for parental strains and four F1 progeny strains of *V. reticuliferus* (Table. 2.4). Parental strains are NIES-3782 (VO-2) and NIES-3783 (VO-3). F1 progeny strains are NIES-3785 (F1-6), NIES-3786 (F1-7), NIES-4110 (F1-9) and NIES-4111 (F1-10). (F): Female, (M): Male strain.

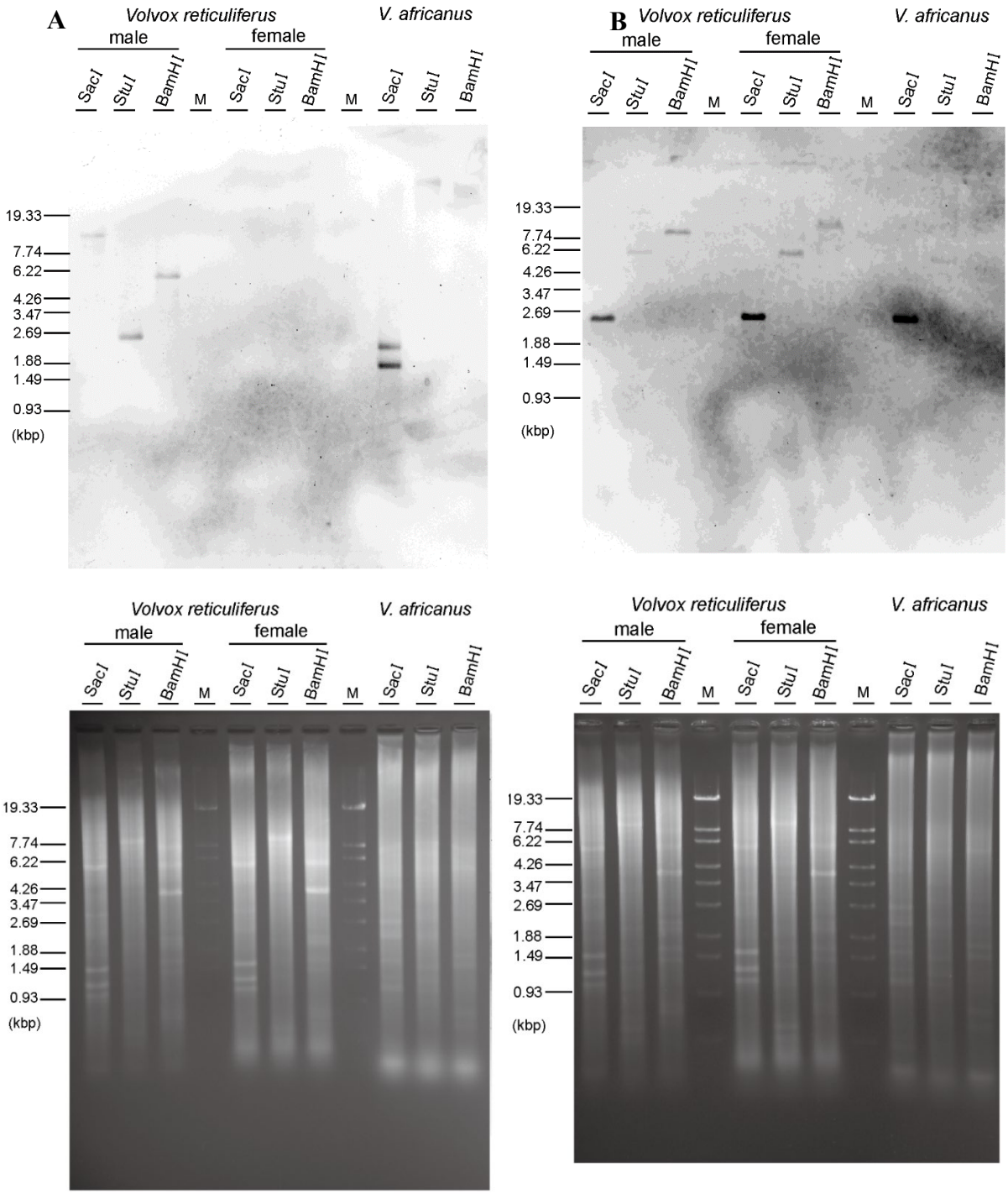

Figure 2.8. Southern blot analysis and gel bands of digested genomic DNA of *V. reticuliferus* and *V. africanus*. A. Southern blotting using Vr*MID* fragment, located in exon1-exon3, shown in Fig. 2.2. B. Southern blotting using *EF1-like* (control) fragment. M: One Step Marker 6 (Nippongene, Tokyo, Japan) for DNA Marker.

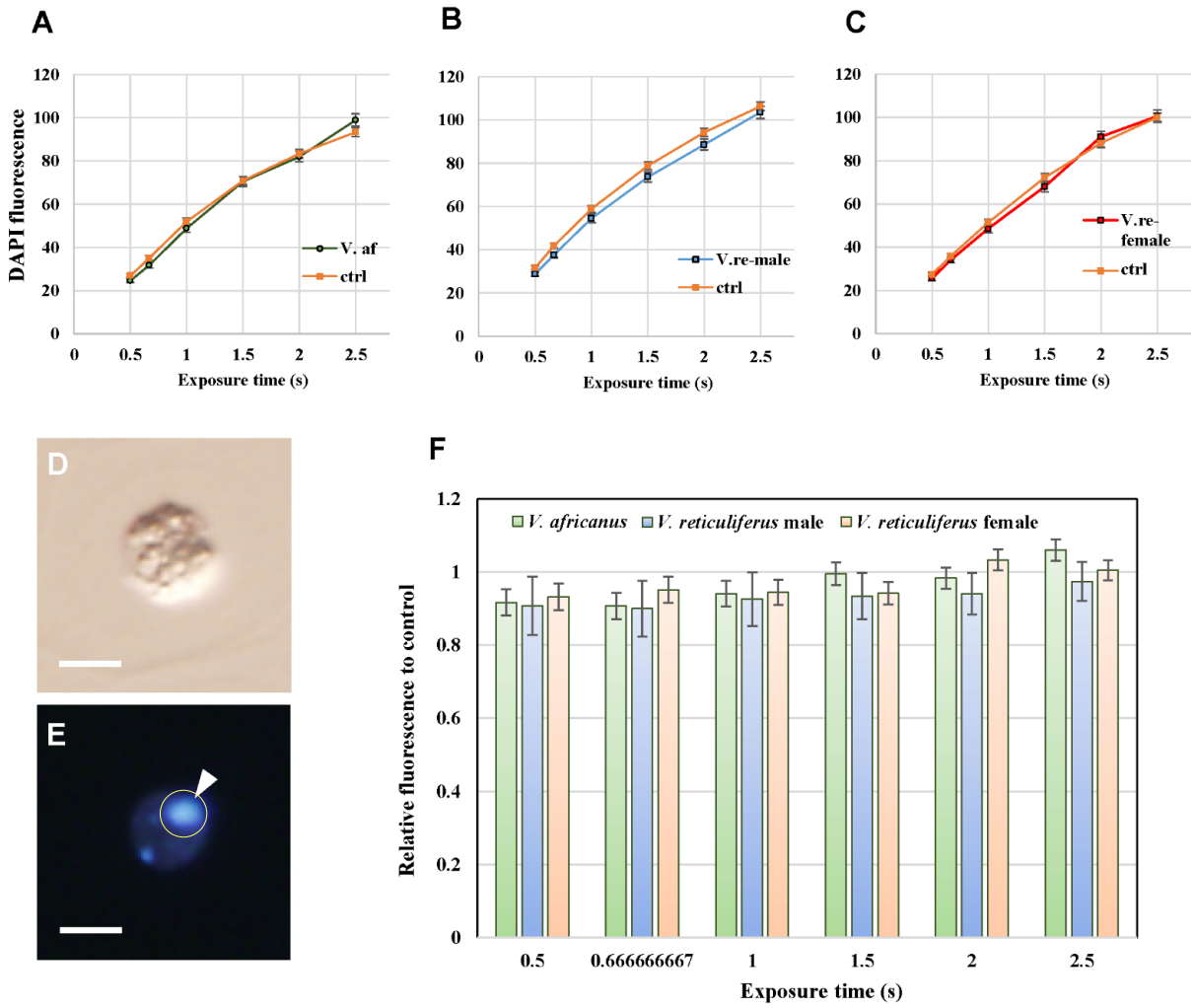

Figure 2.9. DAPI staining for estimating comparative genome size in *V. africanus* and *V. reticuliferus*.

A-C. Mean gray value of ten nuclei with imageJ at 0.5, 0.67, 1.0, 1.5, 2.0, 2.5 s exposure time. Bars show means and standard deviations. ctrl: *V. carteri* EVE strain in the same slide for control. A. *V. africanus*, B. *V reticuliferus* male strain, C. *V reticuliferus* female strain.

D, E. DAPI stained somatic cell of *V. africanus*. D. DIC image, E. DAPI staining image. Arrowhead shows location of a nucleus. Yellow ring shows the region of measurement in image J. Scale bar = 5 μm.

F. Relative fluorescence of stained nuclei of somatic cells in *V. africanus* and *V. reticuliferus* to *V. carteri* EVE strain (control) at each exposure time. Bars show means and standard deviations.

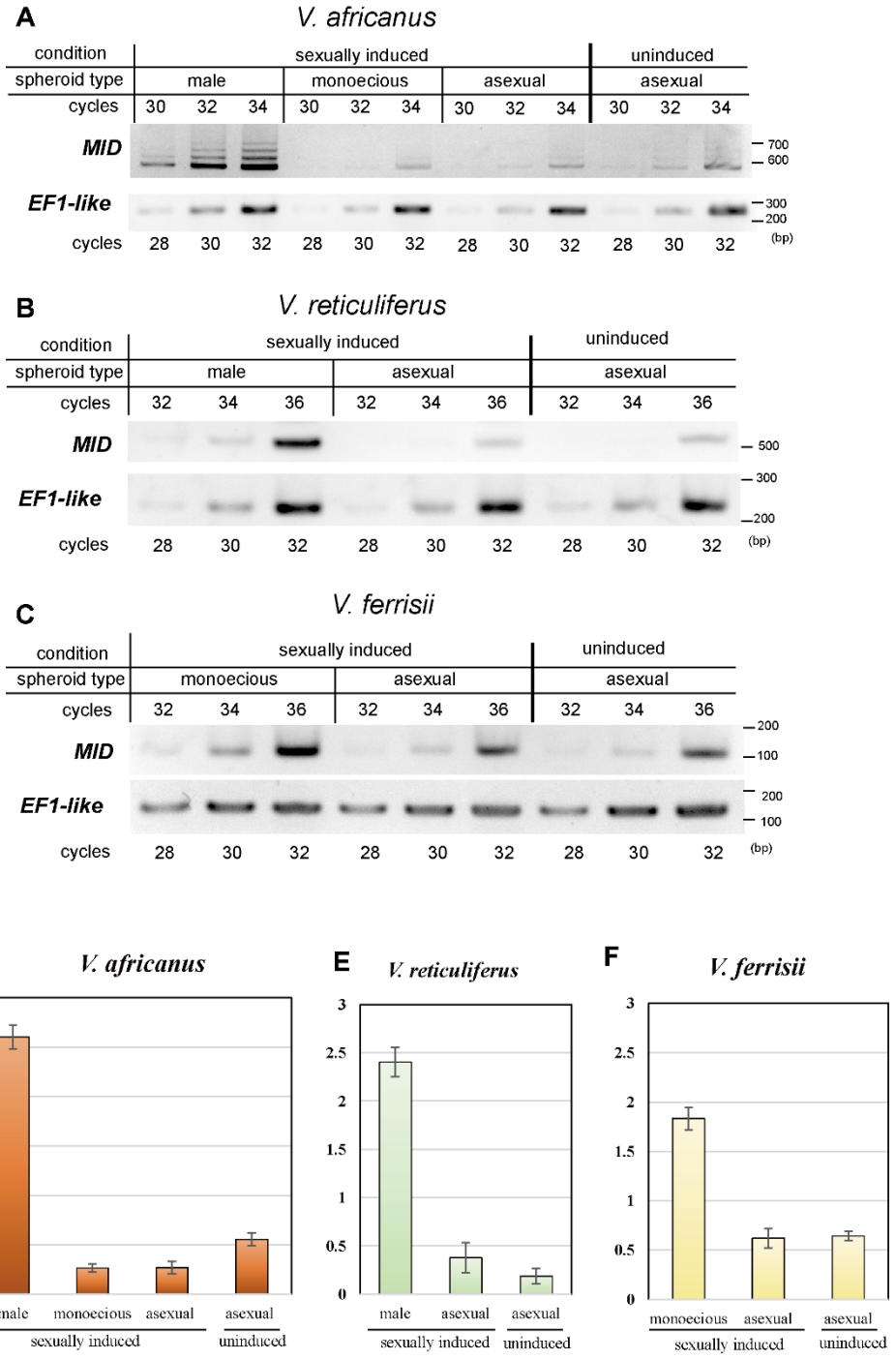

Figure 2.10. Semi-quantitative RT-PCR of *MID* orthologs in three species of *Volvox*.

A-C. Images of gelband. The loading volume for each lane was normalized to the quantity of *EF1-like* (internal control) product.

D-F. Gel band quantification analyses by ImageJ. Bars show means and standard deviations.

TABLES

Table 2.1. List of Volvocales included in the phylogenetic analyses of *MID* sequences and DDBJ/EMBL/GENBANK accession numbers.

Species	**Strain designation**	**Accession number**	**Reference**
V. africanus	NIES-3780 (2013-0703-VO4)	LC274875, LC274876	The present study
V. reticuliferus	NIES-3786 (VO123-F1-7)	LC274879, LC274880	The present study
V. ferrisii	NIES-3986 (2011-929-Vx2-F2-9)	LC274877, LC274878	The present study
V. carteri	UTEX 1886	GU784916.1	Ferris et al. 2010
Pleodorina starrii	NIES-1363	BAF42661	Nozaki et al. 2008
Yamagishiella unicocca	NIES-1859	LC274882	The present study
Eudorina sp. 2006-703-Eu-15	NIES-2735	LC274881	The present study
G. maiaprilis	NIES-2457	AB623044	Setohigashi et al. 2011
G. multicoccum (homothallic)	NIES-1708	AB774226	Hamaji et al. 2013
G. multicoccum (heterothallic)	NIES-1038	AB774225	Hamaji et al. 2013
G. octonarium	NIES-852	AB774227	Hamaji et al. 2013
G. pectorale	NIES-1710	AB353340	Hamaji et al. 2008
G. quadratum	NIES-652	AB774228	Hamaji et al. 2013
G. viridistellatum	NIES-654	AB774224	Hamaji et al. 2013
Chlamydomonas reinhardtii	CC-621	AAC49753	Ferris and Goodenough (1998)
C. globosa	CC-1870	AAB60944.1	Ferris et al. (2010)

Table 2.2. Degenerate primers used in this study.

Primer name	Primer sequence (5' to 3')	forward (F) or reverse (R) primer
SMID-F1	ACIGARTGGYTIAARGAITG	F
SMID-R4	GCITCYTTDATIGGIARRTG	R
SMID-R5	GGDATICCIARYTGICKRCA	R
SMID-R6	GCIACYTTICKRTAIGGCCA	R
dMT-dF3 [a]	RCIMRIAARGCIGAYYTIAC	F

[a] Hamaji et al. (2008)

Table 2.3. Gene specific primers used in this study.

Primer name	Primer sequence (5' to 3')	forward (F) or reverse (R) primer	Gene
VaMID_F1	ACGCGGATATTAGCTGGTTCTTCC	F	*VaMID*
VaMID_F2	TGCCAATTAAAGACGCCTCCAGAG	F	
VaMID_F3	TGGGGCTTTCAACGACATATCTGA	F	
VaMID5'R1	TGCCGGCAGATACGCTTCAGATATGT	R	
VaMID5'R2	CTCTGGAGGCGTCTTTAATTGGCATGTG	R	
VaMID5'R3	TGTCGTTGAAAGCCCCAATTCTCT	R	
VaMID_AR	ACCGCTCATACTTTGCCATTAGAA	F	
VaMID_ValR2	AATACAGTCGCTCCCAAGATGAAA	R	
VfMID_F1	TTGGAAGGATTCGAGCTACAGAAG	F	*VfMID*
VfMID_F2	CATACCTCTTGCAGTGCCGTTCG	F	
VfMID_F3	AAGGCCGACATCTCAAGTCACGAC	F	
VfMID_F4	GGTCGCTAGCCTGGGATTTGACAA	F	
VfMID_F5	GAAACCTTACCCTTCGGCCACTTT	F	
VfMID_F6	AGGCCTGGAAAGGTTGGTGTTCTG	F	
VfMID_R1	AAAACTGGCTGACGTCGTGACTTG	R	
VfMID5'R	TGCCATTGTCCGGTCGCTTCTGTAG	R	
VfMID_Rsp2	CCGCGTTGCCGGCATATTCGCTT	R	
F1-7MID_3'F1	GGACTTTGGCGTTCTATGCGGATT	F	*VrMID*
F1-7MID_3'F2	GACACGCAAAGCAGACCTAACGAA	F	
F1-7MID_R1	GTCCGCGTTCGTTAGGTCTGCT	R	
F1-7MID_R2	TTAGGTCTGCTTTGCGTGTCAA	R	
F1-7MID_AF	TGAAATAAGACATACGCCGGTTTCG	F	
F1-7MID_AR	TGCGAAAATTCACACCGGTATGCA	R	
F1-7_R3	TCGTTAGGTCTGCTTTGCGTGTCA	R	
F1-7MID_E1_F	CAGTTTGTTCTGTTGGCGTCGAC	F	
F1-7_s_MID_R	TCGTTAGGTCTGCTTTGCGTGTC	R	
F1-7_ITS2_F	TCCTTCTTCTTGCATGTGGATATGGC	F	*ITS2* of NIES-3782[a]
F1-7_ITS2_R	TTAACCGAACAACTTGTGCACCCA	R	

Table 2.3. Continued.

CV_EF1A1-R2[b]	CACGCTCGCCTGATCAACCTGCTG	F	*EF1-like*
GpEF1A-INT3-R[b]	GTCCAGACCCTTGATGTTCATGCC	R	
VaEF1_F2	TTGAACTTGTTCGTCACGGTGCCT	F	*EF1-like*
VaEF1_R2	TCGACAGTGAAGACCTTGCCAGTG	R	
F1-7EF1_F	TCAACTTGAAGGGCGAGAAGGTCA	F	
F1-7EF1_R	GTCATTTTCCTGCCCACTCACACC	R	
VfEF1_F2	AAGGAGCGCTACGATGAGATTGCC	F	
VfEF1_R2	TACCACGGCATGTTCTTGGACTCG	R	

[a] Nozaki et al., (2015). [b] Hamaji et al., (2008).

Table 2.4. Six strains of *Volvox reticuliferus* used for genomic PCR of *VrMID* (Fig. 2.7)

Strain designation	Origin	Sex	Origin
NIES-3782 (2013-0703-VO2)	Lake Biwa, Japan	female	Nozaki et al., (2015)
NIES-3783 (2013-0703-VO3)	Lake Biwa, Japan	male	Nozaki et al., (2015)
NIES-3785 (VO123-F1-6)	F_1 progeny strain of 2013-0703-VO1 x VO2 x VO3	female	Nozaki et al., (2015)
NIES-3786 (VO123-F1-7)	F_1 progeny strain of 2013-0703-VO1 x VO2 x VO3	male	Nozaki et al., (2015)
NIES-4110 (VO123-F1-9)	F_1 progeny strain of 2013-0703-VO1 x VO2 x VO3	female	Personal strain from Dr. H. Nozaki
NIES-4111 (VO123-F1-10)	F_1 progeny strain of 2013-0703-VO1 x VO2 x VO3	male	Personal strain from Dr. H. Nozaki

Table 2.5. Conditions for PCR cycles and primers used in semi-quantitative RT- PCR analyses (Fig. 2.10).

Species	**gene**	**PCR cycles**	**forward (F) or reverse (R) primer**	**Primer name (Table 2.2)**	**Sequence (5' to 3')**
V. africanus	*MID*	2 min at 94℃, followed by 32, 34 or 36 cycles of 98℃, 10 sec, 65℃, 30 sec, 68℃, 30 sec.	F	VaMID_AR	ACCGCTCATACTT TGCCATTAGAA
			R	VaMID_ValR2	AATACAGTCGCT CCCAAGATGAAA
	EF1-like	2 min at 94℃, followed by 28, 30 or 32 cycles of 98℃, 10 sec, 63℃, 30 sec. 68℃, 30 sec.	F	VaEF1_F2	TTGAACTTGTTC GTCACGGTGCCT
			R	VaEF1_R2	TCGACAGTGAAG ACCTTGCCAGTG
***V. reticuliferus* male strain**	*MID*	2 min at 94℃, followed by 32, 34 or 36 cycles of 98℃, 10 sec, 68℃, 30 sec.	F	F1-7MID_3'F1	GGACTTTGGCGT TCTATGCGGATT
			R	F1-7_R3	TCGTTAGGTCTG CTTTGCGTGTCA

Table 2.5. Continued.

***V. reticuliferus* male strain**	*EF1-like*	2 min at 94℃, followed by 28, 30 or 32 cycles of 98℃, 10 sec, 68℃, 30 sec.	F	F1-7EF1_F	TCAACTTGAAGGGCGAGAAGGTCA
			R	F1-7EF1_R	GTCATTTTCCTGCCCACTCACACC
V. ferrisii	*MID*	2 min at 94℃, followed by 32, 34 or 36 cycles of 98℃, 10 sec,68℃, 30 sec.	F	VfMID_F3	AAGGCCGACATCTCAAGTCACGAC
			R	VfMID_Rsp2	CCGCGTTGCCGGCATATTCGCTT
	EF1-like	2 min at 94 ℃, followed by 28, 30 or 32 cycles of 98 ℃, 10 sec, 68 ℃, 30 sec.	F	VfEF1_F2	AAGGAGCGCTACGATGAGATTGCC
			R	VfEF1_R2	TACCACGGCATGTTCTTGGACTCG

Chapter 3.

Identification of sex-determining (SD) region in heterothallic *Volvox reticuliferus* and SD-like region in homothallic *V. africanus* by *de novo* whole genome sequencing

INTRODUCTION

To date, genomic studies of volvocine green algae have focused on heterothallic species, but this lineage also underwent numerous transitions between heterothallism and homothallism (Hanschen et al., 2018). In Chapter 2, I noted the presence of a *MID* gene in two homothallic species of the genus *Volvox*, and it was shown that modulation of *MID* expression in a *V. carteri* male strain can create a homothallic phenotype (Geng et al., 2014). However, it remains unknown how a naturally-occurring homothallic mating system might arise from an ancestral UV sex chromosome system (or vice versa).

In Chapter 2, I focused on two closely-related species of *Volvox* that have different sexual systems: *V. reticuliferus* is heterothallic with morphologically differentiated (a.k.a. "special") male and female sexual spheroids, whereas *V. africanus* is homothallic producing "special" male and monoecious spheroids from single clonal cultures (analogous to andromonoecy in land plants) (Nozaki et al., 2015) (Figs. 1.3, 2.1). While ancestral heterothallism in *Merrillosphaera* is more likely than homothallism, statistical support for this inference is not strong, and the directionality of transitions between these two types of sexuality within this clade remains somewhat inconclusive (Hanschen et al., 2018).

In this chapter, I performed *de novo* whole genome sequencing of male and female strains of *V. reticuliferus* and of homothallic *V. africanus* in order to identify their SDR and SD-like regions (SDLRs), respectively. I used this new sequence information to infer the likely ancestral state of heterothallism in this clade and to reconstruct the chromosomal changes which occurred during the evolution of homothallism in *V. africanus*, including tracking the fates of ancestrally sex-limited genes and the resolution of male and female gametologs. Alternative scenarios for the steps leading to homothallism in *V. africanus* are presented and evaluated.

MATERIALS AND METHODS

Algal strains.

V. reticuliferus male and female strains and a homothallic *V. africanus* strain (NIES-3786, 3785 and 3780, respectively; Microbial Culture Collection at the National Institute for Environmental Studies (Kawachi et al., 2013)) were used in the present study (Tables 2.1, 2.4).

Whole-genome sequencing

The cultures were maintained in 300 mL standard *Volvox* medium (SVM) (Kirk and Kirk, 1983) in a silicon-capped 500 mL flask with aeration at 25°C, on a light: dark cycle 12 h: 12 h under cool-white fluorescent lamps at an intensity of 110–150 μmol·m^{-2}·s^{-1}.

Genomic DNAs were prepared according to the method of Miller et al (1993). Approximately 5 mL sample culture was corrected by filtration and transferred to a 15 mL tube, with containing 1/20 of resuspension buffer (50 mM Tris (pH 8.0), 10 mM EDTA), 1/20 of 20% sarcosyl, and approximately 1.5 mL of glass beads (425 to 600 pm; Sigma); the sample was vortexed five times at high speed for 1 min, with 1-min incubations on ice between pulses. The tube was then frozen over 30 minutes and thawed at 37℃ five times. Cell debris and any contaminating beads were pelleted by centrifuging in 3500 rpm 25 min, and the supernatant was then transferred to new 15 mL tubes. An equal volume of 2 x CTAB buffer (2% hexadecyltrimethylammonium bromide [CTAB], 100 mM Tris-HCl (pH 8), 20 mM EDTA(pH 8), 1.4 M NaCl, 1% polyvinylpyrrolidone), prewarmed to 65 ℃, was added and the sample mixed. The tube was then filled with an equal volume of CHCl3, mixed again, and spun in 3500 rpm 25 min; the aqueous layer was transferred to new 15 mL tubes, one-tenth volume 10% CTAB buffer (10% CTAB, 0.7 M NaCl) was added, the tube was mixed, and the sample was extracted with CHCl3 as before; Once again the aqueous layer was transferred to a new Eppendorf tube, and nucleic acids were precipitated by adding an equal volume of CTAB

precipitation buffer (1% CTAB, 50 mM Tris-HCl (pH 8), 10 mM EDTA (pH 8)), mixing, and allowing to stand at room temperature for 30 min; Nucleic acids were pelleted by spinning the tube for 10 min in a microcentrifuge, the supernatant was discarded, and the pellet was resuspended in high-salt TE (10 mM Tris-HCl, pH 8; 1 mM EDTA, pH 8; 1 M NaCl). Nucleic acids were then precipitated with ethanol, resuspended and precipitated again, washed with 70% ethanol, dried, dissolved in TE. After added 18.18 mM spermine-4HCl, precipitated nucleic acids was resuspended in 75 mL of 100 mM EDTA and 65 µl of 4 M NH_4OAc, and left 1 hour at 4℃. Nucleic acids were precipitated with Isopropanol, dissolved in TE, then precipitated again with phenol/$CHCl_3$ pH 8.0 equilibrated with Tris. Contaminating RNA was removed by 10 µg/µl of RNaseA (Nippongene).

The purified DNA was shipped to National Institute of Genetics, Mishima, for generating *de novo* nuclear genome data (Table 3.1) based on sequencing by PacBio Sequel (Pacific Biosciences, Menlo Park, CA, USA) and Illumina HiSeq 2500 sequencers (illumina, San Diego, CA, USA) that were then subjected to assembling. The PacBio data were assembled by Falcon v0.7, Falcon-unzip v0.4 (Chin et al., 2016) and SMRT Link v6.0.0.47841 (Pacific Biosciences), and the Illumina data were then mapped against the PacBio assembly sequence and assembly were corrected using Pilon v1.22 (Walker et al., 2014).

RNA-seq data mapping

The asexual cultures were maintained in 300 mL standard *Volvox* medium (SVM) (Kirk and Kirk, 1983) in a silicon-capped 500 mL flask with aeration at 25°C, on a light: dark cycle 12 h: 12 h under cool-white fluorescent lamps at an intensity of 110–150 µmol·m^{-2}·s^{-1}.

To induce sexual reproduction, about 0.5 ml of growing cultures were transferred into 300 ml of USVT medium (Nozaki et al., 2015) diluted one to two with distilled water in a silicon-capped 500 mL flask with aeration and grown at 25°C on a 12-h light:12-h dark schedule under

cool-white fluorescent lamps at an intensity of 160–180 μmol·m^{-2}·s^{-1}. Sexual spheroids developed after 4~5 days (*V. africanus*) or 7~10 days (*V. reticuliferus*).

Total RNA was extracted from asexual and sexual induced cultures for each strain (Table 3.1) using RNeasy Plant Mini Kit (Qiagen, Hilden, Germany) according to the manufacturer's protocol. Contaminating DNA was removed using RNase-Free DNase I (Takara Bio Inc., Shiga, Japan). The purified RNA was shipped to National Institute of Genetics, Mishima, for generating RNA-seq data (Table 3.2) based on sequencing by Illumina HiSeq 2500 that were then assembled and mapped to the genome data.

Sex-determining region identification

Candidate contigs for the entire SDR or *MT* (*V. reticuliferus* male:contig010; *V. reticuliferus* female: contig011/058) were screened as major significant matching subjects with more than three non-overlapping protein hits (cutoff maximum E-value: 1e−10) by TBLASTN (NCBI) on *de novo* assemblies of *V. reticuliferus* with 80 proteins on *V*. *carteri* female SDR (*MTF*) (Acc. No. GU784915) as queries and then dotplot-analyzed between haplotypes of same species using YASS (https://bioinfo.lifl.fr/yass/index.php) (Noé and Kucherov, 2005) to detect the rearranged genomic regions or SDR. By using the *V. reticuliferus* SDR sequences, a long *SD*-like region (SDLR) was determined in *V. africanus* contig018/132.

Bridging between Contig011 and Contig058 of *Volvox reticuliferus* female strain

Genomic DNA of *V. reticuliferus* female strain NIES-3785 was prepared according to the method of Miller et al. (1993). Specific primers (VrF_058_F1_788.3k and VrF_011_R1_2.7k; Table 3.3) were designed for terminal regions of Contigs 011 and 058 to fill in a gap between the two contigs. PCR was performed using the total DNA and the two specific primers sets with KOD FX Neo (TOYOBO, Osaka, Japan) to amplify DNA fragments of ca. 5 kbp long. PCR schedule

was 2 min at 94°C, followed by 5 cycles of 10 s at 98°C and 60 s at 74°C, 5 cycles of 10 s at 98°C and 60 s at 72°C, 5 cycles of 10 s at 98°C and 60 s at 70°C, 40 cycles of 10 s at 98°C and 60 s at 68°C, 420 s at 68°C. For determining the nucleotide sequences, direct sequencing of the PCR-amplified fragments was carried out by cycle sequencing reactions with BigDye™ Terminator v3.1 Cycle Sequencing Kit (Applied Biosystems™, Thermo Fisher Scientific, Waltham, Massachusetts, USA) using specific primers (Table 3.3). The determined sequence from all sets was 598 bp (Acc. No. LC582539) and demonstrated a bridging between Contig011 (368-1 positions) and Contig058 (790402-790173 positions) without gap between the contigs. Although the 598 bp sequence alternatively suggested another bridging between Contig011 (368-1 positions) and Contig013 (2289448-2289677 positions) without gap between the contigs, this bridging would result in discrepancy in one (*CGL55~THI10*, Fig. 3.3) of the two peripheral regions of SDR which the large male Contig010 completely harbors. Thus, the bridging between Contig011 and Contig058 is more probable than that between Contig011 and Contig013.

Bridging between Contig018 and Contig132 of *Volvox africanus*

Genomic DNA of *V. africanus* strain NIES-3780 was prepared according to the method of Miller et al. (1993) as described above. Specific primers (VxAfr-SF1 and VxAfr-SR3; Table 3.4) were designed for terminal regions of Contig018 and Contig132 to fill in a gap between the two contigs. PCR was performed using the total DNA and the two specific primers (VxAfr-SF1 and VxAfr-SR1/VxAfr-SR3) with Tks Gflex™ DNA Polymerase (Takara Bio., Osaka, Japan) to amplify DNA fragments of ca. 5 kbp long. PCR schedule was 1 min at 94°C, followed by 40 cycles of 10 s at 98°C and 180 s at 68°C. For determining the nucleotide sequences, direct sequencing of the PCR-amplified fragments was carried out by cycle sequencing reactions with BigDye™ Terminator v3.1 Cycle Sequencing Kit using internal primers (Table 3.4). A sequence of 5148 bp (Acc. No. LC582540) was determined just internal to the primer pair (VxAfr-SF1 and

VxAfr-SR3) to bridge Contig018 and Contig132. Based on the blastn search by GenomeMatcher 3.0 (Ohtsubo et al., 2008), 949-5148 positions of the 5148 sequence were best-fitted with the anterior 4198 bp (1-4198 positions) of Contig132 whereas the remaining 948 bp (1-948 positions) of the 5148 bp correspond to 1532837-1533784 positions of Contig018 (1534657 bp). Thus, the most posterior 873 bp (1533785-1534657 positions) of Contig018 were removed for bridging between Contig018 and Contig132.

Identification of *FUS1* sequence of *Volvox africanus*

The polyadenylated mRNAs were directly isolated from *V. africanus* cells using Dynabeads Oligo (dT)25 (Thermo Fisher Scientific), reverse transcribed with Superscript III reverse transcriptase (Thermo Fisher Scientific), and subjected to PCR (2 min at 94℃, followed by 30 cycles of 10 sec at 98℃, 30 sec at 65℃ and 30 sec at 68℃) with two specific primers (FUS1_E2_F1: 5’- CCGTTCGCATTTACAGTGCAGCTC-3’; FUS1_E4_R1: 5’- GACAACCGACGCAGCTGGAGAAA-3’) and KOD FX Neo (TOYOBO, Osaka, Japan). To extend the cDNA sequences, 5′ RACE and 3′ RACE were performed using the GeneRacer kit (Thermo Fisher Scientific) and three specific primers (FUS1_E2_R1: 5’-GCTGTATGGACGCCTCTGATTGGT-3’; FUS1_E2_R2 : 5’-TGCGGAACCTGGCAAGAGTTTACA-3’; FUS1_E4_F1: 5’-TGCGTCGGTTGTCCACATGTTAAG-3’). The PCR products were directly sequenced, or first cloned into the pCR4Blunt-TOPO vector (Thermo Fisher Scientific). For determining the nucleotide sequences, direct sequencing of the PCR-amplified fragments was carried out by cycle sequencing reactions with BigDye™ Terminator v3.1 Cycle Sequencing Kit. Based on the cDNA sequence and genome sequence, only sequence harboring exon2-exon4 of *FUS1* was recognized. No RNA-seq data were obtained regarding *V. africanus FUS1*.

Molecular phylogenetic analyses

Homologous protein sequences of sex-limited genes and gametologs in *V. reticuliferus* and *V. africanus* (Table 3.5) were retrieved from database of other volvocine algae by BLASTP (cutoff maximum E-value: 5e−2) on NCBI. *Chlamydomonas reinhardtii* protein sequences were treated as outgroups. When such an outgroup sequence was not retrieved, homologous sequences were extracted by BLASTP (cutoff maximum E-value: 1e−1) from *Chlamydomonas reinhardtii* v5.5 genome data in phytozome v12.1 (https://phytozome.jgi.doe.gov/pz/portal.html#). Phylogenetic analyses were performed using MUSCLE (Edgar, 2004)-aligned full-length protein sequences of sex-limited genes and gametologs (Figs 3.3B, 3.5-3.7). The maximum likelihood (ML) method was subjected to each alignment with complete deletion option and bootstrap analysis based on 1000 replications by MEGA X (Kumar et al., 2018) using the best-fitted model selected by MEGA X (Table 3.6). In addition, Bayesian inference for the respective alignments was carried out using MrBayes 3.2.7a(Ronquist et al., 2012) with the best-fitted model selected by ModelTest-NG 0.1.6 (Darriba et al., 2020)(Table 3.6), with 1000,000 generations of Markov chain Monte Carlo iterations (discarding the first 25% as burn-in). Convergence of the analysis was confirmed by the average standard deviation of split frequencies below 0.01. The alignments are available in TreeBASE (www.treebase.org/treebase-web/home.html; Study ID S26767).

Molecular evolutionary analysis

Divergence scores of synonymous and non-synonymous substitutions between gametologs were computed using yn00 of the PAML4 package (Yang, 2007); nonsynonymous and synonymous site divergence of aligned coding sequences of gametologs was calculated based on Yang and Nielsen, 2000 with equal weighting between pathways, and the same codon frequency for all pairs.

Timetree analysis of advanced members of the colonial volvocine algae

Tree in Fig. 3.3B topology was inferred by maximum likelihood (ML) analyses of 6021 base pairs of five chloroplast genes (Nozaki et al., 2019) [TreeBase (Piel, W. H. et al., 2009; Vos et al., 2012) ID 26647 plus *Eudorina* sp. NIES-3984 (Acc. No. MH267732)] with a model selected by MEGA X (Kumar et al., 2018). Asterisks on branches indicate 80% or more bootstrap values (based on 1000 replicates) by the ML analyses. A timetree was inferred by applying the RelTime method (Tamura et al., 2012, 2018) to the ML tree whose branch lengths were calculated using the ML method and the General Time Reversible substitution model (Nei and Kumar, 2000). The timetree was computed using two calibration constraints (C1 (65-90 MYA) and C2 (50-90 MYA) based on TimeTree: the Time Scale of Life < http://www.timetree.org/> (Liss et al., 1997; Herron et al., 2009)). The method of Tao et al. (2020) was used to set minimum and maximum time boundaries on nodes for which calibration densities were provided. The estimated log likelihood value of the tree is -38392.49. A discrete Gamma distribution was used to model evolutionary rate differences among sites (5 categories (+G, parameter = 0.8168)). The rate variation model allowed for some sites to be evolutionarily invariable ([+I], 57.55% sites). This analysis involved 46 nucleotide sequences. Codon positions included were 1st+2nd+3rd. There was a total of 6021 positions in the final dataset. Evolutionary analyses were conducted in MEGA X.

RESULTS and DISCUSSIONS

An expanded SDR in heterothallic *Volvox reticuliferus*

De novo sequencing of whole genomes from male and female strains of *V. reticuliferus* was done using a combination of long and short reads and yielded a nuclear genome assembly of around 130 Mbp, similar to that of *V. carteri* and other volvocine species (Tables 3.1, 3.3). Protein coding gene predictions were performed with the assistance of transcriptome data to estimate ca 14,000 genes in each strain (Table 3.1). Here I focused on identifying and analyzing the *V. reticuliferus* SDRs, with some additional whole genome analyses. Comparative genome analyses identified a single large (ca 1 Mbp) heteromorphic and highly divergent *MT* region (SDR) that differed between male and female (Figs. 3.1, 3.3A, 3.8). The male SDR (*MTM*) was 0.98 Mbp long and contained three predicted male-limited genes (*MID*, *MTD1* and *VRM001*) whereas the female SDR (*MTF*) was 1.02 Mbp long with three predicted female-limited genes (*FUS1*, *VRF001* and *VRF002*) (Figs. 3.1, 3.3, 3.4). The male and female SDRs also harbored 24 gametologs (shared genes) (Fig.3.10) distributed throughout the SDR with very little evidence of conserved syntenic bloc structure between haplotypes (Figs. 3.3, 3.8). Like the *V. carteri* SDR, the SDR of *V. reticuliferus* has low gene density (28/Mbp versus 104-105/Mbp genome average) and is strongly enriched for repeats (70% compared with 27% genome average) (Table 3.1), features typical for heteromorphic sex chromosomes and other non-recombining regions of the genomes.

As expected, *MID* was found in the *V. reticuliferus* male SDR, but unlike *V. carteri*, an intact *MTD1* gene was also present (Figs. 3.3, 3.4) supporting the inference that this gene which is widely conserved in male or *minus MT* regions in the volvocine lineage became a pseudogene in the *V. carteri* lineage (Ferris et al., 2010)relatively recently (Fig. 3.1). The presence of *FUS1* in the *V. reticuliferus* female SDR (Figs. 3.3, 3.4) further suggests that this gene--which is conserved in plus and female SDRs in nearly all volvocine species (Hamaji et

al., 2018)--was also lost recently in the *V. carteri* lineage (Fig. 3.1). The remaining three sex-limited SDR genes of *V. reticuliferus* (*VRM001*, *VRF001* and *VRF002*) had no predicted functional domains and no homologs elsewhere in the genome or in other species (Figs. 3.3, 3.4), indicating that, like the case in *V. carteri* which has fifteen predicted non-conserved sex-limited genes, expanded volvocine SDRs may act as reservoirs for genetic novelty or innovation. Whether any of these recently evolved sex-limited genes play roles in male or female sexual differentiation remains to be determined.

16 of the 24 gametologs in the *V. reticuliferus* SDR had homologs in the *V. carteri* SDR suggesting they were present in the ancestral SDR of *Merrillosphaera* (Figs. 3.5-3.7), though the physical order of these 16 gametologs was not conserved between homologous haplotypes (Fig. 3.10). These two species diverged ca 11 MYA, and together with the more distantly-related *V. carteri*, they constitute a monophyletic grouping within the "section *Merrillosphaera*", which is an infrageneric taxon of the polyphyletic genus *Volvox* and originates ca 75 MYA (Fig. 3.2).

Overall, my data support the presence of an expanded and highly differentiated SDR being present at least as far back as the emergence of the *Volvox* sect. *Merrillosphaera* lineage originating around 75 MYA (Figs. 3.1, 3.2) and persisting in extant taxa. Further evidence for shared common ancestry of *Volvox* SDRs based on gametolog molecular evolution data is described below.

An expanded SD-like region in homothallic *Volvox africanus*

De novo whole genome sequencing and annotation for *V. africanus* was done similarly as that for *V. reticuliferus*, revealing a comparable nuclear genome size and protein coding capacity for these two species (Table 3.1). Using *V. reticuliferus* SDR genes to search for *V. africanus* homologs I identified an unusual ca. 1 Mbp genomic region in *V. africanus* that I designated "SDLR" (SD-like region) (Fig. 3.11). The SDLR contained homologs for 20/24 *V. reticuliferus* gametologs and a *FUS1*-related pseudogene (Figs. 3.3, 3.4, 3.12), but no other homologs of

male or female sex-limited genes from *V. reticuliferus*. The SDLR was flanked by sequences corresponding to the pseudo-autosomal regions flanking the *V. reticuliferus* SDR (Figs. 3.3, 3.11), indicating a syntenic chromosomal location for the SDLR and SDR of these two species. Homologs of the four remaining gametologs from *V. reticuliferus* were found in separate, unlinked genomic locations (see below) (Fig. 3.14). Strikingly, the SDLR was similar to *V. reticuliferus* and *V. carteri* SDRs in having a typically low gene density and elevated repeat content compared to other regions of its genome (Table 3.1). These findings strongly suggest a recent origin of the *V. africanus* SDLR from a differentiated heteromorphic U or V sex chromosome.

I searched for homologs of the conserved volvocine sex-limited genes *MID* and *MTD1* in *V. africanus*, as well as for homologs of the non-conserved sex-limited genes of *V. reticuliferus* (*VRM001, VRF001*, *VRF002*) (Fig. 3.1). Interestingly, *V. africanus MID* was found in a short contig as a tandem five-copy array (Fig. 3.15) flanked by three pseudogenes which have intact paralogs in the SDLR (*VAMT051*, *SPS1*, *MTM0397*). I designated this short *MID*-containing contig "short SDLR" because, like the SDLR, it has low gene density (20/Mbp versus 104-105/Mbp genome average) and is strongly enriched for repeats (85% compared with 27% genome average) (Table 3.1) also indicating its recent origin from a heteromorphic sex chromosome.

Phylogenies of SDR, SDLR and short SDLR genes from *V. reticuliferus*, *V. africanus* and *V. carteri*, were used to infer their origins and relationships to one another, and by extension, to understand the origins of the SDLR and short SDLR in *V. africanus* (Fig. 3.1). As expected, the phylogenies of *FUS1*, *MID* and *MTD1* were consistent with vertical inheritance in *Volvox* and other volvocine species, with independent losses or pseudogenization of *FUS1* in *V. carteri* and *V. africanus* (Fig. 3.1B). Of the 20 genes in the *V. africanus* SDLR that it shares with *V. reticuliferus* gametologs, 18 descend from a female SDR ancestor, and in five cases these genes

date back to a common ancestor with a *V. carteri* female SDR homolog (Figs. 3.1, 3.6 and Table 3.5), and in the case of *SPS1*, they go as far back as the SDR from *Eudorina* sp. (Figs. 2.1, 2.2B). In contrast, none of the SDLR predicted proteins grouped with male SDR proteins. In two cases, *VAMT003* and *VAMT030*, the phylogenetic relationships of the *V. africanus* proteins suggests that their corresponding genes entered the SDR/SDLR after the *V. reticuliferus* and *V. africanus* lineages split (Fig. 3.6). There was a single gene likely belonging to the ancestral female SDR, *VAMT041*, that was not present in the *V. africanus* SDLR, but instead was found inserted into an autosome-like region (Figs. 3.1, 3.3). Taken together these data strongly support the origin of the *V. africanus* SDLR from an ancestral female U chromosome that was retained almost completely intact after the transition to homothallism, though it did undergo intra-locus rearrangements relative to the *V. reticuliferus* female SDR (Fig. 3.1). These results also unequivocally support the ancestral state of the *Merrillosphaera* clade as being heterothallic with large non-recombining SDRs, and the transition to homothallism in *V. africanus* as being a derived feature.

If *V. africanus* descended from an ancestor with UV sex chromosomes, then what were the fates of the male SDR genes from that ancestor? As described above, the sex-related genes *MID* and *MTD1* are present elsewhere in the *V. africanus* genome. Strikingly, only three male-SDR-derived gametologs (*MME6, MOT41, TOC34*) were retained intact in *V. africanus*; and all three are found inserted into different unlinked autosomal locations (Figs. 3.1, 3.3, 3.14). Notably, female-derived homologs of these three genes are absent from the SDR and other autosomal regions suggesting the female alleles were lost after the transition to homothallism. Three pseudogenes in short SDLR (*VAMT051*, *SPS1*, *MTM0397*) are male-derived and have female-derived paralogs in the SDLR (Figs. 3.1, 3.7). In no case, did I find intact male-derived and female-derived copies of gametologs in *V. africanus*.

Taken together, those data allow me to draw several conclusions regarding the transition from heterothallism to homothallism in the *V. africanus* algae. First, I conclude that maleness is

mainly conferred by the conserved genes *MID* and *MTD1*, possibly along with the male gametologs retained from a heterothallic ancestor. In volvocine algae female (or *plus*) gamete production is the default state when *MID* is absent (Ferris and Goodenough, 1994). However, it is likely that the female-derived SDLR has retained some sex-specific functions. This inference of sex specific functions encoded in the female SDLR is supported by data from *V. carteri* where developmental and fertility defects were observed in a chromosomally male strain that was converted to an egg-producing pseudo-female by suppression of *MID* expression (Geng et al., 2014). These fertility defects were likely due to the absence of female SDR genes in this strain. The loss of the only conserved female gene, *FUS1*, from the SDLR in *V. africanus* suggests that its function became partly or wholly dispensable for female gamete function or was replaced by something else. In *Chlamydomonas* FUS1 protein localizes to the site of membrane fusion during fertilization and is essential to complete fertilization (Ferris et al., 1996). Precedent for the dispensability of *FUS1* comes from heterothallic *V. carteri* which also lost *FUS1* but which still can produce fertilizable eggs in a chromosomally male SDR background (Ferris et al., 1996, 2010), implying that other female-limited SDR genes did not replace *FUS1* function in this species. The other losses from the ancestrally female SDLR in *V. africanus* were gametologs that each has a male-derived allele inserted into an autosomal location (Figs. 3.1, 3.3, 3.14). This finding suggests that retention of two copies for all of the gametologs was unstable, and raises the question of why the ancestral female gametolog copy was not retained for all of the SDLR genes? While I cannot rule out that the loss or retention of male versus female gametologs was largely stochastic, I speculate that in the cases where a male-derived gametolog copy was retained (*MME6, MOT41, TOC34*), the male gametolog may have had a history of sexually antagonistic selection in the heterothallic ancestor resulting in a differential fitness penalty for retaining male versus female allele (see below). Interestingly, one of the three male-SDR-derived gametologs in *V. africanus*, *MOT41*, encodes a homolog of IFT43, an intraflagellar transport

protein that plays an essential role in flagellar biogenesis (Zhu et al., 2017). Although functional flagella must be produced in somatic cells of both sexes of *Volvox*, it is possible that the ancestrally male allele of *MOT41* was needed for some critical aspect of sperm motility which could not be adequately fulfilled by the female allele. The potential for sexually antagonistic functions of MME6, a subunit of the NADP malic enzyme (Dubini et al., 2009), and TOC34, a chloroplast outer membrane transit peptide receptor (Kalanon and McFadden, 2008) are less clear, but they could be involved in specialized aspects of sperm cell energy metabolism and chloroplast biogenesis, respectively.

FIGURES

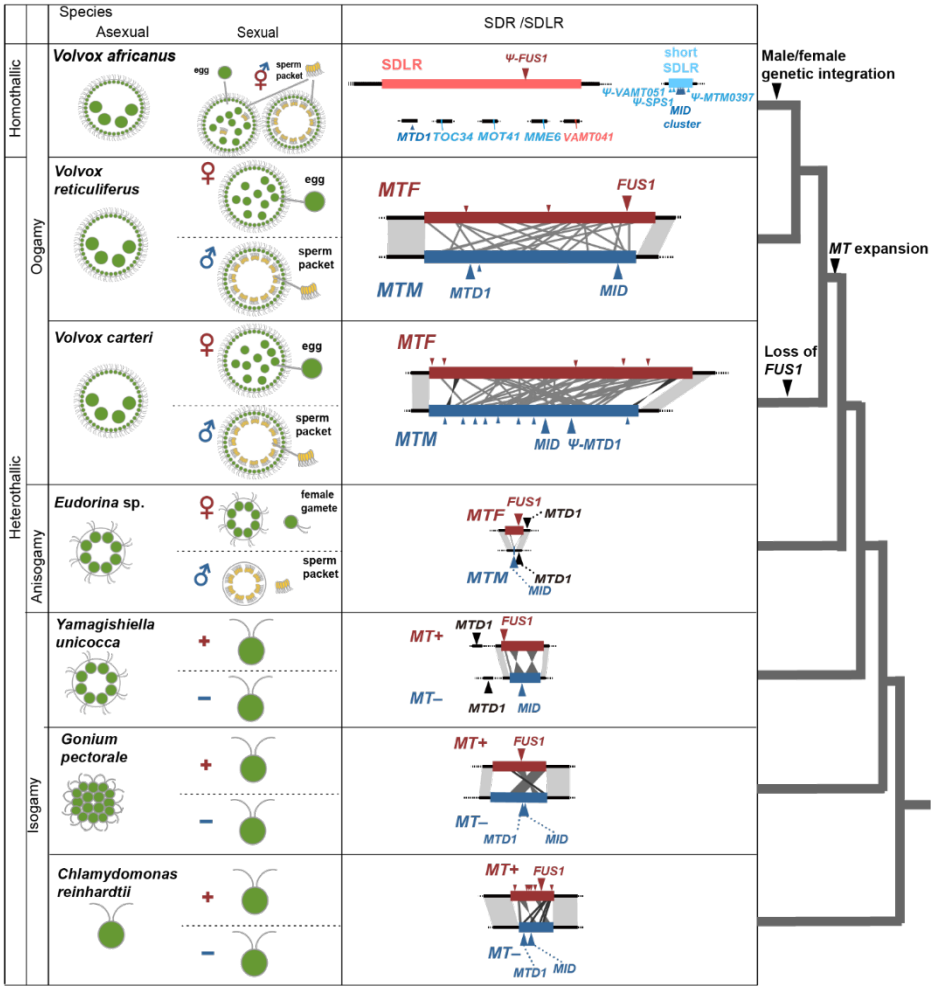

Figure 3.1. Volvocine green algal phylogeny and sex-determining region (SDR) or mating-type locus (*MT*) evolution. Asexual or vegetative phase, sexual phase, SDR or *SD*-like region (SDLR) and phylogenetic positions of *Volvox reticuliferus* and *V. africanus* are illustrated with those of five other species previously studied (*Chlamydomonas reinhardtii*, *Gonium pectorale*, *Yamagishiella unicocca*, *Eudorina* sp. and *V. carteri* (Ferris and Goodenough, 1994; Ferris et al., 2010; Hamaji et al., 2016, 2018; Umen and Coelho, 2019). Note that all of these three *Volvox* species belongs to the section *Merrillosphaera* (Fig. 3.2).

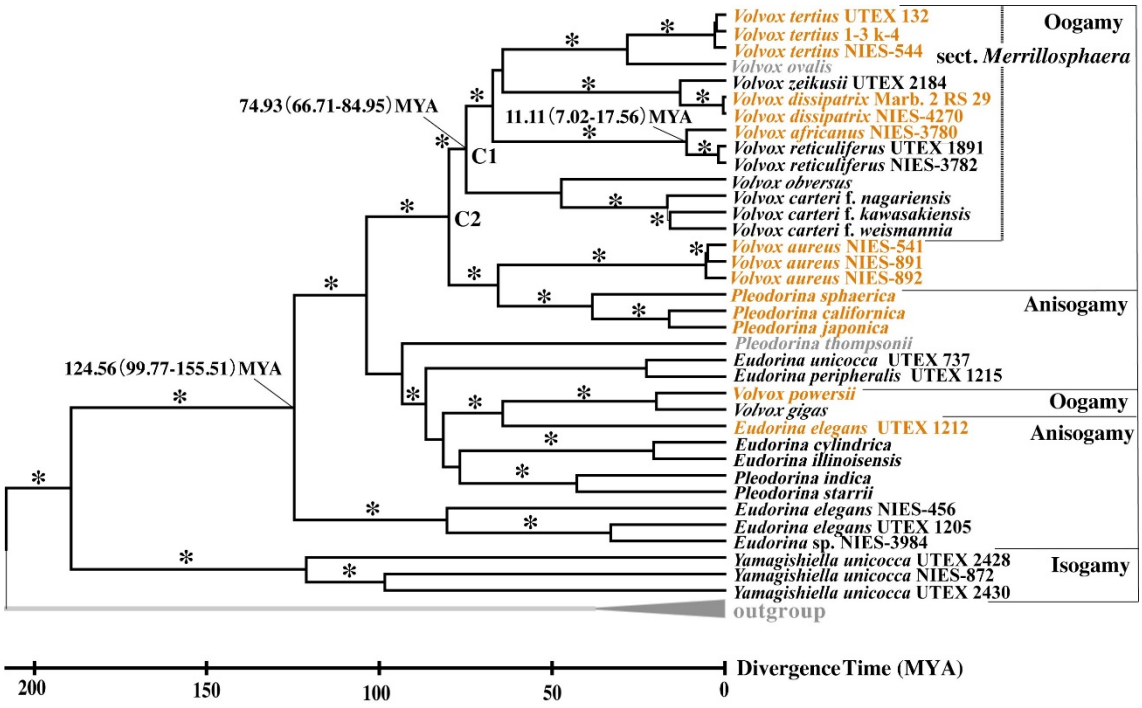

Figure 3.2. Timetree analysis of advanced members of the colonial volvocine algae. Note that the divergence time between heterothallic *Volvox reticuliferu*s and homothallic *V. africanus* is "11.11 (7.02-17.56) MYA". Species names in orange or black indicate homothallic or heterothallic sexuality, respectively.

A

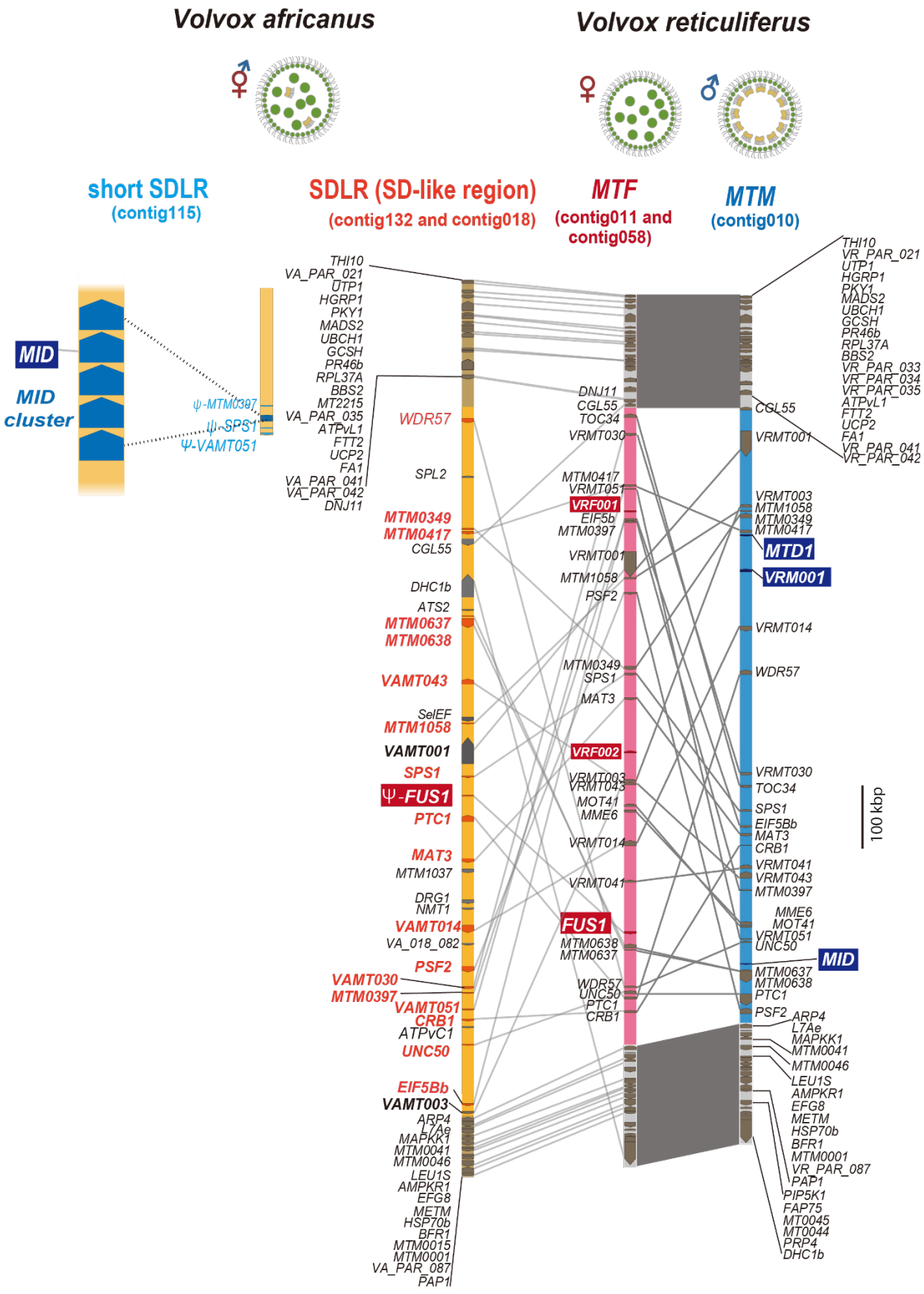
Volvox africanus
Volvox reticuliferus
short SDLR
(contig115)
SDLR (SD-like region)
(contig132 and contig018)
MTF
(contig011 and contig058)
MTM
(contig010)
MID
MID cluster
ψ-MTM0397
ψ-SPS1
Ψ-VAMT051
100 kbp

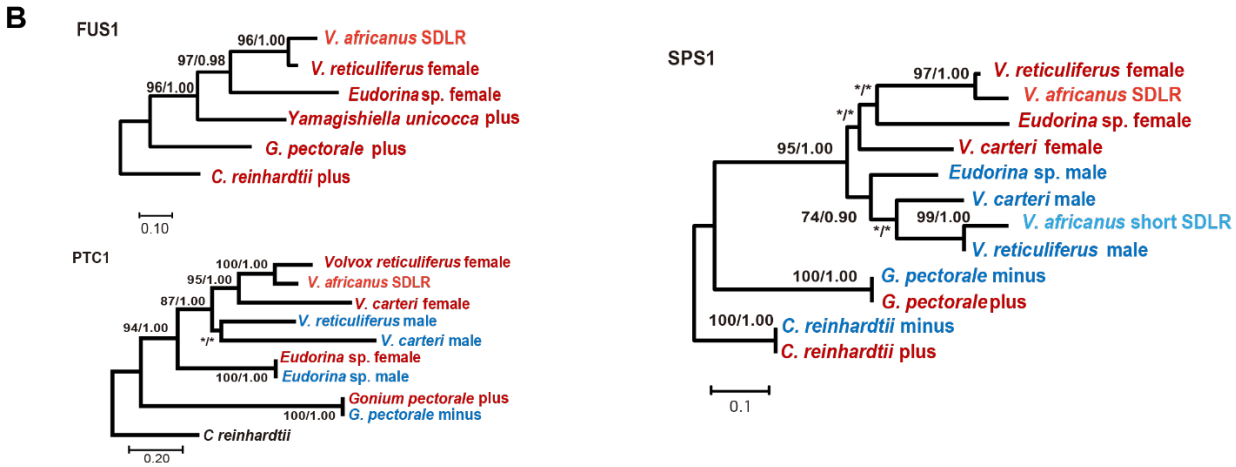

Figure 3.3. Sex-determining region (SDR) or Mating-type locus (*MT*) of heterothallic *Volvox reticuliferu*s (male and female) and two *SD*-like regions (SDLR and short SDLR) in homothallic *V. africanus* and phylogeny of four genes in SDR and two *SD*-like regions. **A**. Comparison of homothallic *V. africanus SD*-like regions (accession nos. LC586641LC58662) and *V. reticuliferus* male and female SDR (*MTM* and *MTF*, respectively; accession nos. LC586643–LC586644). Note male- and female-limited genes (backed blue and backed red, respectively) and gametologs of *V. reticuliferus* and their homologs in *SD*-like regions of *V. africanus.* Red and blue regions represent *MTM* and *MTF*, respectively. Yellow regions represent SDLR and short SDLR. Gray shading indicates a syntenic bloc of pseudo autosomal regions. Red and blue homologs in SDLR and short SDLR represent *MTF*- and *MTM*-origin, respectively (deduced from phylogenetic analyses; B and Figs. 3.5-3.7). **B.** Maximum likelihood (ML) phylogeny of homologs of the sex-limited genes *FUS1* and two gametologs (*PTC1* and *SPS1*). Red and blue represent homologs of gametologs/sex limited genes from female and male *MT* (SDLR and short SDLR*),* respectively. Note that *V. africanus* has male-related and female-related *SP1* homologs in short SDLR and SDLR, respectively. Numbers in left and right sides at branches indicate bootstrap values of *ML* analysis and posterior probabilities of Bayesian inference, respectively. For phylogenetic analyses of homologs of male-limited *MTD1* and other gametologs, see Figs. 3.5-3.7

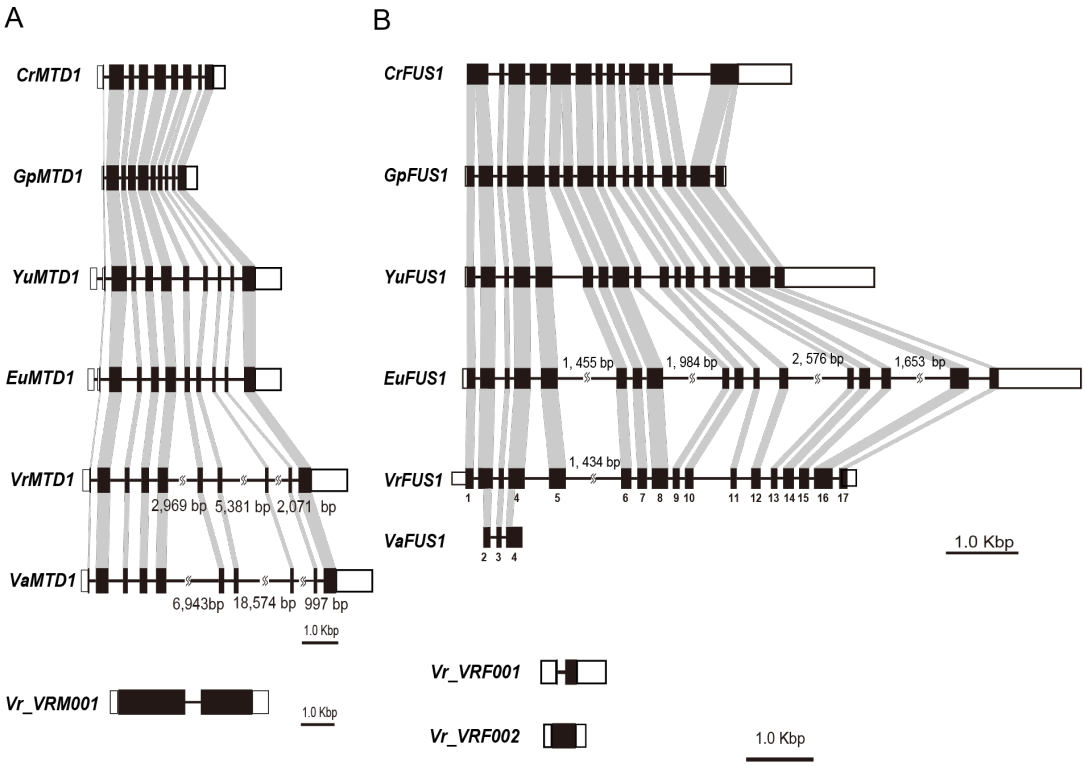

Fig. 3.4. The exon-intron structures of sex-limited genes of *Volvox reticuliferus* and their homologs in other volvocine species (Figs. 3.2, 3.4, 3.13). *Cr*, *Gp*, *Yu*, *Eu*, *Vr* and *Va* at the prefixes of gene names represent *Chlamydomonas reinhardtii*, *Gonium pectorale*, *Yamagishiella unicocca*, *Eudorin*a sp., *V. reticuliferus* and *V. africanus*, respectively.

Filled and open boxes represent coding and non-coding exon sequences, respectively.

Lines between boxes represent introns. Gray boxes link homologous coding sequences.

A. Two male-limited genes: *MTD1* and *VRM001*. For *MID* homologs, see Fig. 2.5. **B.** Three female-limited genes: *FUS1*, *VRF001* and *VRF002*. Numbers below boxes for *VrFUS1*and *VaFUS1* indicate exon numbers.

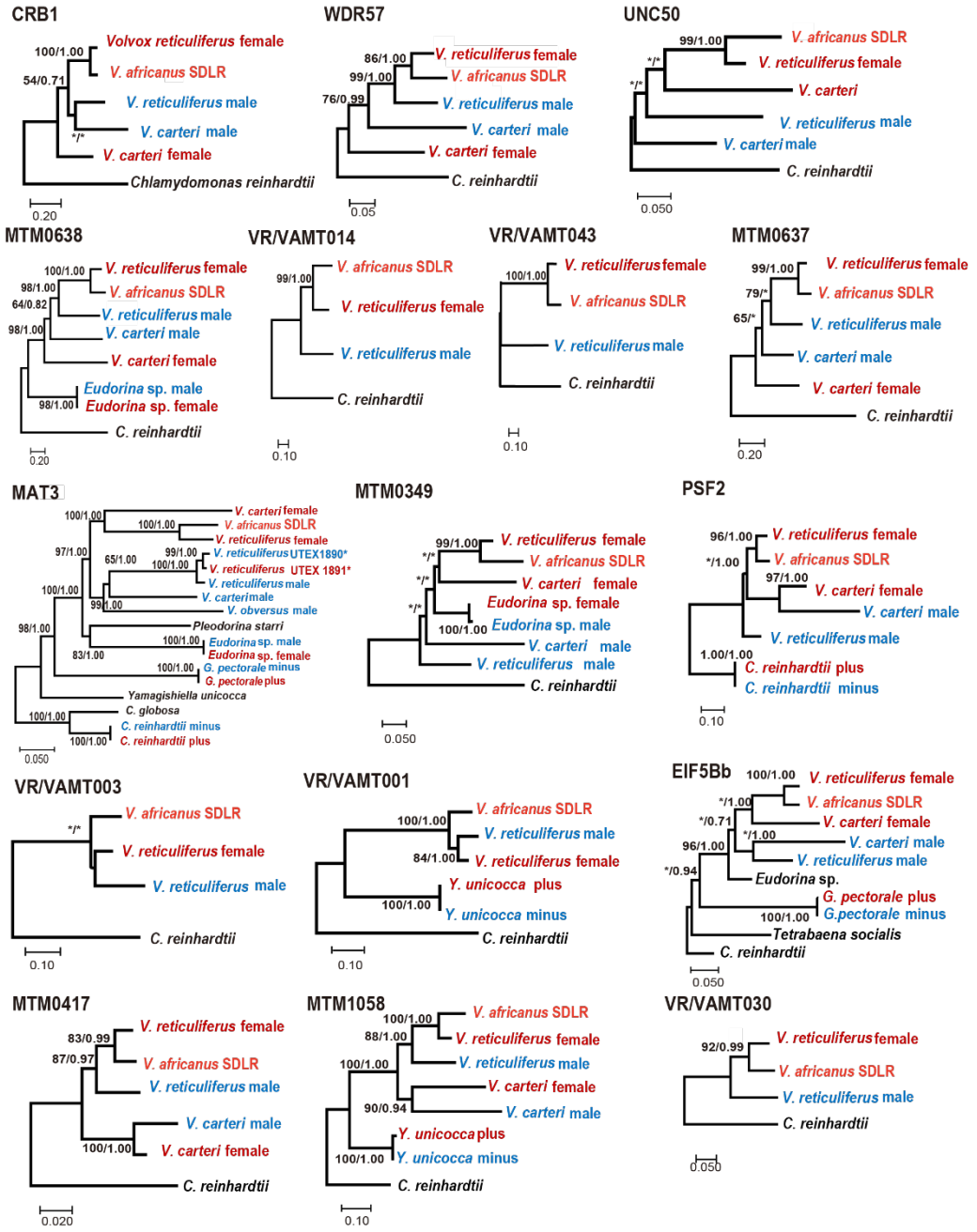

Figure 3.5. Maximum likelihood (ML) phylogeny of 16 homologs of gametologs harboring in *Volvox africanus* SDLR (Fig. 3.3). Red and blue represent homologs of gametologs from female SDR (SDLR) and male SDR, respectively. Note that 14 *V. africanus* homologs represent *V. reticuliferus* female SDR-related whereas male- or female-relation of the other two (*VAMT003* and *VAMT001*) are ambiguous. Numbers in left and right sides at branches indicate bootstrap values of *ML* analysis and posterior probabilities of Bayesian inference, respectively. For the other four gametolog homologs in *Volvox africanus* long *MT-like*, see Fig. 3.3B and Fig. 3.6.

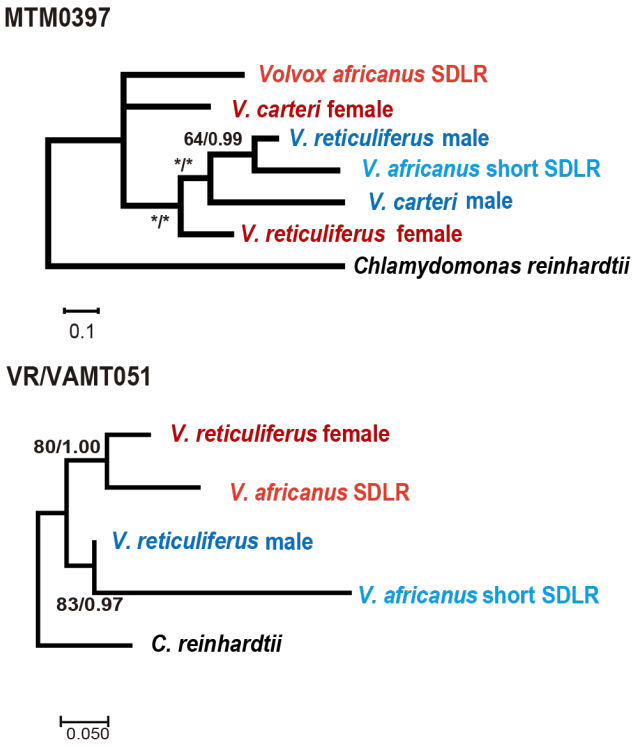

Figure 3.6. Maximum likelihood (ML) phylogeny of two homologs of gametologs harboring in both SDLR and short SDLR of *Volvox africanus* (Fig. 3.3). Red and blue represent homologs of gametologs from female SDR (SDLR) and male SDR (short SDLR), respectively. Numbers in left and right sides at branches indicate bootstrap values of *ML* analysis and posterior probabilities of Bayesian inference, respectively.

For the other gametolog homologs in *Volvox africanus* SDLR and short SDLR, see Fig. 3.3B and Fig. 3.5.

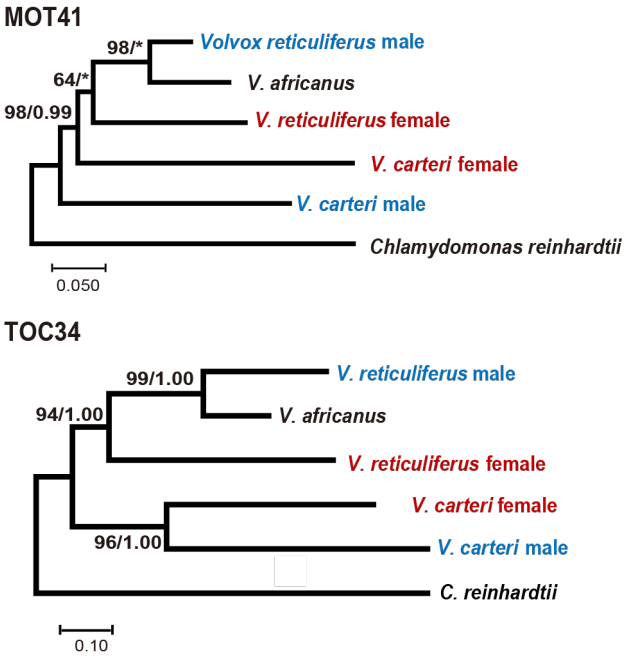

Figure 3.7. Maximum likelihood (ML) phylogeny of and two gametologs of *Volvox reticuliferus*. Red and blue gene names represent gametologs from female and male SDR, respectively. Note that two *V. africanus* homologs are found within autosome-like regions (outside SDLR and short SDLR) (Fig. 3.13A). Numbers in left and right sides at branches indicate bootstrap values of ML analysis and posterior probabilities of Bayesian inference, respectively.

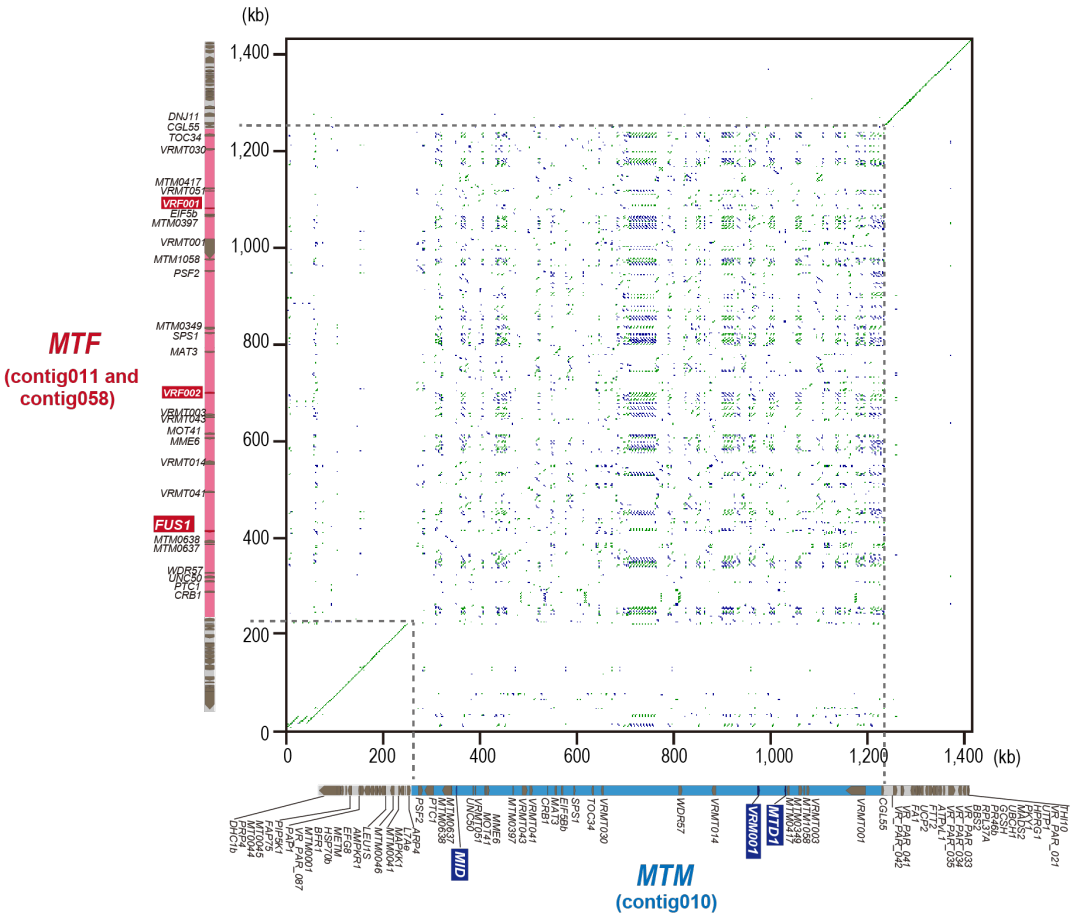

Fig. 3.8. *Volvox reticuliferus* dotplot between male (vertical) and female (horizontal) specific regions [*MTM* (blue) and *MTF* (red), respectively] and parts of pseudo autosomal regions (gray). Green and blue dots indicate forward and reverse alignments, respectively. For details of *MTM* and *MTF,* see Fig. 3.3A.

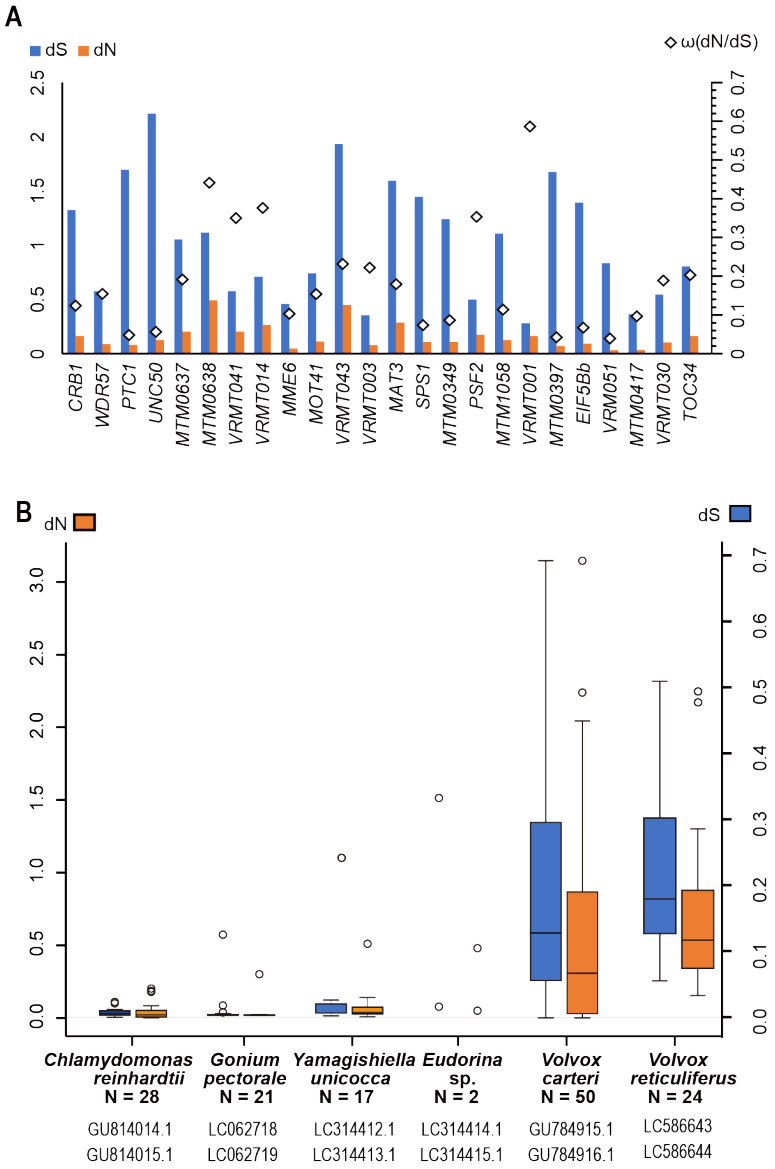

Figure 3.9. Molecular evolutionary analyses of gametologs in *Volvox reticuliferus*. A. dN/dS ratios of gametologs in rearranged regions or sex-determining regions (SDR*s*) of *V. reticuliferus*. There are no prominently dimorphic gametologs under positive selection between sexes (dN/dS > 1). B. Box-whisker plots comparing the distributions of synonymous (dS, blue/left) and non-synonymous (dN, orange/right) substitution values for gametolog pairs found in SDR*s* of volvocine algal haploid sex chromosomes. Open dots are outliers from interquartile ranges except for those of *Eudorina* sp. which indicate two gametologs.

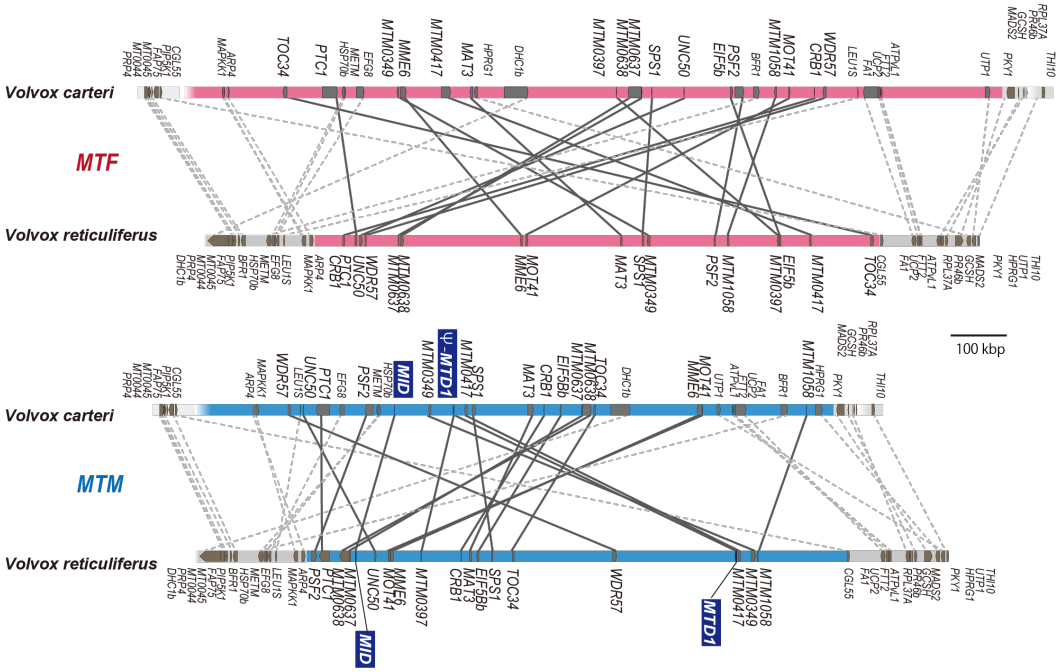

Figure 3.10. Comparison of homologous genes in expanded sex-determining regions (SDRs) of *Volvox carteri* and *V. reticuliferus*. Red, blue and gray regions represent male SDR (*MTM*), female SDR (*MTF*) and pseudo autosomal regions, respectively. Note two male-limited genes (backed blue) in *MTM* and 16 gametologs in *MTM* and *MTF* for each species. Only homologous genes between *V. carteri* and *V. reticuliferus* are shown. Based on the present study (Fig. 3.3A) and Ferris et al., 2010.

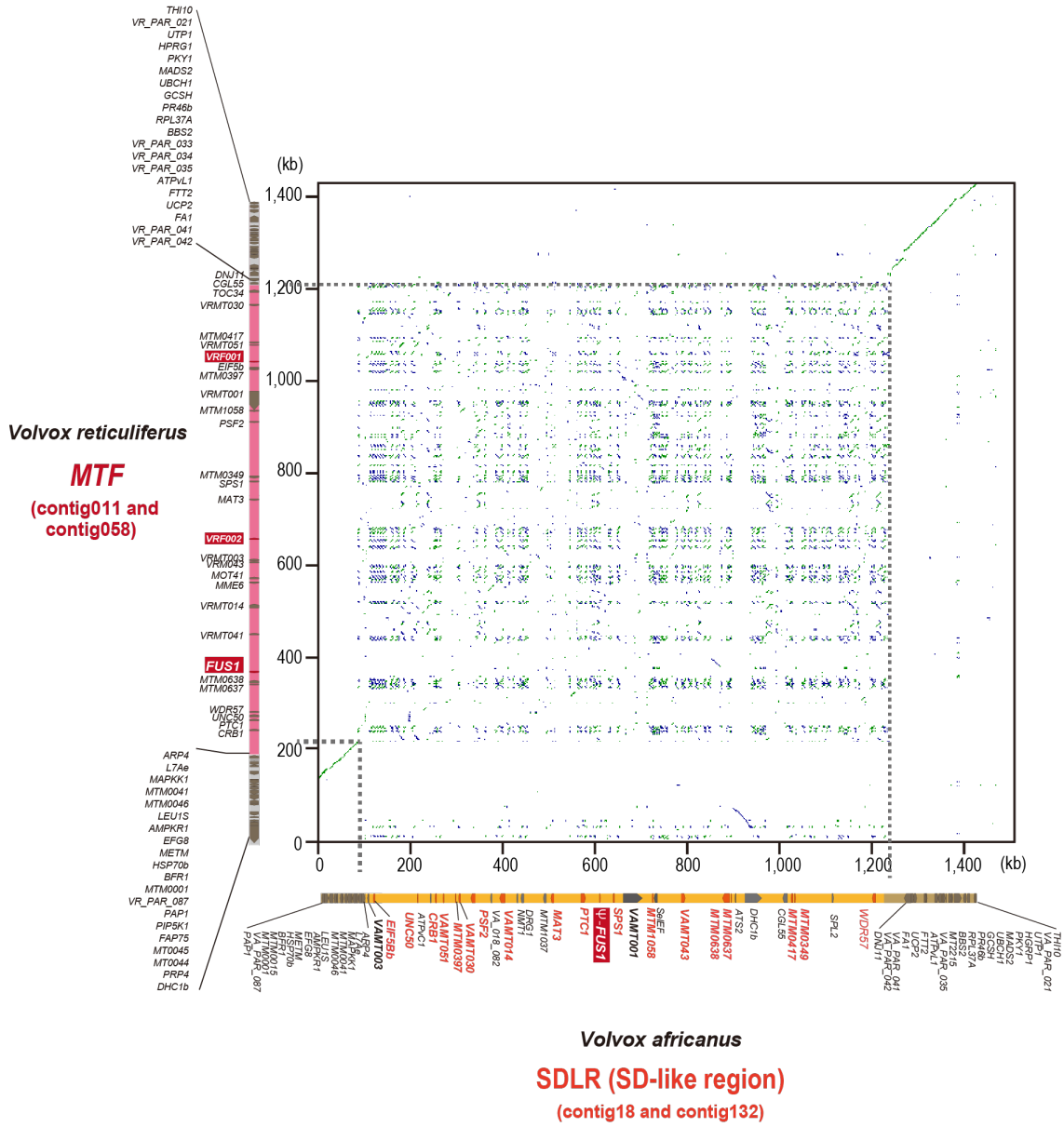

Figure 3.11. Dotplot between *Volvox reticuliferus* female-limited region (vertical, female SDR or *MTF*) and its homologous region of *Volvox africanus* (horizontal, SDLR) and parts of flanking or pseudo autosomal regions (gray). Green and blue dots indicate forward and reverse alignments, respectively. For details of *MTF* and SDLR, see Fig. 3.3A.

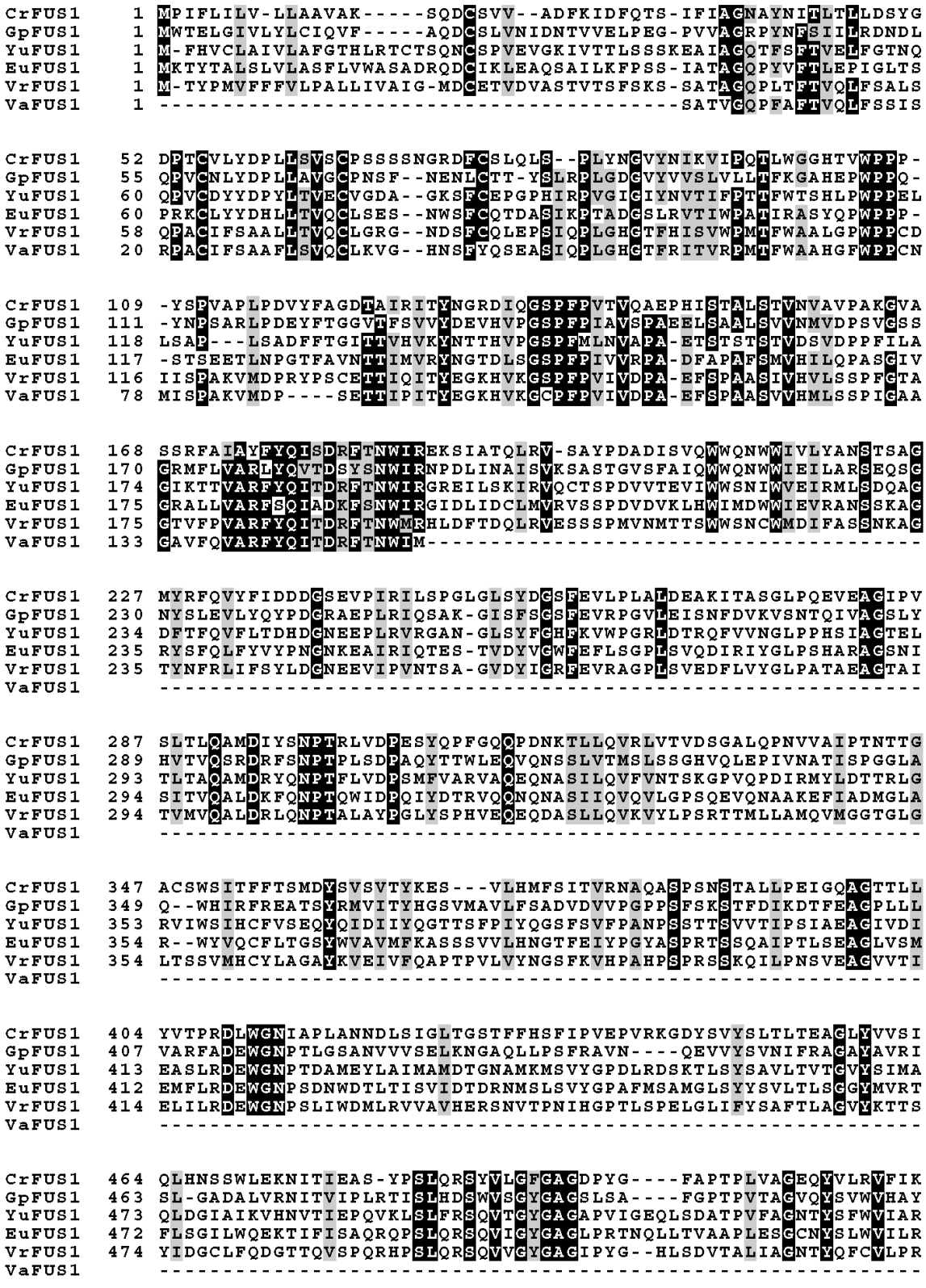
CrFUS1 1 MPIFLILV-LLAAVAK-----SQDCSVV--ADFKIDFQTS-IFIAGNAYNITLTLLDSYG
GpFUS1 1 MWTELGIVLYLCIQVF-----AQDCSLVNIDNTVVELPEG-PVVAGRPYNFSIILRDNDL
YuFUS1 1 M-FHVCLAIVLAFGTHLRTCTSQNCSPVEVGKIVTTLSSSKEAIAGQTFSFTVELFGTNQ
EuFUS1 1 MKTYTALSLVLASFLVWASADRQDCIKLEAQSAILKFPSS-IATAGQPYVFTLEPIGLTS
VrFUS1 1 M-TYPMVFFFVLPALLIVAIG-MDCETVDVASTVTSFSKS-SATAGQPLTFTVQLFSALS
VaFUS1 1 ----------SATVGQPFAFTVQLFSSIS
CrFUS1 52 DPTCVLYDPLLSVSCPSSSSNGRDFCSLQLS--PLYNGVYNIKVIPQTLWGGHTVWPPP-
GpFUS1 55 QPVCNLYDPLLAVGCPNSF--NENLCTT-YSLRPLGDGVYVVSLVLLTFKGAHEPWPPQ-
YuFUS1 60 QPVCDYYDPYLTVECVGDA--GKSFCEPGPHIRPVGIGIYNVTIFPTTFWTSHLPWPPEL
EuFUS1 60 PRKCLYYDHLLTVQCLSES--NWSFCQTDASIKPTADGSLRVTIWPATIRASYQPWPPP-
VrFUS1 58 QPACIFSAALLTVQCLGRG--NDSFCQLEPSIQPLGHGTFHISVWPMTFWAALGPWPPCD
VaFUS1 20 RPACIFSAAFLSVQCLKVG--HNSFYQSEASIQPLGHGTFRITVRPMTFWAAHGFWPPCN
CrFUS1 109 -YSPVAPLPDVYFAGDTAIRITYNGRDIQGSPFPVTVQAEPHISTALSTVNVAVPAKGVA
GpFUS1 111 -YNPSARLPDEYFTGGVTFSVVYDEVHVPGSPFPIAVSPAEELSAALSVVNMVDPSVGSS
YuFUS1 118 LSAP---LSADFFTGITTVHVKYNTTHVPGSPFMLNVAPA-ETSTSTSTVDSVDPPFILA
EuFUS1 117 -STSEETLNPGTFAVNTTIMVRYNGTDLSGSPFPIVVRPA-DFAPAFSMVHILQPASGIV
VrFUS1 116 IISPAKVMDPRYPSCETTIQITYEGKHVKGSPFPVIVDPA-EFSPAASIVHVLSSPFGTA
VaFUS1 78 MISPAKVMDP----SETTIPITYEGKHVKGCPFPVIVDPA-EFSPAASVVHMLSSPIGAA
CrFUS1 168 SSRFAIAYFYQISDRFTNWIREKSIATQLRV-SAYPDADISVQWWQNWWIVLYANSTSAG
GpFUS1 170 GRMFLVARLYQVTDSYSNWIRNPDLINAISVKSASTGVSFAIQWWQNWWIEILARSEQSG
YuFUS1 174 GIKTTVARFYQITDRFTNWIRGREILSKIRVQCTSPDVVTEVIWWSNIWVEIRMLSDQAG
EuFUS1 175 GRALLVARFSQIADKFSNWIRGIDLIDCLMVRVSSPDVDVKLHWIMDWWIEVRANSSKAG
VrFUS1 175 GTVFPVARFYQITDRFTNWMRHLDFTDQLRVESSSPMVNMTTSWWSNCWMDIFASSNKAG
VaFUS1 133 GAVFQVARFYQITDRFTNWIM----------
CrFUS1 227 MYRFQVYFIDDDGSEVPIRILSPGLGLSYDGSFEVLPLALDEAKITASGLPQEVEAGIPV
GpFUS1 230 NYSLEVLYQYPDGRAEPLRIQSAK-GISFSGSFEVRPGVLEISNFDVKVSNTQIVAGSLY
YuFUS1 234 DFTFQVFLTDHDGNEEPLRVRGAN-GLSYFGHFKVWPGRLDTRQFVVNGLPPHSIAGTEL
EuFUS1 235 RYSFQLFYVYPNGNKEAIRIQTES-TVDYVGWFEFLSGPLSVQDIRIYGLPSHARAGSNI
VrFUS1 235 TYNFRLIFSYLDGNEEVIPVNTSA-GVDYIGRFEVRAGPLSVEDFLVYGLPATAEAGTAI
VaFUS1 ----------
CrFUS1 287 SLTLQAMDIYSNPTRLVDPESYQPFGQQPDNKTLLQVRLVTVDSGALQPNVVAIPTNTTG
GpFUS1 289 HVTVQSRDRFSNPTPLSDPAQYTTWLEQVQNSSLVTMSLSSGHVQLEPIVNATISPGGLA
YuFUS1 293 TLTAQAMDRYQNPTFLVDPSMFVARVAQEQNASILQVFVNTSKGPVQPDIRMYLDTTRLG
EuFUS1 294 SITVQALDKFQNPTQWIDPQIYDTRVQQNQNASIIQVQVLGPSQEVQNAAKEFIADMGLA
VrFUS1 294 TVMVQALDRLQNPTALAYPGLYSPHVEQEQDASLLQVKVYLPSRTTMLLAMQVMGGTGLG
VaFUS1 ----------
CrFUS1 347 ACSWSITFFTSMDYSVSVTYKES---VLHMFSITVRNAQASPSNSTALLPEIGQAGTTLL
GpFUS1 349 Q--WHIRFREATSYRMVITYHGSVMAVLFSADVDVVPGPPSFSKSTFDIKDTFEAGPLLL
YuFUS1 353 RVIWSIHCFVSEQYQIDIIYQGTTSFPIYQGSFSVFPANPSSTTSVVTIPSIAEAGIVDI
EuFUS1 354 R--WYVQCFLTGSYWVAVMFKASSSVVLHNGTFEIYPGYASPRTSSQAIPTLSEAGLVSM
VrFUS1 354 LTSSVMHCYLAGAYKVEIVFQAPTPVLVYNGSFKVHPAHPSPRSSKQILPNSVEAGVVTI
VaFUS1 ----------
CrFUS1 404 YVTPRDLWGNIAPLANNDLSIGLTGSTFFHSFIPVEPVRKGDYSVYSLTLTEAGLYVVSI
GpFUS1 407 VARFADEWGNPTLGSANVVVSELKNGAQLLPSFRAVN----QEVVYSVNIFRAGAYAVRI
YuFUS1 413 EASLRDEWGNPTDAMEYLAIMAMDTGNAMKMSVYGPDLRDSKTLSYSAVLTVTGVYSIMA
EuFUS1 412 EMFLRDEWGNPSDNWDTLTISVIDTDRNMSLSVYGPAFMSAMGLSYYSVLTLSGGYMVRT
VrFUS1 414 ELILRDEWGNPSLIWDMLRVVAVHERSNVTPNIHGPTLSPELGLIFYSAFTLAGVYKTTS
VaFUS1 ----------
CrFUS1 464 QLHNSSWLEKNITIEAS-YPSLQRSYVLGFGAGDPYG----FAPTPLVAGEQYVLRVFIK
GpFUS1 463 SL-GADALVRNITVIPLRTISLHDSWVSGYGAGSLSA----FGPTPVTAGVQYSVWVHAY
YuFUS1 473 QLDGIAIKVHNVTIEPQVKLSLFRSQVTGYGAGAPVIGEQLSDATPVFAGNTYSFWVIAR
EuFUS1 472 FLSGILWQEKTIFISAQRQPSLQRSQVIGYGAGLPRTNQLLTVAAPLESGCNYSLWVILR
VrFUS1 474 YIDGCLFQDGTTQVSPQRHPSLQRSQVVGYGAGIPYG--HLSDVTALIAGNTYQFCVLPR
VaFUS1 ----------

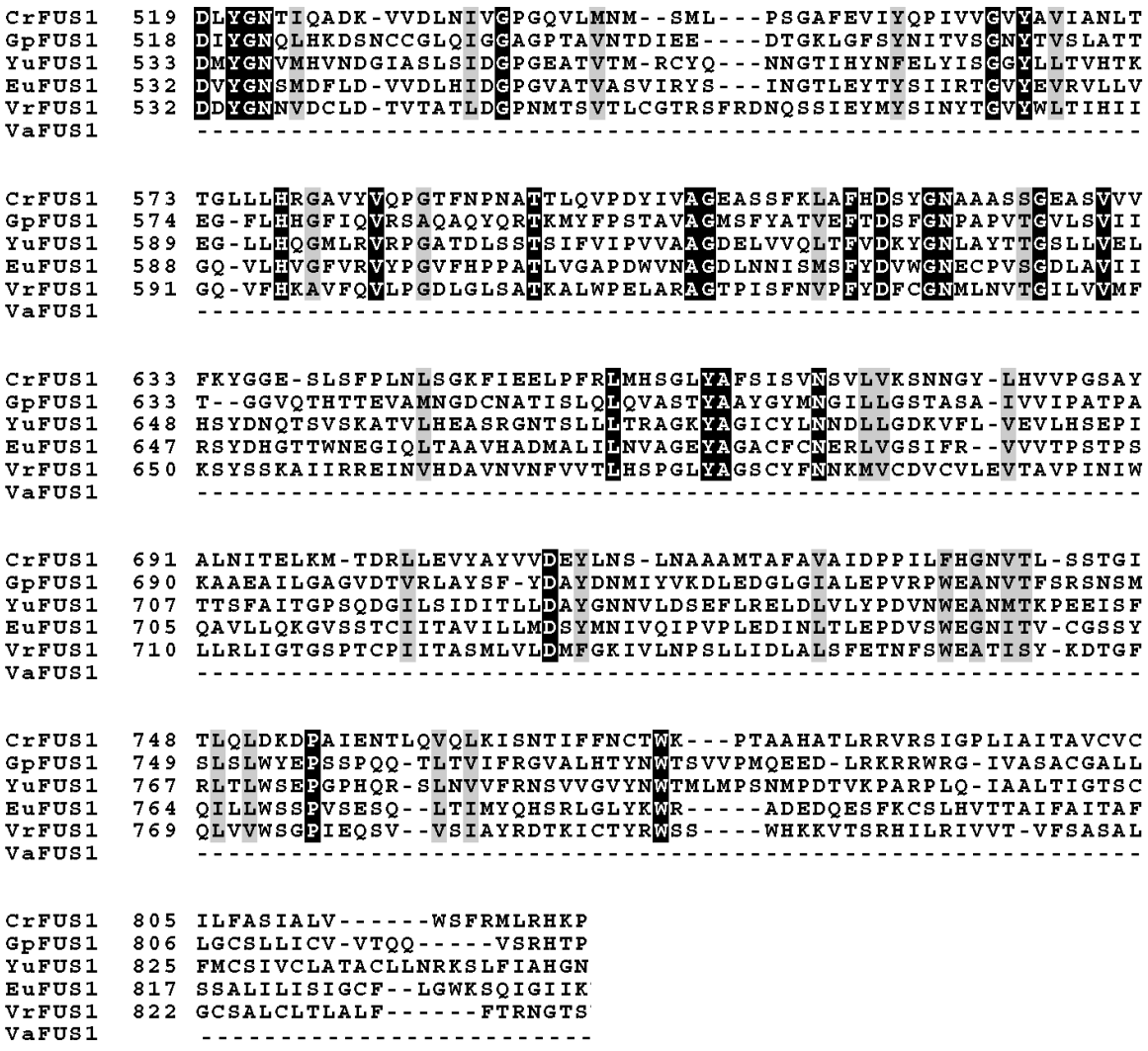

Figure 3.12 Alignment of female-limited FUS1 amino acid sequences. The FUS1 sequences of *C. reinhardtii* (CrFUS1, accession number AAC49416), *G. pectorale* (GpFUS1, accession number BAU61607), *Y. unicocca* (YuFUS1, identified in this study) and *Eudorina* sp. (EuFUS1, identified in this study) were aligned using MEGA X with manual adjustments. Acids identically in five sequences are shaded in black, and over 70% of identity or similarity are shaded in gray, respectively.

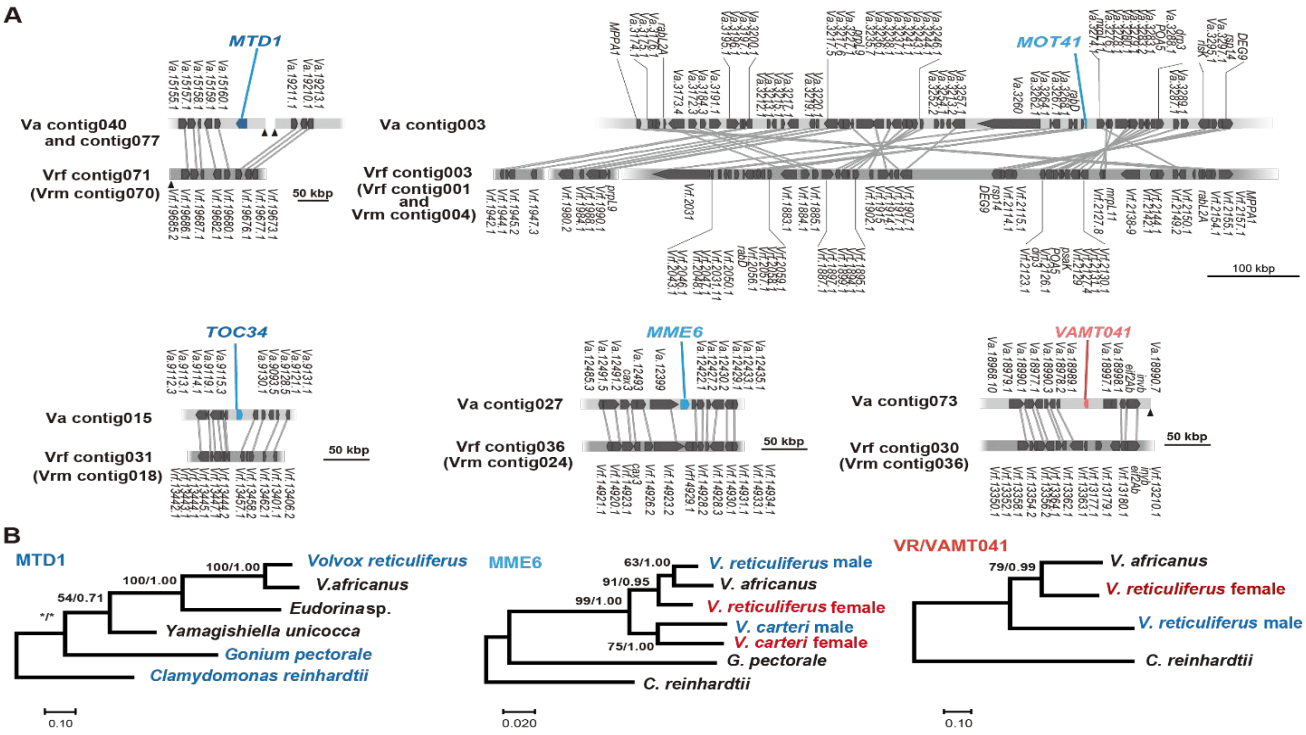

Figure 3.13. *Volvox africanus* autosome-like regions inserted by homologs of the male-limited *MTD1* and four gametologs of *Volvox reticuliferus* (Fig. 3.3A).

A. Comparison between autosome-like regions inserted by SDR-related gene homologs in homothallic *V. africanus* (Va, upper bars) and their homologous autosomal regions of heterothallic *V. reticuliferus* female (Vrf, lower bars). Contigs harboring the corresponding autosomal regions of *V. reticuliferus* male (Vrm) are described within parentheses and have the same gene arrangements as in Vrf autosomal regions shown here. Blue and red color of the gene names of *V. africanus* represents homologs of male or female gametologs of *V. reticuliferus*, respectively, based on the phylogenetic analyses.

B. Maximum likelihood (ML) phylogeny of homologs of *MTD1* and two gametologs (*MME-6* and *VR/VAMT041*). Red and blue gene names represent gametologs/sexlimited genes from female SDR (*MTF*) and male SDR (*MTM*), respectively. Numbers in left and right sides at branches indicate bootstrap values of *ML* analysis and posterior probabilities of Bayesian inference, respectively. For *MOT41* and *TOC34*, see Fig. 3.7.

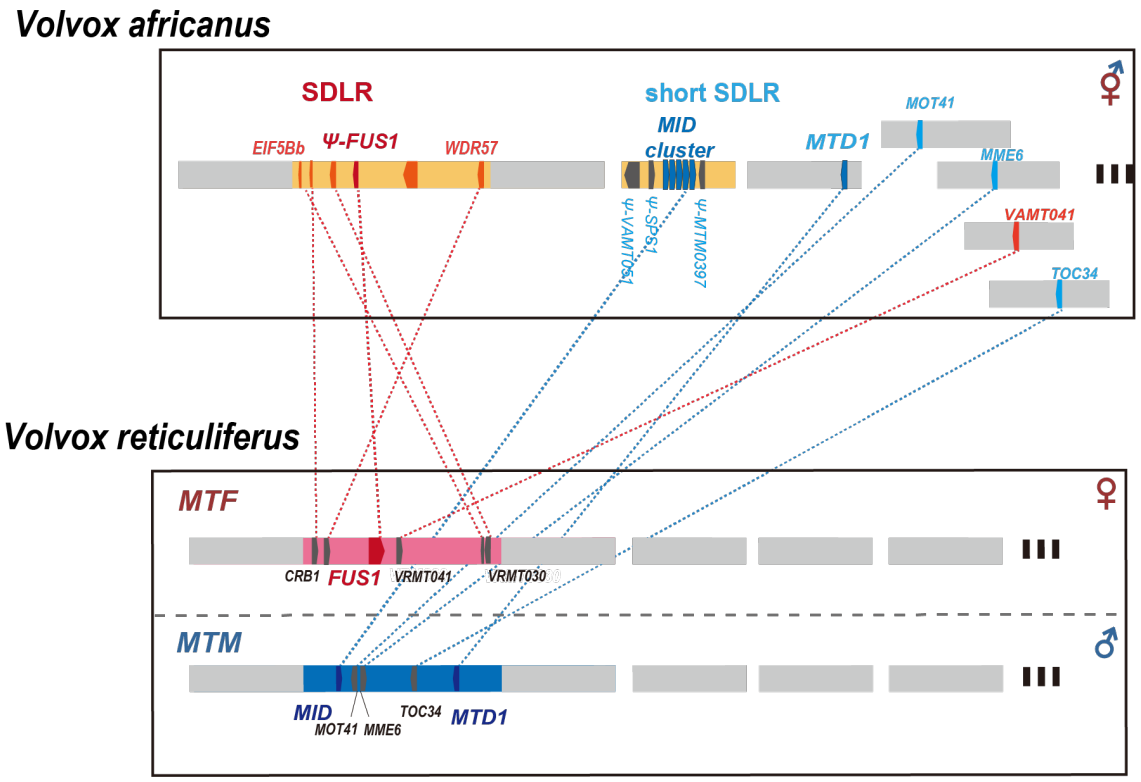

Figure 3.14 Diagrammatic comparison between sex-determining region (SDR)-like sequences (SDLR and short SDLR) of homothallic *V. africanus* (upper panel) and female SDR (*MTF*) and male SDR (*MTM*) of heterothallic *Volvox reticuliferus* (lower panel). Only four homologs of female-related gametologs in SDLR are shown. Based on the present study.

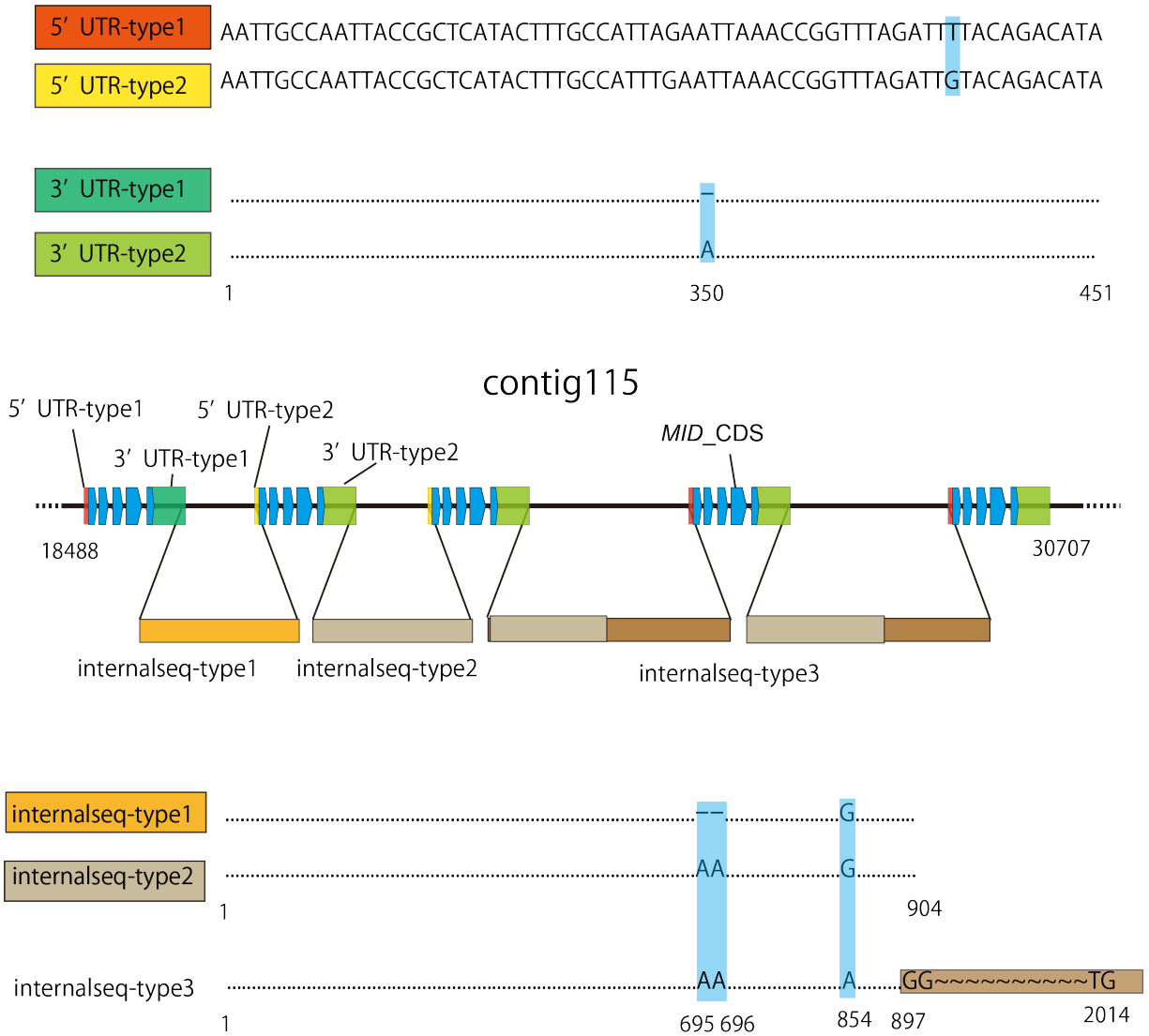

Figure 3.15. The outline of *VaMID* tandem repeat in contig115.

All CDS region had same sequences. 5’ UTR and 3’ UTR were sorted two types and diverted by single nucleotide (blue box). Four Internal regions were sorted three types. Type1 and type2 were diverted by double nucleotides (blue box). Type3 had type2 sequences of 897 bp, and unique sequences continued until 2014bp (brown box).

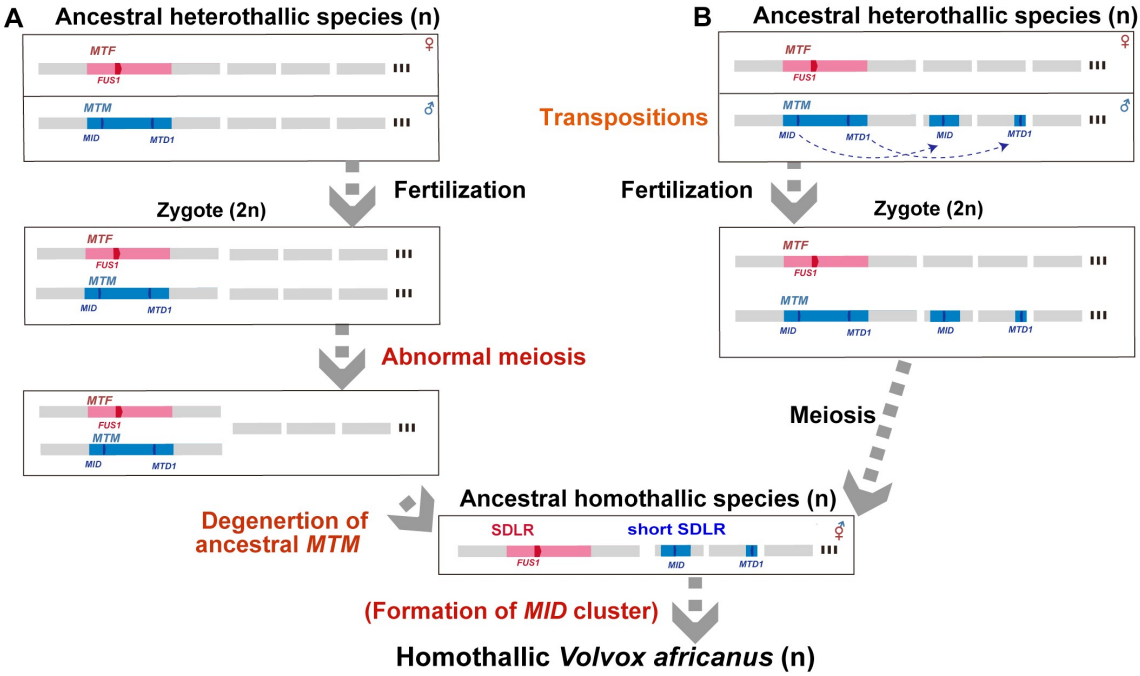

Figure 3.16. Two alternative hypotheses for evolution of homothallic *Volvox africanus*. Transpositions of three male and one female gametologs to autosomal regions (Fig. 3.13) that must have taken place during the evolution of *V. africanus* are not described. Based on the present study.

TABLES

Table 3.1. Comparison of details of whole nuclear genomes and SDR or SDLR/short SDLR of three *Volvox* strains.

	Species	*V. reticuliferus*		*V. africanus*
	Mating type/ sex (strain)	Female (NIES-3786)	Male (NIES-3785)	Homothallic (NIES-3780)
Whole genome	Size/total length(bp)	133,065,142	133,961,728	129,328,469
	Number of contigs	200	230	448
	Min (bp)	18,733	21,643	10,030
	Max(bp)	4,940,096	5,524,336	6,701,515
	contig N50	1,907,605	1,866,906	13,568,98
	%GC	54	54	53
	Number of genes	13,860	14,050	12,903
	Gene density (genes/Mb)	104.2	104.9	99.7
	Repeats (%) *	26.82	26.82	25.85
SDR or SDLR/short SDLR	Size (Mbp)	1.01	0.97	1.02/0.20
	%GC	51	51	51/50
	Number of genes	28	28	30/4
	Gene density (genes/Mb)	27.64	28.82	29.44/20.00
	Repeats (%) *	70.15	70.20	74.83/84.83

*Repetitive sequences identified using RepeatMasker-open-4-0-9 (http://www.repeatmasker.org) with Dfam3.0, generated libraries of repeats by RepeatScout (http://bix.ucsd.edu/repeatscout/).

Table 3.2. Results of RNA-seq.

Species	*V. reticuliferus*				*V. africanus*	
Mating type/ sex (strain)	Female (NIES-3786)		Male (NIES-3785)		Homothallic (NIES-3780)	
Culture condition	asexual	Sexual induced	asexual	Sexual induced	asexual	Sexual induced
Size/total length(bp)	7,194,367,200	8,947,862,000	6,981,367,600	8,839,040,600	6,893,563,600	7,070,441,600
Number of read-pairs	35,971,836	44,739,310	34,906,838	44,195,203	34467818	35,352,208

Table 3.3. Comparison of whole genome and SDR or SDLR/short SDLR properties of the volvocine algae (Fig. 3.1) *.

		Whole genome				
Species	Mating type/ sex	Size/total length (Mb)	%GC	Number of genes	Gene density (genes/Mb)	DDBJ/ENA/GenBank accessions no.
V. reticuliferus	Female	133	54	13860	104.2	BNCP01000001-BNCP01000200
	Male	134	54	14050	104.8	BNCQ01000001-BNCQ01000230
V. africanus	Homothallic	127	53	13716	108.1	BNCO01000001-BNCO01000448
V. carteri	Female	131.1	56.1	14958	114	GCA_000143455.1
	Male	N.d.	N.d.	N.d.**	N.d.	N.d.
Eudorina sp.	Female	184	61	N.d.	N.d.	GCA_003117195.1
	Male	168.6	61.3	N.d.	N.d.	GCA_003117095.1
Y. unicocca	Plus	134.2	61.1	N.d.	N.d.	GCA_003116995.1
	Minus	140.8	60.8	N.d.	N.d.	GCA_003117035.1
G. pectorale	Plus	149	64.5	17990	121	GCA_001584585.1
	Minus	N.d.	N.d.	N.d.	N.d.	N.d.
C. reinhardtii	Plus	111.1	64.1	17732	159.6	GCA_000002595.2
	Minus	N.d.	N.d.	N.d.	N.d.	N.d.

Table 3.3. Continued.

				SDR or SDLR/short SDLR		
Species	Mating type/ sex	Size (Mb)	%GC	Number of genes	Gene density (genes/Mb)	DDBJ/ENA/GenBank accessions no.
V. reticuliferus	Female	1.01	51	28(25***)	27.7	LC586643
	Male	0.98	51	28(25)	28.6	LC586644
V. africanus	Homothallic	1.02	51/50	30/4	29.4/20	LC586641/ LC58664 2
V. carteri	Female	1.51	52	55(50)	39	GU784915.1
	Male	1.13	53	60(50)	54	GU784916.1
Eudorina sp.	Female	0.09	53.9	3(2)	33.3	LC314414.1
	Male	0.007	51.4	3(2)	428	LC314415.1
Y. unicocca	Plus	0.268	60.1	18(17)	67.2	LC314412.1
	Minus	0.165	60.3	18(17)	109	LC314413.1
G. pectoral	Plus	0.366	59.7	24(21)	58	LC062718
	Minus	0.499	61	24(21)	46	LC062719
C. reinhardtii	Plus	0.31	60	35(22)	109	GU814014.1
	Minus	0.204	61	25(22)	118	GU814015.1

*References: *V. reticuliferus* and *V. africanus* (the present study); *C. reinhardtii* (Ferris et al., 2010); *G. pectorale* (Hamaji et al., 2016); *Y. unicocca* and *Eudorina* sp. (Hamaji et al., 2018) ;*V. carteri* (Ferris et al., 2010).

**Not determined.

***The number of gametologs in parentheses.

Table 3.4. Primers used for amplification and sequencing of the DNA fragments filling in a gap between Contigs 011 and 058 of *Volvox reticuliferus* female strain.

Primer name	Sequence ('5'-3')	Nucleotide positions
VrF_058_F1_788.3k	ATCACGACGAAGGGTATCATCATTAGGC	788289 -788316 in Contig058
VrF_058_F2_790.1k	TGCCTAGCTTTCTTTGCCGCAATAGAC	790135 -790161 in Contig058
VrF_011_R2_0.2k	CATTAGGCTGCTTTAGTTCGCGTATGTG	209 - 183in Contig011
VrF_011_R1_2.7k	GGTTGCATGCACTCCCATTTCTTCAG	2751 - 2726 in Contig011

Table 3.5. Primers used for amplification and sequencing of the DNA fragments filling in a gap between Contigs 018 and 132 of *Volvox africanus*.

Primer name	Sequence ('5'-3')	Nucleotide positions
VxAfr-SF1	GCCTGAGCTCGGTGATACTGACTTCGGGAG	1532807-1532836 in Contig018
VxAfr-SR3	AACGTGCTGGGGTGAATCATACCCTTGGCG	4228-4199 in Contig132
VxAFr-In1	TCGGAGGGACAGATGGTTTTGCTGAGCACT	1123-1152[1]
VxAfr-In2	GGGATAACTCACAATATTCGACTCGCGTCG	1398-1427[1]
VxAfr-In3	GGCCTTGATTGAGCAGACGAGGAGGCTGAG	2372-2401[1]
VxAfr-In4	CGTGAACGGATACTTGCTGTATCTGACCGG	2408-2437[1]
VxAfr-In5	GTGCGCAGCGTCGTAAGCCGGATCCTGTGC[2]	3436-3407[1]
VxAfr-In6	GGTGCGCACGACCGTTGTCGCAGCGGTAGG	3493-3464[1]
VxAfr-In7	GTCCGGATCCAGCAGTAAGGCCCACTTAGT	181-152[1]
VxAfr-In8	GTTTAACGGTGTGGATGTAGCAGGCGTGCC	4222-4251[1]
VxAfr-In9	TCTTCGCTTATGCAAGGGGACTCTGTTGGG	4714-4743[1]
VxAfr-In10	GGTGGTTCAGGTCGACCTTGGTGGTTGTTT	4399-4428[1]
VxAfr-In11	GGCGTGCCGGTTCCGTTGACGGGGCCGGCA	4244-4273[1]
VxAfr-SF2	ACTAAGTGGGCCTTACTGCTGGATCCGGAC	152-181[1]
VxAfr-SR1	TGCCGGCCCCGTCAACGGAACCGGCACGCC	4273-4244[1]
VxAfr-SR2	GCAAACGACACGAAGGGTACCTTGCCCAAC	4767-4738[1]
VxAfrR-3	ATCTGGCGAACAACAGAAAGACTTAGC	1230-1204[1]
VxAfrR-4	AAATTCGCTCGGACAGTATTCACAAAG[2]	1594-1568[1]

[1] Nucleotide positions in the bridging sequence (5148 bp.: Acc. No. LC582540) between VxAF-SF1 (Contig018) and VxAF-SPR3 (Contig132).

[2] Not completely identical to the bridging sequence.

Table 3.6. List of genes in SDR and pseudo autosomal regions of *Volvox reticuliferu*s (Fig. 3.3) and their orthologs in *V. africanus* and *V. carteri*. Genes in SDR or R domain are shown in bold.

V. reticuliferus gene	*V. africanus* ortholog		*V. carteri* ortholog
	Location	Name	
THI10	autosome-like	THI10	THI10
VR_PAR_021	autosome-like	VA_PAR_021	-
UTP1	autosome-like	UTP1	**UTP1**
HGRP1	autosome-like	HGRP1	**HGRP1**
PKY1	autosome-like	PKY1	PKY1
MADS2	autosome-like	mads2	MADS2
UBCH1	autosome-like	UBCH1	UBCH1
GCSH	autosome-like	GCSH	GCSH
PR46b	autosome-like	PR46b	PR46b
RPL37A	autosome-like	RPL37A	RPL37a
BBS2	autosome-like	BBS2	BBS2
VR_PAR_033	-	-	VOLCADRAFT_99150
VR_PAR_034	-	-	VOLCADRAFT_99151
VR_PAR_035	-	-	-
ATPvL1	autosome-like	ATPvL1	**ATPvL1**
FTT2	autosome-like	FTT2	**FTT2**
UCP2	autosome-like	UCP2	**UCP2**
FA1	autosome-like	FA1	**FA1**
VR_PAR_041	autosome-like	VA_PAR_041	
VR_PAR_042	autosome-like	VA_PAR_042	VOLCADRAFT_88639
DNJ11	autosome-like	DNJ11	dnj11
CGL55	SDLR	CGL55	CGL55
VRMT001	SDLR	VAMT001	-
VRMT003	SDLR	VAMT003	-
MTM1058	SDLR	MTM1058	**MTM1058**
MTM0349	SDLR	MTM0349	**MTM0349**
MTM0417	SDLR	MTM0417	**MTM0417**

Table 3.6 Continued.

MTD1*	autosome-like	MTD1	**ψ-MTD1***
VRM001*	-	-	-
VRMT014	SDLR	VAMT014	-
WDR57	SDLR	WDR57	**WDR57**
VRMT030	SDLR	VAMT030	VOLCADRAFT_89775
TOC34	autosome-like	TOC34	**TOC34**
SPS1	SDLR/short SDLR	SPS1/ψ-SPS1	**SPS1**
EIF5Bb	SDLR	EIF5Bb	**EIF5Bb**
MAT3	SDLR	MAT3	**MAT3**
CRB1	SDLR	CRB1	**CRB1**
VRMT041	autosome-like	VAMT041	-
VRMT043	SDLR	VAMT043	-
MTM0397	SDLR/short SDLR	MTM0397/	**MTM0397**
		ψ-MTM0397	
MME6	autosome-like	MME6	**MME6**
MOT41	autosome-like	MOT41	**MOT41**
VRMT051	SDLR/short SDLR	VAMT051	-
UNC50	SDLR	UNC50	**UNC50**
MID*	short SDLR	MID	**MID***
MTM0637	SDLR	MTM0637	**MTM0637**
MTM0638	SDLR	MTM0638	**MTM0638**
PTC1	SDLR	PTC1	**PTC1**
PSF2	SDLR	PSF2	**PSF2**

Table 3.6 Continued.

ARP4	autosome-like	ARP4	**ARP4**
L7Aef	autosome-like	L7Ae	**L7Ae**
MAPKK1	autosome-like	MAPKK1	**MAPKK1**
MTM0041	autosome-like	MTM0041	**MTM0041**
MTM0046	autosome-like	MTM0046	**MTM0046**
LEU1S	autosome-like	LEU1S	**LEU1S**
AMPKR1	autosome-like	AMPKR1	**AMPKR1**
EFG8	autosome-like	EFG8	**EFG8**
METM	autosome-like	METM	**METM**
HSP70b	autosome-like	HSP70b	**HSP70**
BFR1	autosome-like	BFR1	**BFR1**
MTM0001	autosome-like	MTM0001	**MTM0001**
VR_PAR_087	autosome-like	VA_PAR_087	VPS53
PAP1	autosome-like	PAP1	PAP1
PIP5K1	-	-	PIP5K1
FAP75	-	-	FAP75
MT0045	autosome-like	Va.22190.1	MT0045
MT0044	autosome-like	MT0044	MT0044
PRP4	autosome-like	PRP4	PRP4
DHC1b	SDLR	DHC1b	**DHC1b**
VRF001**	-	-	-
VRF002**	-	-	-
FUS1**	SDLR	ψ-FUS1	-

*Male-limited gene.

**Female-limited gene.

Table 3.7. Models used for the maximum likelihood analyses (ML) and Bayesian inference (BI) in molecular phylogenetic analyses of homologs of sex-limited genes and gametologs of *Volvox reticuliferus* and *V. africanus* (Figs. 3.3B, 3.5-3.7 and 3.13B).

Gene name	ML_model*	BI_model**	Figure
CRB1	JTT +G	Dayhoff	Figure 3.5
WDR57	JTT+G	WAG	Figure 3.5
PTC1	JTT+G	WAG	Figure 3.3B
UNC50	JTT+G	Cprev	Figure 3.5
MTM0637	JTT+G+I	Dayhoff	Figure 3.5
MTM0638	JTT+G+I+F	WAG	Figure 3.5
VR/VAMT041	JTT+G	Dayhoff	Figure3.13B
VR/VAMT014	JTT+G	Vt	Figure 3.5
MME6	JTT+G	WAG	Figure3.13B
MOT41	JTT+G	WAG	Figure 3.7
VR/VAMT043	JTT+G	WAG	Figure 3.5
VR/VAMT003	LG+G [f]	Dayhoff	Figure 3.5
MAT3	JTT+G	Dayhoff	Figure 3.5
SPS1	JTT+G	Dayhoff	Figure 3.3B
MTM0349	JTT+G	WAG	Figure 3.5
PSF2	JTT+G	Dayhoff	Figure 3.5
MTM1058	JTT+G	Dayhoff	Figure 3.5
VR/VAMT001	JTT+G+F	WAG	Figure 3.5
MTM0397	LG+G	WAG	Figure 3.6
eif5Bb	JTT+I	Dayhoff	Figure 3.5
VR/VAMT051	JTT	Vt	Figure 3.6
MTM0417	JTT+G	Dayhoff	Figure 3.5
VR/VAMT030	LG+G	Vt	Figure 3.5
TOC34	JTT+G	WAG	Figure 3.7
MTD1	JTT+G	WAG	Figure3.13B
FUS1	JTT+G	WAG	Figure 3.3B

*The best-fitted model selected by MEGA X (Kumar et al., 2018).

**The best-fitted model was selected by Modeltest-NG 0.1.6 (Darriba et al., 2020).

Chapter 4.

General discussion

The phenotype of sexual spheroids in homothallic *Volvox*

In chapter 2, *MID* orthologs in two homothallic species of *Volvox* were identified. The phenotype of sexual spheroids was different between those two *Volvox*; *V. africanus* formed monoecious and male spheroids; *V. ferrisii* formed only monoecious spheroids. The ratio of male and female gametes in the latter species is enough to form zygote by selfing or outcrossing between nearby individuals. However, the former species formed too many numbers of sperm in sexual reproduction phase.

Such sexual system found in some diploid species. 1.7% of angiosperms have "andromonoecious (male and hermaphrodite flowers in same individual)" sexual system (Yampolsky and Yampolsky, 1922), that evolved from hermaphrodite ancestors in the result of avoidance self-fertilization and inbreeding (Charlesworth and Charlesworth, 1978). "Androdioecy (male and hermaphrodite individuals in same population)" is strictly different from *V. africanus* situation, but there seems to be some points of arguments in androdioecy from hermaphrodite ancestors, similar to *V. africanus.* For example, some androdioecy evolved in the result of acquisition of male function in females which lose chance of mating (Pannell, 2002; Russell and Pannell, 2015).

However, to discuss the strategy of *V. africanus,* difference of male and monoecious spheroids in *V. africanus* (Fig. 2.1E, F, G), such as population, motility and conditions of sex reproduction in nature, should be clarified.

Transition from heterothallism to homothallism in a UV chromosome system

The presence of a long female-derived SDLR in *V. africanus* indicates that this locus remained largely intact during the transition from heterothallism to homothallism (Fig. 3.14). Starting with this observation, I can begin to infer how homothallism arose in *V. africanus* (Fig 3.16). My hypotheses are based on the assumptions that *MID* (and probably *MTD1*) is essential for male

gametogenesis and that none of the female-limited genes in the heterothallic ancestor were absolutely essential for female gametogenesis, though ancestrally female gametologs probably did play a role as described below. In addition, it is also assumed that some modulation of *MID* and *MTD1* expression during sexual development are essential to allow female sexual differentiation to occur in *V. africanus* since the MID pathway is dominant for sex determination. This is consistent with chapter 1 data for *V. africanus* where *MID* transcripts were much more abundant in pure males versus monoecious spheroids. Experiments in *V. carteri* also showed that a homothallic phenotype could be induced when *MID* expression was partly suppressed in a male strain (Geng et al., 2014). The intriguing observation that *MID* became incorporated into tandem array in *V. africanus* raises additional questions about how this arrangement relates to *MID* expression and the mechanism by which *MID* remains active (or not) in male versus monoecious spheroids.

One scenario for the transition to homothallism in *V. africanus* involves meiotic non-disjunction as an initiating event that placed male and female SDRs together into a single progeny. Degeneration of the male SDR with loss of most of its genes, amplification of the *MID* gene on the remnant male short SDLR fragment, and several autosomal insertions of male gametologs, with losses of the corresponding female gametologs, would have led to the current state in *V. africanus* (Figs. 3.14, 3.16A). This scenario is somewhat problematic as it does not explain the strong female bias for gametolog retention.

An alternative scenario starts with a short *MID*-containing male SDLR precursor fragment transposing to an autosome or becoming an independent genetic element, followed by the transposition of other male SDR genes into autosomes (Fig. 3.16B). These transposition events would include *MTD1*, and three autosomal gametologs that are male-derived (see above and Fig. 3.14), followed by introgression of these loci into a chromosomally female strain after outcrossing. The difficulty of this scenario comes from the need to introgress and maintain

multiple unlinked autosomal male loci in an otherwise chromosomally female strain. I envision that the *MID* transposition event to form a short SDLR occurred first, and may have spread in the outcrossing population, behaving similarly to the extrachromosomal *MID* array discovered previously in *Chlamydomonas reinhardtii* (Ferris and Goodenough, 1997). The short SDLR alone might have been sufficient to cause some degree of homothallism when present in a chromosomally female strain (Geng et al., 2014), and could have spread or been fixed under conditions when outcrossing was inefficient (e.g. low population density, imbalanced sex ratio due to genetic drift). Additional male SDR-to-autosomal transposition events (*MTD1* and three male gametologs) that combined with the short SDLR and female chromosome in a nascent homothallic strain may have conferred a male fitness advantage. While these ideas for the evolution of homothallism are speculative (Fig. 3.16), they are potentially testable using molecular genetic manipulations of *V. africanus*, *V. reticuliferus* and/or *V. carteri* where an artificially-created selfing strain has been previously reported (Geng et al., 2014).

Further prospects to understand the evolution of sexual system

Transitions between haploid dioicy and monoicy have been documented in haploid bryophytes (McDaniel et al., 2013) and in brown algae (Heesch et al., 2019), but the molecular nature of sex determination and histories of sex chromosomes are not well understood in either group. Here it can infer how a fully differentiated UV sex chromosome system in volvocine algae was modified to produce a homothallic mating system in *V. africanus*. The remnant female SDLR in *V. africanus* with distinct properties of a sex chromosome (low gene density, high repeat content) may only suggest that this transition may have been recent as such features might be expected to be purged over time in a normally recombining SDLR. However, it is highly likely that the SDR and SDLR regions of *Volvox* have a role in the development of "special" sexual spheroids in *Volvox* where males and females are morphologically different from asexual spheroids in

arrangement of somatic and reproductive cells (Figs. 1.2, 1.3) (Starr, R.C., 1969; Hanschen et al., 2016). Geng et al. (2014) demonstrated that in *V. carteri* genes on SDR controlled aspects of male versus female special sexual developmental patterning independently of the MID pathway. I showed here that *V. reticuliferus* has 16 gametologs in common with *V. carteri* SDR (Fig. 3.10) that are strong candidates for playing a conserved role in distinct aspects of dimorphic sexual development (e.g. sexual germ cell precursor number/size). The *V. africanus* SDLR harbors at least 18 female-derived genes that have common ancestors with *V. reticuliferus* female gametologs, and 5 of the 18 also have a common ancestor with the *V. carteri* female SDR making them ancestrally female in the section *Merrillosphaera* (Figs. 3.1, 3.2). The *V. africanus* female-like SDLR genes may therefore play a role in governing developmental patterning that gives rise to monoecious versus male sexual forms in this species (Figs. 1.2, 1.3). In the future, the functions of SDLR female lineage genes and male lineage genes that intervene in the autosomal homology region will be analyzed; and genomic analysis using different homothallic strains described by Starr (1971), that has a different lineage and sexual expression from the current *V. africanus* will further elucidate the molecular genetic basis of the evolution of *Volvox* from heterothallism to homothallism.

Acknowledgements

First of all, I would like to express my sincere gratitude to Dr. Hisayoshi Nozaki (University of Tokyo) for his encouragements, suggestions, critical proofreading of this manuscript and giving me the opportunity to study in his laboratory.

I am grateful to Drs. Hiroko Kawai-Toyooka (University of Tokyo) and Takashi Hamaji (Kyoto University) for technical guidance, discussions, and encouragements.

I also thank Dr. Fumio Takahashi (Ritsumeikan University) for sampling *Volvox africanus* and *V. reticuliferus* from Lake Biwa; Drs. Yuki Tsuchikane and Hiroyuki Sekimoto (Japan Women's University) for the technical guidance of estimation of genome sizes with DAPI and the helpful discussions; Drs. Yohei Minakuchi, Masanobu Kawachi, and Atsushi Toyoda (National Institute of Genetics) for the technical guidance, sequencing and assembling of *Volvox africanus and Volvox reticuliferus* whole genome and transcriptome data; Dr. Yoko Arakaki (University of Tokyo) for the DNA extraction for whole genome; Dr. Kaoru Kawafune (Tokyo Institute of Technology) for the technical assistance of the analyses using the genome data and encouragements; Dr. Ryo Matsuzaki (National Institute for Environmental Studies) for technical guidance of the phylogenetic analyses; Drs. Patrick J. Ferris and James G. Umen (Donald Danforth Plant Science Center) for helpful advice to write the manuscript, helpful discussions and comments ; Drs. Yoshiki Nishimura (Kyoto University), Masanobu Kawachi (National Institute for Environmental Studies) and Toshiyuki Mori (Osaka University) for helpful discussions and comments.

I am also grateful to all the current and former members of the Laboratory of Origin of Eukaryote Biodiversity (University of Tokyo) for their friendship, discussions, and encouragements.

Finally, I really thank to my family for their supports and encouragements.

A part of Chapter 2 was reproduced from Yamamoto et al. (2017, *PLoS ONE* **12**: e0180313).

References

Charlesworth, B., and Charlesworth, D. (1978). A model for the evolution of dioecy and gynodioecy. Am. Nat. *112*, 975–997.

Charlesworth, D., Morgan, M.T., and Charlesworth, B. (1990). Inbreeding depression, genetic load, and the evolution of outcrossing rates in a multilocus system with no linkage. Evol. Int. J. Org. Evol. *44*, 1469–1489.

Chin, C.-S., Peluso, P., Sedlazeck, F.J., Nattestad, M., Concepcion, G.T., Clum, A., Dunn, C., O'Malley, R., Figueroa-Balderas, R., Morales-Cruz, A., et al. (2016). Phased diploid genome assembly with single-molecule real-time sequencing. Nat. Methods *13*, 1050–1054.

Coelho, S.M., Gueno, J., Lipinska, A.P., Cock, J.M., and Umen, J.G. (2018). UV chromosomes and haploid sexual systems. Trends Plant Sci. *23*, 794–807.

Coleman, A.W. (1999). Phylogenetic analysis of "Volvocacae" for comparative genetic studies. Proc. Natl. Acad. Sci. U. S. A. *96*, 13892–13897.

Darriba, D., Posada, D., Kozlov, A.M., Stamatakis, A., Morel, B., and Flouri, T. (2020). ModelTest-NG: A new and scalable tool for the selection of dna and protein evolutionary models. Mol. Biol. Evol. *37*, 291–294.

Darwin, C., and Burkhardt, F. (1861). The correspondence of Charles Darwin. 9. 1861 (Cambridge University Press).

Dubini, A., Mus, F., Seibert, M., Grossman, A.R., and Posewitz, M.C. (2009). Flexibility in anaerobic metabolism as revealed in a mutant of *Chlamydomonas reinhardtii* lacking hydrogenase activity. J. Biol. Chem. *284*, 7201–7213.

Edgar, R.C. (2004). MUSCLE: multiple sequence alignment with high accuracy and high throughput. Nucleic Acids Res. *32*, 1792–1797.

Ferris, P.J., and Goodenough, U.W. (1994). The mating-type locus of *Chlamydomonas reinhardtii* contains highly rearranged DNA sequences. Cell *76*, 1135–1145.

Ferris, P.J., and Goodenough, U.W. (1997). Mating type in *Chlamydomonas* is specified by mid,

the minus-dominance gene. Genetics *146*, 859–869.

Ferris, P., Olson, B.J.S.C., De Hoff, P.L., Douglass, S., Diaz-Cano, D.C., Prochnik, S., Geng, S., Rai, R., Grimwood, J., Schmutz, J., et al. (2010). Evolution of an expanded sex determining locus in *Volvox*. Science *328*, 351–354.

Ferris, P.J., Woessner, J.P., and Goodenough, U.W. (1996). A sex recognition glycoprotein is encoded by the plus mating-type gene fus1 of *Chlamydomonas reinhardtii*. Mol. Biol. Cell *7*, 1235–1248.

Geng, S., De Hoff, P., and Umen, J.G. (2014). Evolution of sexes from an ancestral mating-type specification pathway. PLoS Biol. *12*, e1001904.

Hamaji, T., Ferris, P.J., Coleman, A.W., Waffenschmidt, S., Takahashi, F., Nishii, I., and Nozaki, H. (2008). Identification of the minus-dominance gene ortholog in the mating-type locus of *Gonium pectorale*. Genetics *178*, 283–294.

Hamaji, T., Mogi, Y., Ferris, P.J., Mori, T., Miyagishima, S., Kabeya, Y., Nishimura, Y., Toyoda, A., Noguchi, H., Fujiyama, A., et al. (2016). Sequence of the *Gonium pectorale* mating locus reveals a complex and dynamic history of changes in volvocine algal mating haplotypes. G3 Bethesda Md *6*, 1179–1189.

Hamaji, T., Kawai-Toyooka, H., Uchimura, H., Suzuki, M., Noguchi, H., Minakuchi, Y., Toyoda, A., Fujiyama, A., Miyagishima, S., Umen, J.G., et al. (2018). Anisogamy evolved with a reduced sex-determining region in volvocine green algae. Commun. Biol. *1*, 17.

Hanschen, E.R., Marriage, T.N., Ferris, P.J., Hamaji, T., Toyoda, A., Fujiyama, A., Neme, R., Noguchi, H., Minakuchi, Y., Suzuki, M., et al. (2016). The Gonium pectorale genome demonstrates co-option of cell cycle regulation during the evolution of multicellularity. Nat. Commun. *7*, 11370.

Hanschen, E.R., Herron, M.D., Wiens, J.J., Nozaki, H., and Michod, R.E. (2018). Repeated evolution and reversibility of self-fertilization in the volvocine green algae*. Evolution *72*,

386–398.

Heesch, S., Serrano-Serrano, M., Luthringer, R., Peters, A.F., Destombe, C., Cock, J.M., Valero, M., Roze, D., Salamin, N., and Coelho, S. (2019). Evolution of life cycles and reproductive traits: insights from the brown algae. BioRxiv 530477.

Herron, M.D., Hackett, J.D., Aylward, F.O., and Michod, R.E. (2009). Triassic origin and early radiation of multicellular volvocine algae. Proc. Natl. Acad. Sci. *106*, 3254–3258.

Hiraide, R., Kawai-Toyooka, H., Hamaji, T., Matsuzaki, R., Kawafune, K., Abe, J., Sekimoto, H., Umen, J., and Nozaki, H. (2013). The evolution of male-female sexual dimorphism predates the gender-based divergence of the mating locus gene *MAT3/RB*. Mol. Biol. Evol. *30*, 1038–1040.

Isaka, N., Kawai-Toyooka, H., Matsuzaki, R., Nakada, T., and Nozaki, H. (2012). Description of two new monoecious species of *Volvox* sect. *Volvox* (Volvocaceae, Chlorophyceae), based on comparative morphology and molecular phylogeny of cultured material. J. Phycol. *48*, 759–767.

Jarne, P., and Auld, J.R. (2006). Animals Mix It up Too: The Distribution of self-Fertilization among hermaphroditic animals. Evolution *60*, 1816–1824.

Jones, D.T., Taylor, W.R., and Thornton, J.M. (1992). The rapid generation of mutation data matrices from protein sequences. Bioinformatics *8*, 275–282.

Kalanon, M., and McFadden, G.I. (2008). The chloroplast protein translocation complexes of *Chlamydomonas reinhardtii*: a bioinformatic comparison of Toc and Tic components in plants, green algae and red algae. Genetics *179*, 95–112.

Kasai, F., Kawachi, M., Erata, M., Mori, F., Yumoto, K., Sato, M., and Ishimoto, M. (2009). NIES-Collection, List of strains, 8th edition. Jpn J Phycol *57*, Supplement: 1–350, plates 1–7.

KATO, S. (1982). Laboratory culture and morphology of *Colacium vesiculosum* Ehrb. (Euglenophyceae). Jpn J Phycol *30*, 63–67.

Kianianmomeni, A., Ong, C.S., Rätsch, G., and Hallmann, A. (2014). Genome-wide analysis of alternative splicing in *Volvox carteri*. BMC Genomics *15*, 1117.

Kirk, D.L. (2005). A twelve-step program for evolving multicellularity and a division of labor. BioEssays News Rev. Mol. Cell. Dev. Biol. *27*, 299–310.

Kirk, D.L., and Kirk, M.M. (1983). Protein synthetic patterns during the asexual life cycle of *Volvox carteri*. Dev. Biol. *96*, 493–506.

Kumar, S., Stecher, G., Li, M., Knyaz, C., and Tamura, K. (2018). MEGA X: Molecular Evolutionary Genetics Analysis across Computing Platforms. Mol. Biol. Evol. *35*, 1547–1549.

Le, S.Q., and Gascuel, O. (2008). An improved general amino acid replacement matrix. Mol. Biol. Evol. *25*, 1307–1320.

Liss, M., Kirk, D.L., Beyser, K., and Fabry, S. (1997). Intron sequences provide a tool for high-resolution phylogenetic analysis of volvocine algae. Curr. Genet. *31*, 214–227.

M. Kawachi et al. (2013). MCC-NIES list of strains, 9th Edition, microbial culture collection at National Institute for Environmental Studies, Tsukuba, Japan.

McDaniel, S.F., Atwood, J., and Burleigh, J.G. (2013). Recurrent evolution of dioecy in bryophytes. Evolution *67*, 567–572.

Miller, S.M., Schmitt, R., and Kirk, D.L. (1993). Jordan, an active *Volvox* transposable element similar to higher plant transposons. Plant Cell *5*, 1125–1138.

Nei, M., and Gojobori, T. (1986). Simple methods for estimating the numbers of synonymous and nonsynonymous nucleotide substitutions. Mol. Biol. Evol. *3*, 418–426.

Nei, M., and Kumar, S. (2000). Molecular Evolution and Phylogenetics.

Noé, L., and Kucherov, G. (2005). YASS: enhancing the sensitivity of DNA similarity search. Nucleic Acids Res. *33*, W540-543.

Nozaki, H. (1983). Sexual reproduction in *Eudorina elegans* (chlorophyta, volvocales). Bot. Mag. Shokubutsu-Gaku-Zasshi *96*, 103–110.

Nozaki, H., Mori, T., Misumi, O., Matsunaga, S., and Kuroiwa, T. (2006). Males evolved from the dominant isogametic mating type. Curr. Biol. CB *16*, R1018-1020.

Nozaki, H., Matsuzaki, R., Yamamoto, K., Kawachi, M., and Takahashi, F. (2015). Delineating a new heterothallic species of *volvox* (volvocaceae, chlorophyceae) using new strains of "*Volvox africanus*." PLOS ONE *10*, e0142632.

Nozaki, H., Takusagawa, M., Matsuzaki, R., Misumi, O., Mahakham, W., and Kawachi, M. (2019). Morphology, reproduction and taxonomy of *Volvox dissipatrix* (Chlorophyceae) from Thailand, with a description of *Volvox zeikusii* sp. nov . Phycologia *58*, 1–8.

Ohtsubo, Y., Ikeda-Ohtsubo, W., Nagata, Y., and Tsuda, M. (2008). GenomeMatcher: a graphical user interface for DNA sequence comparison. BMC Bioinformatics *9*, 376.

Pannell, J.R. (2002). The Evolution and maintenance of androdioecy. Annu. Rev. Ecol. Syst. *33*, 397–425.

Piel, W. H., Chan, L., Dominus, V. Tannen, M. J., Ruan, J, and ., Vos, R. A., (2009). TreeBASE v. 2: A Database of Phylogenetic Knowledge. E-BioSphere.

Ronquist, F., Teslenko, M., van der Mark, P., Ayres, D.L., Darling, A., Höhna, S., Larget, B., Liu, L., Suchard, M.A., and Huelsenbeck, J.P. (2012). MrBayes 3.2: efficient Bayesian phylogenetic inference and model choice across a large model space. Syst. Biol. *61*, 539–542.

Russell, J.R.W., and Pannell, J.R. (2015). Sex determination in dioecious *Mercurialis annua* and its close diploid and polyploid relatives. Heredity *114*, 262–271.

Smith, G.M. (1944). A Comparative study of the species of *Volvox*. Trans. Am. Microsc. Soc. *63*, 265–310.

Starr, R.C. (1969). Structure, reproduction and differentiation in *Volvox carteri* f. nagariensis Iyengar, strains HK9 & 10. Arch Protistenkd. *111*, 204–222.

Starr RC (1971). Sexual reproduction in *Volvox africanus*. In Contribution in Phycology, (Allen Press), pp. 59–66.

Tamura, K., Battistuzzi, F.U., Billing-Ross, P., Murillo, O., Filipski, A., and Kumar, S. (2012). Estimating divergence times in large molecular phylogenies. Proc. Natl. Acad. Sci. *109*, 19333–19338.

Tamura, K., Stecher, G., Peterson, D., Filipski, A., and Kumar, S. (2013). MEGA6: Molecular evolutionary genetics analysis version 6.0. Mol. Biol. Evol. *30*, 2725–2729.

Tamura, K., Tao, Q., and Kumar, S. (2018). Theoretical foundation of the reltime method for estimating divergence times from variable evolutionary rates. Mol. Biol. Evol. *35*, 1770–1782.

Tao, Q., Tamura, K., Mello, B., and Kumar, S. (2020). Reliable confidence intervals for reltime estimates of evolutionary divergence times. Mol. Biol. Evol. *37*, 280–290.

Umen, J., and Coelho, S. (2019). Algal sex determination and the evolution of anisogamy. Annu. Rev. Microbiol. *73*, 267–291.

Vos, R., Balhoff, J., Caravas, J., Holder, M., Lapp, H., Maddison, W., Midford, P., Priyam, A., Sukumaran, J., Xia, X., et al. (2012). NeXML: rich, extensible, and verifiable representation of comparative data and metadata. Syst. Biol. *61*, 675–689.

Walker, B.J., Abeel, T., Shea, T., Priest, M., Abouelliel, A., Sakthikumar, S., Cuomo, C.A., Zeng, Q., Wortman, J., Young, S.K., et al. (2014). Pilon: an integrated tool for comprehensive microbial variant detection and genome assembly improvement. PLoS ONE *9*, e112963.

Wong, J.L., and Wolfner, M.F. (2017). Is gender just a category? The two-plus sex advantage. Mol. Reprod. Dev. *84*, 89–90.

Yamamoto, K., Oda, Y., Haseda, A., Fujito, S., Mikami, T., and Onodera, Y. (2014). Molecular evidence that the genes for dioecism and monoecism in *Spinacia oleracea* L. are located at different loci in a chromosomal region. Heredity *112*, 317–324.

Yampolsky, C., and Yampolsky, H. (1922). Distribution of sex forms in phaerogamic flora (Biblio. Genet.).

Yang, Z. (2007). PAML 4: phylogenetic analysis by maximum likelihood. Mol. Biol. Evol. *24*,

1586–1591.

Yang, Z., and Nielsen, R. (2000). Estimating synonymous and nonsynonymous substitution rates under realistic evolutionary models. Mol. Biol. Evol. *17*, 32–43.

Zhu, B., Zhu, X., Wang, L., Liang, Y., Feng, Q., and Pan, J. (2017). Functional exploration of the IFT-A complex in intraflagellar transport and ciliogenesis. PLOS Genet. *13*, e1006627.